Durham E-Theses

Stability Analyses for Porous Convection Including Second Sound Effects

HADDAD, SHATHA,AHMED,MAHDI

Stability Analyses for Porous Convection Including Second Sound Effects

Shatha Haddad

A Thesis presented for the degree of
Doctor of Philosophy

Numerical Analysis
Department of Mathematical Sciences
University of Durham
England

June 2014

Dedicated to

My family

with love and gratitude.

Stability Analyses for Porous Convection Including Second Sound Effects

Shatha Haddad

Submitted for the degree of Doctor of Philosophy

June 2014

Abstract

We investigate various models of thermal convection in a fluid saturated porous medium of both Darcy and Brinkman types. The linear instability and global (unconditional) nonlinear stability thresholds are analysed. Analytical solutions and numerical solutions are obtained by employing the D^2 Chebyshev tau and compound matrix techniques, and we investigate the effect that the inertia term and other physical parameters have on the stability of the system. The thesis is split into two parts. In Part I we consider a coupled model of thermal convection in a fluid saturated porous material and theories of viscous fluid motion which allows heat to travel as a wave. This is discussed in the first three chapters.

In Chapter 2 the instability mechanism is investigated in complete detail and it is shown that stationary convection is likely to prevail under normal terrestrial conditions, but if the thermal relaxation time is sufficiently large there is a possible parameter range which allows for oscillatory convection. However, the presence of the Guyer-Krumhansl terms has the effect of damping the oscillatory convection and returning the instability mechanism to one of stationary convection.

In Chapter 3 the constitutive equation for the heat flux is governed by a couple of the Guyer-Krumhansl equations and the Cattaneo-Fox law. In particular, we study the effects of the Guyer-Krumhansl terms on oscillatory convection. It is found that for a certain range of the Guyer-Krumhansl coefficient stationary convection occurs while changing the range results in oscillatory convection. Numerical results quantify this effect.

The thermal instability in a Brinkman porous medium incorporating fluid inertia for both free–free and fixed–fixed boundaries is considered in Chapter 4. We have incorporated the Cattaneo–Christov theory in the constitutive equation for the heat flux. For fixed surfaces, the results are generated by using the D^2 Chebyshev tau method. The results reveal that employing the Cattaneo–Christov theory has a pronounced effect in determining the convection instability threshold.

Part II concerns the effect of an anisotropic permeability on thermal instability in the modelling problems of thermal convection of Darcy type with and without the inclusion of an inertia term, which represented the last three chapters.

In Chapter 5 we allow a non-zero inertia term and also allow the permeability to be an anisotropic tensor. For particular numerical results we consider the case when the vertical component of the permeability tensor is variable. Linear instability results are calculated numerically and it is proved that the nonlinear energy stability bound is the same as the linear one. We perform the linear instability and nonlinear stability analysis, in the case where the inertial term vanishes, to investigate the effect of anisotropy with rotation on the stability thresholds in Chapter 6, showing that the nonlinear critical Rayleigh numbers coincide with those of the linear analysis. The results reveal that the inclusion of the inertial term for this model can play an important role on the onset of convection in Chapter 7.

Declaration

The work in this thesis is based on research carried out at the University of Durham, the Department of Mathematical Sciences, the Numerical Analysis Group, England. No part of this thesis has been submitted elsewhere for any other degree or qualification and it all my own work with the exception of Chapter 2, which was written in collaboration with Prof. B. Straughan of the University of Durham. The contents of Chapters 2 to 5 are published in [45–48].

Acknowledgements

I would like to take this opportunity to express my sincere thanks to my supervisor Prof. Brian Straughan for his effort, encouragement, constructive guidance, and supplying his insight into my research work during my PhD Study which has enabled me to complete my work in my thesis.

I am also grateful to many staff members in St. Cuthbert's Society for their professional and administrative support. In particular, I wish to express my gratitude to Mrs. Carol Philipson who has provided me with love and support and who has made my time in Durham enjoyable.

Special thanks go to my mother, my brothers, and my sisters for their constant love, support, and encouragement which has helped me to keep going throughout the completion of this thesis.

My thanks go to my friends. In particular, Dr. Alaa Abdulhseen Salih and his wife, I greatly appreciate the kind help and generosity received from them during my first year in Durham.

I would also like to acknowledge the financial support which I received from the Iraq Ministry of Higher Education and Scientific Research and thanks goes to the Iraqi Cultural Office in London for their efforts during my the study period.

Finally, thanks to Dr. M. Imran for preparing the LaTeX template which has helped me to write this thesis.

Contents

List of Figures

List of Tables

Chapter 1

Introduction

Thermal convection in porous media is a subject which has immense application. For instance, in geophysics, in star evolution, in crystal growth, and many other areas, see e.g. the accounts in the books by Straughan [115, 116, 121] and Nield and Bejan [84]. It is a topic which has a long history but due to its importance in real life applications it is still attracting much interest from prominent writers, see e.g. Nield and Kuznetsov [82, 83], Nield and Barletta [80], Rionero [92, 94, 95], Agarwal and Bhadauria [1], Bagchi and Kulacki [3], Bera and Khalili [4], Bera et al. [5], Capone et al. [7–10], Carotenuto and Minale [14], Chen et al. [20], Diaz and Brevdo [30], Kaloni and Mahajan [56], Kumar et al. [58, 59], Kuznetsov and Nield [63], Lee et al. [67], Malashetty and Biradar [72, 73], Nanjundappa et al. [79], Saravanan and Sivakumar [101], Shivakumara et al. [104–107], Simitev [108], Straughan [116], Sunil et al. [124], Usha et al. [127], Yang et at. [139], and the references therein.

The main aims of this thesis are to investigate the stability of thermal convection in a fluid saturated porous material of both Darcy and Brinkman types. To achieve this goal, the linear instability and nonlinear analysis are performed to study the changes in the behaviour of the onset of thermal convection in a fluid saturated porous medium due to the effects various parameters on heat transfer. The work in this thesis is divided into two parts. In the first part, Chapters 2, 3, and 4, we turn our attention to the Cattaneo theories, see Straughan [121], for the heat flux to study the effect of thermal waves (second sound) on the stability threshold via

linear instability analysis. We employ a linear analysis since this yields meaningful Rayleigh number threshold. The hyperbolic nature of the equations, leading to second sound has to date prevented useful analyses by nonlinear stability methods. The second part, Chapters 5, 6, and 7, deal with the thermal convection in a fluid saturated Darcy porous medium when the permeability is anisotropic. In particular, the effects of anisotropic permeability with and without inclusion the fluid inertia term. Both linear and nonlinear stability analyses are employed. The nonlinear work is very important since it shows the linear work is correctly capturing the physics of the onset thermal convection. cf. Rionero [96–98], Hill and Malashetty [51], and Lombardo et al. [68].

In the next Section, we introduce standard notation and some useful inequalities that are used through the thesis and then in Section 1.2, we illustrate the basic concept of stability theory in porous media.

1.1 Notation, definition and useful inequalities

In this Section, we introduce standard indicial notation with the Einstein summation convection for the repeated indices, which is used throughout the thesis. The standard vector is denoted by bold type. For example, for $\mathbf{q}(\mathbf{x}) = (q_1, q_2, q_3)$ with $\mathbf{x} = (x_1, x_2, x_3)$, or for $q(x)$ a scalar function of x, we have

$$q_x \equiv \frac{\partial q}{\partial x} \equiv q_{,x}, \qquad q_{i,t} \equiv \frac{\partial q_i}{\partial t}, \qquad \text{div } \mathbf{q} \equiv q_{i,i} \equiv \frac{\partial q_i}{\partial x_i} \equiv \sum_{i=1}^{3} \frac{\partial q_i}{\partial x_i},$$

$$q_j q_{i,j} \equiv q_j \frac{\partial q_i}{\partial x_j} \equiv \sum_{j=1}^{3} q_j \frac{\partial q_i}{\partial x_j}, \;\; i = 1, 2 \text{ or } 3.$$

The material derivative of a function $\mathbf{q}$ is given by

$$\dot{q}_i \equiv \frac{\partial q_i}{\partial t} + v_j \frac{\partial q_i}{\partial x_j},$$

where $\mathbf{v}$ is the velocity of the moving body at point $\mathbf{x}$.

Throughout the thesis we deal with a convection cell which is periodic in the (x, y) plane. Thus, suppose $z \in (0, 1)$ and Γ denotes the cell shape in the horizontal, (x, y), direction. Then the period cell V is denoted by $\Gamma \times \{z \in (0, 1)\}$.

The norm and the inner product on $L^2(V)$, where V is a periodic cell are denoted, respectively, by $\|\cdot\|$, $(\cdot, \cdot)$. For example, for two functions f and g we define

$$\|f\|^2 = \int_V f^2 dV,$$

and

$$(f, g) = \int_V f g dV.$$

The Kronecker delta δ_{ij} and the three dimensional Levi–Civita function ε_{ijk} are defined by

$$\delta_{ij} = \begin{cases} 1 & \text{if} \quad i = j, \\ 0 & \text{if} \quad i \neq j, \end{cases}$$

$$\varepsilon_{ijk} = \begin{cases} 1 & \text{if} \quad ijk = 123, 312, \text{ or } 231, \\ -1 & \text{if} \quad ijk = 132, 321, \text{ or } 213, \\ 0 & \text{if} \quad i = j \text{ or } j = k \text{ or } k = i, \end{cases}$$

In addition, we present some useful inequalities which are used in the energy stability theory as follows

1. The Cauchy–Schwarz inequality

$$(f, g) \leq \|f\| \, \|g\| \, .$$

2. The arithmetic–geometric mean inequality

    For $a, b \in \mathbb{R}$, with a constant weight $\alpha > 0$. Then

$$ab \leq \frac{1}{2\alpha} a^2 + \frac{\alpha}{2} b^2.$$

3. The Young's inequality

    For $a, b \in \mathbb{R}$, and $p, q \geq 1$ such that $1/p + 1/q = 1$. Then

$$ab \leq \frac{|a|^p}{p} + \frac{|b|^q}{q}.$$

4. The Poincaré inequality

    Let V be a three dimensional cell. Assume for simplicity V has dimensions $0 \leq x < 2a_1$, $0 \leq y < 2a_2$, and $0 < z < 1$, and assume u is a function periodic

in x, y, of period $2a_1$, $2a_2$, respectively, and $u = 0$ on $z = 0, 1$. Then the Poincaré inequality may be written as follows

$$\langle u_i u_i \rangle \leq \frac{1}{\pi^2} \langle u_{i,j} u_{i,j} \rangle \,,$$

where $\langle \cdot \rangle$ denotes integration over V. Alternatively this may be written as

$$\|\mathbf{u}\|^2 \leq \frac{1}{\pi^2} \|\nabla \mathbf{u}\|^2 \,.$$

1.2 Stability theory in porous media

Before proceeding to the body of the thesis and discussing the stability of the system of the thermal convection in porous media problems in some details we briefly clarify the linear instability and nonlinear stability theories used to find the stability threshold. For purposes of illustration, we provide an example of the Bénard problem for the Brinkman model, see Straughan [116].

Let us consider a layer of saturated porous material bounded by two horizontal planes $z = 0$ and $z = d$. We assume the porous medium occupies the three dimensional region $\{(x, y) \in \mathbb{R}^2\} \times \{z \in (0, d)\}$. The fluid is assumed to be incompressible. The Boussinesq approximation is adopted and so we write the density as

$$\rho(T) = \rho_0 \left[1 - \alpha \left(T - T_L \right) \right],$$

where T is temperature, ρ_0 is the density at T_L, and α is the thermal expansion coefficient. The governing system of equations incorporating fluid inertia for thermal convection according to the Brinkman model are as follows

$$\hat{a} v_{i,t} = -p_{,i} - \frac{\mu}{\mathrm{K}} v_i + \hat{\lambda} \Delta v_i - k_i g \rho(T),$$
$$v_{i,i} = 0, \tag{1.2.1}$$
$$T_{,t} + v_i T_{,i} = \kappa \Delta T,$$

where $\mathbf{v}, p, \mu, g$, and $\hat{a}$ are, respectively, velocity field, pressure, dynamic viscosity, gravity, and inertia coefficient. Additionally, K is the permeability, $\hat{\lambda}$ is referred to as an equivalent viscosity, and $\mathbf{k} = (0, 0, 1)$. The boundary conditions are

$$v_i = 0 \,, \qquad z = 0, d \,, \tag{1.2.2}$$

$$T = T_L, \qquad z = 0; \quad T = T_U, \ z = d, \tag{1.2.3}$$

where T_L, T_U are constants with $T_L > T_U$.

From the boundary conditions (1.2.2), the basic conduction solution, which is motionless, to (1.2.1) is $\mathbf{v} = 0$. Assuming that $T = T(z)$, and substituting these values into equations (1.2.1) yields

$$p_{,i} = -g\rho_0 \left[1 - \alpha \left(T - T_L\right)\right] k_i, \qquad (1.2.4)$$

$$\Delta T = 0. \qquad (1.2.5)$$

In fact T is a function of z only, then we may write (1.2.5) as

$$\frac{d^2 T}{dz^2} = 0. \qquad (1.2.6)$$

Upon integration (1.2.6) as a linear function and using the boundary conditions (1.2.2), we get

$$T = -\beta z + T_L, \qquad (1.2.7)$$

where

$$\beta = \frac{T_L - T_U}{d}.$$

Then, substituting equation (1.2.7) into equation (1.2.4) to obtain

$$p_{,i} = -gk_i \rho_0 \left[1 + \alpha\beta z\right].$$

An integration yields

$$\bar{p} = -gk_i x_i \rho_0 \left[1 + \frac{1}{2}\alpha k_j x_j\right],$$

then for $k_i = \delta_{i3}$, we see that

$$p = p_0 - g\rho_0 z - \frac{1}{2}\alpha\beta g\rho_0 z^2, \qquad (1.2.8)$$

where p_0 is the pressure at $z = 0$.

To study the stability of the steady conduction solutions $\left(\bar{\mathbf{v}}, \bar{T}, \bar{p}\right)$ we introduce a perturbation (u_i, ϑ, π) of the form

$$v_i = \bar{v}_i + u_i, \qquad T = \bar{T} + \vartheta, \qquad p = \bar{p} + \pi.$$

The nonlinear perturbation equations arising from (1.2.1) are

$$\hat{a} u_{i,t} = -\pi_{,i} - \frac{\mu}{\mathrm{K}} u_i + \hat{\lambda}\Delta u_i + k_i g\rho_0 \alpha\vartheta,$$

$$u_{i,i} = 0, \qquad (1.2.9)$$

$$\vartheta_{,t} + u_i \vartheta_{,i} = \beta w + \kappa\Delta\vartheta,$$

where $w = u_3$. We then introduce the non-dimensionalisations

$$x_i = dx_i^*, \quad u_i = \frac{\kappa}{d}u_i^*, \quad t = \frac{d^2}{\kappa}t^*, \quad \pi = \frac{\mu\kappa}{\mathrm{K}}\pi^*,$$

$$a_0 = \frac{\hat{a}\mathrm{K}}{\mu}, \quad \lambda = \mathrm{K}\hat{\lambda}/d^2\mu, \quad \vartheta = \sqrt{\frac{\beta\mu\kappa}{\mathrm{K}\rho_0\alpha\mathrm{g}}}\vartheta^*,$$

and the Rayleigh number $R_a = R^2$ is defined as

$$R^2 = \frac{d^2\rho_0 g\alpha\beta\mathrm{K}}{\mu\kappa}.$$

The non-dimensional perturbation equations arising from (1.2.9) are (dropping $*$'s)

$$a_0 u_{i,t} = -\pi_{,i} - u_i + \lambda\Delta u_i + R\vartheta k_i,$$

$$u_{i,i} = 0, \qquad\qquad (1.2.10)$$

$$\vartheta_{,t} + u_i\vartheta_{,i} = Rw + \Delta\vartheta.$$

The corresponding boundary conditions are

$$u_i = 0, \quad \vartheta = 0, \quad z = 0, 1, \qquad\qquad (1.2.11)$$

and u_i, ϑ, π satisfy a plane tiling periodicity in the x, y directions, we refer the reader to Chandrasekhar [19, p.43], and Straughan [115, p. 51].

1.3   Linear instability analysis

To find threshold for linear instability we first remove the nonlinear term of (1.2.10), and assume a time dependence like $u_i = u_i(\mathbf{x})\,e^{\sigma t}$, $\vartheta = \vartheta(\mathbf{x})\,e^{\sigma t}$, $\pi = \pi(\mathbf{x})\,e^{\sigma t}$, σ is a general eigenvalue. Upon substituting into equation (1.2.10) and removing of the exponential parts we arrive at the system

$$\sigma a_0 u_i = -\pi_{,i} - u_i + \lambda\Delta u_i + R\vartheta k_i,$$

$$u_{i,i} = 0, \qquad\qquad (1.3.1)$$

$$\sigma\vartheta = Rw + \Delta\vartheta.$$

In general $\sigma = \sigma_r + i\sigma_1$, $\sigma_r, \sigma_1 \in \mathbb{R}$. If in a system the growth rate $\sigma \in \mathbb{R}$ it said that the exchange of stabilities hold automatically. When $\sigma_1 \neq 0$ implies $\sigma_r < 0$, we say that the principle of exchange of stabilities holds and so the convection

mechanism commence as stationary convection. Whereas if $\sigma = i\sigma_1$ with $\sigma_1 \neq 0$, the convection mechanism sets in as oscillatory convection. When $\sigma > 0$ the solution grows exponentially in time and is unstable. Thus when exchange of stabilities holds we solve the linearised system for the smallest value of R^2 and it sufficient to consider the system for $\sigma = 0$.

Accordingly, we now multiply $(1.3.1)_1$ by u_i^*(the complex conjugate of u_i), $(1.3.1)_3$ by ϑ^*(the complex conjugate of ϑ) and integrate over V to obtain

$$\sigma a_0 \left\| \mathbf{u} \right\|^2 = - \left\| \mathbf{u} \right\|^2 - \lambda \left\| \nabla \mathbf{u} \right\|^2 + R(\vartheta, w^*), \tag{1.3.2}$$

$$\sigma \left\| \vartheta \right\|^2 = - \left\| \nabla \vartheta \right\|^2 + R(w, \vartheta^*). \tag{1.3.3}$$

Next, add (1.3.2) to (1.3.3) to find

$$\sigma(a_0 \left\| \mathbf{u} \right\|^2 + \left\| \vartheta \right\|^2) = - \left\| \mathbf{u} \right\|^2 - \lambda \left\| \nabla \mathbf{u} \right\|^2 - \left\| \nabla \vartheta \right\|^2 + R[(\vartheta, w^*) + (w, \vartheta^*)]. \tag{1.3.4}$$

The imaginary part of the foregoing equation yields

$$\sigma_1(a_0 \left\| \mathbf{u} \right\|^2 + \left\| \vartheta \right\|^2) = 0.$$

Thus, $\sigma_1 = 0$ and so $\sigma \in \mathbb{R}$. Therefore, the principle of exchange of stabilities holds and it is sufficient to set $\sigma = 0$ into equation (1.3.1) to find instability boundary. The system (1.3.1) may be reduced to

$$\pi_{,i} = - u_i + \lambda \Delta u_i + R\vartheta k_i,$$
$$u_{i,i} = 0, \tag{1.3.5}$$
$$0 = Rw + \Delta \vartheta.$$

We now take curl curl of equation $(1.3.5)_1$ and retain the third component to obtain

$$\Delta w = \lambda \Delta^2 w + R \Delta^* \vartheta,$$
$$0 = Rw + \Delta \vartheta, \tag{1.3.6}$$

where $\Delta^* = \partial^2/\partial x^2 + \partial^2/\partial y^2$ is the horizontal Laplacian operator.

Assuming a normal mode representation of w and ϑ of the form

$$w = W(z)f(x, y), \qquad \vartheta = \Theta(z)f(x, y),$$

where $f(x, y)$ is a planform which tiles the plan (x, y) with $\Delta^* f = -a^2 f$, where a is the horizontal wave number, see Straughan [115]. Upon applying the normal mode representation to equation (1.3.6), one arrives at

$$
\begin{aligned}
\left(D^2 - a^2\right) W &= \lambda \left(D^2 - a^2\right)^2 W - a^2 R\Theta, \\
0 &= RW + \left(D^2 - a^2\right)\Theta,
\end{aligned}
\tag{1.3.7}
$$

where $D = d/dz$. The corresponding boundary conditions are

$$
W = \Theta = 0, \quad \text{at } z = 0, 1.
\tag{1.3.8}
$$

To solve this system we need two more conditions with respect to which we consider solutions of system for either fixed surfaces or free surfaces. If either one is fixed then the system would have to be solved numerically by using efficient techniques, namely the compound matrix method, and the D^2 Chebyshev tau method. In case we consider two stress free surfaces we need further boundary conditions. To illustrate, we begin by imposing the following boundary condition

$$
D^2 W = 0, \quad \text{at } z = 0, 1.
\tag{1.3.9}
$$

Next, we eliminate the variable Θ from equation (1.3.7) to have sixth order ordinary differential equation

$$
\lambda \left(D^2 - a^2\right)^3 W - \left(D^2 - a^2\right)^2 W + a^2 R^2 W = 0,
\tag{1.3.10}
$$

and from equations (1.3.7), (1.3.8), and (1.3.9) we find

$$
W = D^2 W = D^4 W = 0, \quad \text{at } z = 0, 1.
$$

Applying these boundary conditions to equation (1.3.10) yield

$$
D^6 W = 0, \quad \text{at } z = 0, 1.
$$

By further differentiation of (1.3.10), an even number of times with respect to z, and this may be repeated to deduce

$$
D^{(2n)} W = 0, \quad at\ z = 0, 1, \quad \text{for } n = 0, 1, \dots.
\tag{1.3.11}
$$

From this it follows that $W(z)$ is taken as $\sin n\pi z$, for $n \in \mathbb{N}$. Hence equation (1.3.10) leads to

$$R^2 = \frac{\lambda \left(n^2\pi^2 + a^2\right)^3 + \left(n^2\pi^2 + a^2\right)^2}{a^2}. \tag{1.3.12}$$

To find the lowest value of R, we minimise the Rayleigh number $R^2 = R^2(n^2, a^2)$. Hence, the minimum occurs when $n = 1$. By calculating dR^2/da^2 we then obtain

$$a_c^2 = \frac{-\left(\lambda\pi^2 + 1\right) + \left(\lambda\pi^2 + 1\right)\sqrt{1 + 8\pi^2\lambda/\left(\lambda\pi^2 + 1\right)}}{4\lambda}.$$

When $\lambda \to 0$ and then $a_c^2 = \pi^2$, $R_c^2 = 4\pi^2$ we recover the result for Darcy model. Also as $\lambda \to \infty$, $a_c^2 = \dfrac{\pi^2}{2}$ and $R_c^2 = \dfrac{27\pi^2}{4}$ as in the fluid case.

It is noteworthy that the linear instability theory only provides a boundary for instability, i.e. for which all Rayleigh number R greater than the critical Rayleigh number result in instability, but it yields no information on stability when the Rayleigh number below this boundary. The solution of the nonlinear system possibly becomes unstable before the stability boundary for values $R < R_c$, therefore subcritical stability may arise. However, nonlinear methods must be performed [113].

1.4 Nonlinear stability analysis

To investigate the possibility of obtaining global nonlinear instability, we multiply $(1.2.10)_1$ by u_i and $(1.2.10)_3$ by ϑ, and integrate the results over V using (1.2.11) to obtain

$$\frac{a_0}{2}\frac{d}{dt}\|\mathbf{u}\|^2 = -\|\mathbf{u}\|^2 - \lambda\|\nabla\mathbf{u}\|^2 + R(\vartheta, w), \tag{1.4.1}$$

$$\frac{1}{2}\frac{d}{dt}\|\vartheta\|^2 = -\|\nabla\vartheta\|^2 + R\left(\vartheta, w\right). \tag{1.4.2}$$

We introduce a positive coupling parameter $\hat{\xi}$. Upon addition of (1.4.1) and $\hat{\xi}$(1.4.2) one finds

$$\frac{dE}{dt} = RI - D, \tag{1.4.3}$$

where

$$E(t) = \tfrac{1}{2}(a_0 \left\|\mathbf{u}\right\|^2 + \hat{\xi} \left\|\vartheta\right\|^2), \tag{1.4.4}$$

$$I = (1 + \hat{\xi})(\vartheta, w), \tag{1.4.5}$$

$$D = \left\|\mathbf{u}\right\|^2 + \lambda \left\|\nabla\mathbf{u}\right\|^2 + \hat{\xi} \left\|\nabla\vartheta\right\|^2. \tag{1.4.6}$$

To proceed from (1.4.3), define R_E by

$$\frac{1}{R_E} = \max_{\mathcal{H}} \frac{I}{D}, \tag{1.4.7}$$

where $\mathcal{H} = \{u_i, \vartheta | u_i \in H^1(V), \vartheta \in H^1(V), u_{i,i} = 0, u_i, \vartheta \text{ are periodic in } x, y\}$, is the space of admissible functions. It now follows from (1.4.3) that (cf. Straughan [113])

$$\frac{dE}{dt} \leq -D\left(1 - \frac{R}{R_E}\right). \tag{1.4.8}$$

Thus, provided $R < R_E$, put $\hat{c} = \left(1 - \dfrac{R}{R_E}\right) > 0$, and from the Poincaré inequality

$$D \geq \pi^2 \lambda \left\|\mathbf{u}\right\|^2 + \hat{\xi}\pi^2 \left\|\vartheta\right\|^2.$$

Hence, from (1.4.8) where $\lambda = a_0$,

$$\frac{dE}{dt} \leq -2\pi^2 \hat{c} E(t).$$

By integration and rearranging

$$E(t) \leq e^{-2\pi^2 \hat{c}t} E(0).$$

Thus, one deduces exponential decay of $E(t)$ and hence global nonlinear stability follows provided $R_E > R$. To complete the analysis we derive the Euler–Lagrange equations for (1.4.7). To this end, we rescale ϑ to $\sqrt{\hat{\xi}}\vartheta$ and put $g(\hat{\xi}) = \left(1 + \hat{\xi}\right)/2\sqrt{\hat{\xi}}$. Then the maximum problem (1.4.7) is

$$\frac{1}{R_E} = \max_{\mathcal{H}} \frac{g(\hat{\xi})(\vartheta, w)}{\left\|\mathbf{u}\right\|^2 + \lambda \left\|\nabla\mathbf{u}\right\|^2 + \left\|\nabla\vartheta\right\|^2}.$$

The Euler-Lagrange equations arising from (1.4.7) are determined from

$$R_E \delta I - \delta D = 0. \tag{1.4.9}$$

This can be calculated by using calculus of variations technique, we refer the reader to Courant and Hilbert [27].

Let consider the solution of the form $u_i + \varepsilon h_i$ and $\vartheta + \varepsilon \eta$ where ε is constant, and h_i, η arbitrary functions which satisfy the boundary conditions $h_i = \eta = 0$ on ∂V. Hence

$$\delta I = \left. \frac{d}{d\varepsilon} \int_V \left(g(\hat{\xi})(\vartheta + \varepsilon\eta)(w + \varepsilon h_3) - 2\pi(u_{i,i} + \varepsilon h_{i,i}) \right) dV \right|_{\varepsilon=0},$$

$$= \left. \int_V \left(g(\hat{\xi}) \left(\eta(w + \varepsilon h_3) + h_3(\vartheta + \varepsilon\eta) \right) - 2h_{i,i}\pi \right) dV \right|_{\varepsilon=0},$$

and

$$\delta D = \left. \frac{d}{d\varepsilon} \int_V \left((u_i + \varepsilon h_i)^2 + \lambda(\nabla(u_i + \varepsilon h_i))^2 + (\nabla(\vartheta + \varepsilon\eta))^2 \right) dV \right|_{\varepsilon=0},$$

$$= \left. \int_V \left(2h_i(u_i + \varepsilon h_i) + 2\lambda \left(\nabla(u_i + \varepsilon h_i)\nabla h_i \right) + 2 \left(\nabla(\vartheta + \varepsilon\eta)\nabla\eta \right) \right) dV \right|_{\varepsilon=0},$$

where the constraint $u_{i,i} = 0$ is included and π is now a Lagrange multiplier. After some integrations by parts, one finds

$$\delta I = \int_V \left(g(\hat{\xi}) \left(\eta w + h_3 \vartheta \right) - 2h_i \pi_{,i} \right) dV,$$

$$\delta D = \int_V (2u_i h_i - 2\lambda \Delta u_i h_i - 2\eta \Delta \vartheta) dV.$$

Since h_i and η were chosen arbitrary functions, hence from equation (1.4.9) we must have

$$R_E \frac{g(\hat{\xi})}{2} \vartheta k_i - u_i + \lambda \Delta u_i = \pi_{,i},$$

$$u_{i,i} = 0, \tag{1.4.10}$$

$$R_E \frac{g(\hat{\xi})}{2} w + \Delta \vartheta = 0.$$

The idea is now to use the parametric differentiation method to find the optimal value of $\hat{\xi}$ which maximises R_E. Thus put $g(\hat{\xi})/2 = \zeta$, and let $(R_E^1, u_i^1, \vartheta^1, \pi^1)$ be a solution to the eigenvalue problem arising from equation (1.4.10) on V for $\hat{\xi} = \hat{\xi}^1 > 0$, and likewise let $(R_E^2, u_i^2, \vartheta^2, \pi^2)$ be a solution for $\hat{\xi} = \hat{\xi}^2 > 0$, $\hat{\xi}^1 \neq \hat{\xi}^2$.

Now multiply equations $(1.4.10)_1$ by u_i^1 holding for $\hat{\xi} = \hat{\xi}^2$, $(1.4.10)_1$ by u_i^2 holding for $\hat{\xi} = \hat{\xi}^1$, $(1.4.10)_3$ by ϑ^1 holding for $\hat{\xi} = \hat{\xi}^2$, and $(1.4.10)_3$ by ϑ^2 holding for $\hat{\xi} = \hat{\xi}^1$. After integration over V we find

$$R_E^2 \zeta^2 \left(\vartheta^2, w^1\right) - \left(u_i^2, u_i^1\right) - \lambda \left(\nabla u_i^2, \nabla u_i^1\right) = 0, \tag{1.4.11}$$

$$R_E^1 \zeta^1 \left(\vartheta^1, w^2\right) - \left(u_i^1, u_i^2\right) - \lambda \left(\nabla u_i^1, \nabla u_i^2\right) = 0, \tag{1.4.12}$$

$$R_E^2 \zeta^2 \left(w^2, \vartheta^1\right) - \left(\nabla \vartheta^2, \nabla \vartheta^1\right) = 0, \tag{1.4.13}$$

$$R_E^1 \zeta^1 \left(w^1, \vartheta^2\right) - \left(\nabla \vartheta^1, \nabla \vartheta^2\right) = 0. \tag{1.4.14}$$

Next, combine (1.4.11) - (1.4.12) + (1.4.13) - (1.4.14) to obtain

$$\left(R_E^2 \zeta^2 - R_E^1 \zeta^1\right) \left[\left(w^1, \vartheta^2\right) + \left(w^2, \vartheta^1\right)\right] = 0.$$

Now, we write $(R_E^2 \zeta^2 - R_E^1 \zeta^1) = (R_E^2 \zeta^2 - R_E^2 \zeta^1) + (R_E^2 \zeta^1 - R_E^1 \zeta^1)$, and recall $\hat{\xi}^1 \neq \hat{\xi}^2$, divide by $\hat{\xi}^2 - \hat{\xi}^1 \neq 0$. Thus we have

$$\left[\frac{R_E^2 \left(\zeta^2 - \zeta^1\right)}{\hat{\xi}^2 - \hat{\xi}^1} + \frac{\zeta^1 \left(R_E^2 - R_E^1\right)}{\hat{\xi}^2 - \hat{\xi}^1}\right] \left[\left(w^1, \vartheta^2\right) + \left(w^2, \vartheta^1\right)\right] = 0.$$

Take the limit $\hat{\xi}^2 \to \hat{\xi}^1$, this leads to

$$\left[R_E \frac{\partial \zeta}{\partial \hat{\xi}} + \zeta \frac{\partial R_E}{\partial \hat{\xi}}\right] (w, \vartheta) = 0. \tag{1.4.15}$$

Here R_E^1, ζ^1, w^1, and ϑ^1 are replaced by R_E, ζ, w, and ϑ.

Then we multiply equations $(1.4.10)_1$ by u_i, $(1.4.10)_3$ by ϑ, add the result and integrate by parts to obtain

$$R_E \left(g(\hat{\xi})\right) (w, \vartheta) = \|\mathbf{u}\|^2 + \lambda \|\nabla \mathbf{u}\|^2 + \|\nabla \vartheta\|^2$$

By substituting into the equation (1.4.15) for (w, ϑ), one may deduces

$$\left[\frac{\|\mathbf{u}\|^2 + \lambda \|\nabla \mathbf{u}\|^2 + \|\nabla \vartheta\|^2}{g(\hat{\xi}) R_E}\right] \left[R_E \frac{\partial g(\hat{\xi})}{\partial \hat{\xi}} + g(\hat{\xi}) \frac{\partial R_E}{\partial \hat{\xi}}\right] = 0. \tag{1.4.16}$$

The maximum value of R_E satisfies $\partial R_E / \partial \hat{\xi} = 0$, and so $\partial g / \partial \hat{\xi} = 0$ gives the best value of $\hat{\xi}$. Thus the optimal value of $\hat{\xi}$ is $\hat{\xi} = 1$, with $\hat{\xi} = 1$ equation (1.4.10) becomes

$$R_E \vartheta k_i - u_i + \lambda \Delta u_i = \pi_{,i},$$

$$u_{i,i} = 0, \tag{1.4.17}$$

$$R_E w + \Delta \vartheta = 0.$$

These equations (1.4.17) are the same as equations (1.3.5). This means that for all initial data the linear instability boundary coincides with the nonlinear stability one, therefore no subcritical instability may arise.

We now commence with the new results obtained in this thesis. In Part I, Chapters 2–4, we concentrate on convection problems in porous media, taking into account second sound, i.e. thermal waves. Part II, Chapters 5–7, concentrates on thermal convection in anisotropic porous media.

Part I. Thermal convection with Cattaneo theories

The propagation of thermal waves (second sound) is of particular importance to the field continuum mechanics, see e.g., Straughan [121, chap. 9]. The investigation of the effect of thermal wave on the onset of convection instability by generalising the Fourier law for heat conduction was initiated by Straughan and Franchi [110]. Some other investigations are due to Lebon and Cloot [65], Franchi and Straughan [38], and Vadasz et al. [134].

Recently, Straughan [117–120], adapted an objective derivative for the heat flux to study thermal convection in a fluid and in fluid saturated Darcy porous media. In this Part we investigate the effect of thermal waves on the onset convection instability in a fluid saturated porous medium. In particular, we present the case of employing an objective derivative, namely, the Cattaneo-Fox and the Cattaneo-Christov derivatives for the heat flux (see Appendix A.1). Also, we present the linear instability theory to establish the instability boundary for a horizontal layer of both Darcy and Brinkman porous material saturated with an incompressible Newtonian fluid.

The layout of this Part is as follows. In Chapter 2 we develop a theory for thermal convection in a fluid saturated porous material when the temperature may propagate as a thermal wave. In particular, we are interested in the mechanism of thermal oscillation and so allow for Guyer-Krumhansl effects but employ a heat flux equation developed by Christov and by Morro. We show that the inclusion Guyer-Krumhansl terms have a pronounced effect on the convection mechanism. The work in this chapter has been published in Haddad and Straughan [45].

In Chapter 3 we investigate a model of the coupled Guyer-Krumhansl equation with the Cattaneo-Fox law for the temperature and heat flux fields (see Appendix A.2) to study thermal convection in a fluid saturated Darcy porous material. By performing the linear instability analysis we find a range of the Guyer-Krumhansl values which allow transition from oscillatory convection to stationary convection with narrower cells. The work in this chapter has been published in Haddad [46]

Chapter 4 is devoted to the study the thermal instability in a saturated porous material of Brinkman type. We describe the linear instability analysis to find the lowest instability boundary for two free surfaces. For two fixed surfaces , the D^2 Chebyshev tau method (see Appendix B) is used to solve the eigenvalue problem which arises in linear instability analysis. We discuss the effects of the presence of the Brinkman term, inertia term, and other parameters on the onset of thermal instability. The work in this chapter has been published in Haddad [47]

Chapter 2

Porous convection and thermal oscillations

Recently it has been suggested that the phenomenon of "heat waves" or "second sound" may radically alter predictions for convection in porous body and this may have a profound effect on star formation and stellar evolution, see Herrera and Falcón [49], Falcón [35], Straughan [117, 120], and the account in Section 9.2.2 of the book by Straughan [121]. At the same time, phonon oscillations are believed to be a key ingredient in assisting heat transport by a temperature wave procedure, as witnessed in the recent work of Cimmelli et al. [26], Jou et al. [54], Jou et al. [55], Sellitto et al. [102, 103], see also the work of Cimmelli et al. [25]. To incorporate phonon oscillations the cited articles employ a heat flux equation which originates from work of Guyer and Krumhansl [42–44].

The objective of this Chapter is to develop and analyse a model for thermal convection in a fluid saturated porous medium when the heat flux satisfies an equation of Guyer - Krumhansl type. In order to achieve this we employ Christov's [21] derivative for the heat flux, a rigorous thermodynamical basis for which has been presented by Morro [77,78] who also includes Guyer-Krumhansl terms. We take this opportunity to point out that the Christov formulation has been employed in acoustic wave analysis by Straughan [119], and analytical properties of the solution to the Christov-Morro equations are presented by Ciarletta and Straughan [23], Ciarletta et al. [24], and by Tibullo and Zampoli [125].

In the next section, we present the appropriate equations for thermal convection in a fluid saturated porous material.

2.1 Basic equations

The fluid velocity in the porous medium satisfies a Darcy law of form, cf. Vadasz [131], Straughan [114],

$$\hat{a}v_{i,t} = -p_{,i} - \frac{\mu}{\mathrm{K}}v_i + k_i g\rho_0\alpha T, \tag{2.1.1}$$

$$v_{i,i} = 0, \tag{2.1.2}$$

where $\mathbf{v}$ is the velocity field, p is the pressure, T is temperature, $\hat{a}$ is an inertia coefficient, μ is the dynamic viscosity, K is the permeability, $\mathbf{k} = (0,0,1)$, g is gravity, α is the thermal expansion coefficient of the fluid, and ρ_0 is the constant density assuming the Boussinesq approximation has been employed to derive (2.1.1).

To complete the system of equations requires a suitable balance law for the temperature field. To this end we derive an energy balance equation together with the Christov [21], Morro [77, 78] equations for the heat flux. The procedure is as in Straughan [117, 120] or Straughan [121], Chapter 8, where we write separate equations for the fluid part of the porous medium by

$$(\rho_o c_p)_f(T_{,t} + V_i T_{,i}) = -Q_{i,i}, \tag{2.1.3}$$

$$\tau_f(Q_{i,t} + V_j Q_{i,j} - Q_j V_{i,j}) = -Q_i - \kappa_f T_{,i} + (\xi_1)_f \Delta Q_i + (\xi_2)_f Q_{k,ki}, \tag{2.1.4}$$

and for solid part by

$$(\rho_o c)_s T_{,t} = -Q_{i,i}, \tag{2.1.5}$$

$$\tau_s Q_{i,t} = -Q_i - \kappa_s T_{,i} + (\xi_1)_s \Delta Q_i + (\xi_2)_s Q_{k,ki}, \tag{2.1.6}$$

where Q_i denotes the heat flux, c_p is the specific heat at constant pressure in the fluid, c refers to the specific heat in the porous medium, κ the thermal diffusivity. Here τ being relaxation times, and ξ_1 and ξ_2 are Guyer-Krumhansl terms derived by Morro [77, 78], f refers to fluid and s denotes the solid skeleton of the porous medium.

To derive equations for the porous medium as a combined unit, we multiply equations governing fluid part (2.1.3), and (2.1.4) by φ and equations governing solid part (2.1.5), and (2.1.6) by $(1 - \varphi)$ and combine them suitably so that

$$(\rho_o c)_m T_{,t} + (\rho_o c_p)_f v_i T_{,i} = -Q_{i,i}, \tag{2.1.7}$$

$$\tau Q_{i,t} + \tau_f (v_j Q_{i,j} - Q_j v_{i,j}) = -Q_i - k_m T_{,i} + (\xi_1)_m \Delta Q_i + (\xi_2)_m Q_{k,ki}, \tag{2.1.8}$$

where V_i is the fluid velocity averaged over the fluid phase so that with φ being porosity, $v_i = \varphi V_i$ is the average of the fluid velocity over the fluid and solid phases, and $\tau = \varphi \tau_f + (1 - \varphi) \tau_s$, m refers to the porous medium where the coefficients k_m, $(\rho_o c)_m$, $(\xi_1)_m$, and $(\xi_2)_m$ are given by

$$k_m = \kappa_s (1 - \varphi) + \kappa_f \varphi,$$

$$(\rho_o c)_m = \varphi (\rho_0 c_p)_f + (\rho_0 c)_s (1 - \varphi),$$

$$(\xi_1)_m = \varphi (\xi_1)_f + (\xi_1)_s (1 - \varphi),$$

$$(\xi_2)_m = \varphi (\xi_2)_f + (\xi_2)_s (1 - \varphi).$$

We divide equation (2.1.7) by $(\rho_0 c_p)_f$ and redefine Q_i to be $Q_i / (\rho_0 c_p)_f$. Further, denote by

$$M = \frac{(\rho_0 c_p)_f}{(\rho_0 c)_m}, \qquad \kappa = \frac{k_m}{(\rho_0 c_p)_f},$$

and for simplicity call $(\xi_1)_m$ and $(\xi_2)_m$ simply ξ_1, ξ_2. Then equations (2.1.7) and (2.1.8) become

$$\frac{1}{M} T_{,t} + v_i T_{,i} = -Q_{i,i}, \tag{2.1.9}$$

$$\tau Q_{i,t} + \tau_f (v_j Q_{i,j} - Q_j v_{i,j}) = -Q_i - \kappa T_{,i} + \xi_1 \Delta Q_i + \xi_2 Q_{k,ki}. \tag{2.1.10}$$

We suppose the fluid saturated porous medium satisfies equations (2.1.1), (2.1.2), (2.1.9), and (2.1.10), and occupies the spatial domain $\Omega = \{(x, y) \in \mathbb{R}^2\} \times \{z \in (0, d)\}$, and let $\mathbf{n}$ is the unit outward so that $\mathbf{n} = (0, 0, 1)$ on $z = d$ and $\mathbf{n} = (0, 0, -1)$ on $z = 0$. The boundary conditions are

$$v_i n_i = 0, \qquad \text{at } z = 0, d,$$

$$T = T_L, \ z = 0; \quad T = T_U, \ z = d, \tag{2.1.11}$$

where T_L, T_U are constants with $T_L > T_U$. In addition the heat flux satisfies

$$\varepsilon_{ijk} n_j Q_k = 0, \qquad z = 0, d, \tag{2.1.12}$$

cf. Straughan [121], p. 193. System (2.1.1), (2.1.2), (2.1.9), (2.1.10), and (2.1.11), (2.1.12) possesses the steady conduction solution

$$\bar{v}_i \equiv 0, \qquad \bar{T} = -\beta z + T_L, \qquad \bar{\mathbf{Q}} = (0, 0, \kappa\beta),$$

$$\bar{p} = p_0 - g\rho_0 z - \frac{1}{2}\alpha\beta g\rho_0 z^2, \tag{2.1.13}$$

where

$$\beta = \frac{T_L - T_U}{d}.$$

To investigate the stability of this solution, we introduce perturbations to $\bar{v}_i$, $\bar{T}$, $\bar{Q}_i$ by putting

$$v_i = \bar{v}_i + u_i, \qquad T = \bar{T} + \vartheta, \qquad Q_i = \bar{Q}_i + q_i$$

and we derive equations for the perturbations $(u_i, \vartheta, q_i, \pi)$ where π is the pressure perturbation. The perturbation equations are non-dimensionalised with the scalings (see [117, 120, 121]),

$$\mathbf{x} = d\mathbf{x}^*, \qquad \mathbf{u} = \frac{\mu d}{\rho_0 K}\mathbf{u}^*, \qquad \mathbf{q} = \kappa U \sqrt{\frac{\beta\mu}{K\rho_0\alpha g\kappa}}\mathbf{q}^*,$$

$$t = \frac{K\rho_0}{\mu}t^*, \qquad \pi = \frac{\mu U d}{K}\pi^*, \qquad \vartheta = dU\sqrt{\frac{\beta\mu}{\kappa\rho_0\alpha g K}}\vartheta^*,$$

where U is a velocity scale, although additionally we here require non-dimensional equivalents of $\hat{a}$, ξ_1 and ξ_2 by scalings

$$\hat{a} = \rho_0 a^*, \qquad \xi_1 = d\xi_1^*, \qquad \xi_2 = d\xi_2^*.$$

In terms of the Prandtl number $Pr = \mu/\rho_0\kappa$ and the key non-dimensional numbers

$$R = \sqrt{\frac{\alpha g d^2 \beta K\rho_0}{\mu\kappa}}, \qquad Da = \frac{K}{d^2}, \qquad Sg = \frac{\tau\mu}{\rho_0 d^2}, \qquad \hat{\tau} = \frac{\tau_f}{\tau}$$

we derive a non-dimensional set of equations for the perturbation variables $(u_i, \vartheta, q_i, \pi)$. In the above $R = \sqrt{Ra}$ where Ra is the Rayleigh number, Da is the Darcy number, Sg is a parameter introduced in Papanicolaou et al. [85], and $\hat{\tau}$ is a relative relaxation time.

The non-dimensional perturbation equations are (omitting the stars)

$$Au_{i,t} = -\pi_{,i} + Rk_i\vartheta - u_i, \tag{2.1.14}$$

$$u_{i,i} = 0, \tag{2.1.15}$$

$$\frac{Pr}{Da}(\frac{1}{M}\vartheta_{,t} + u_i\vartheta_{,i}) = Rw - q_{i,i}, \tag{2.1.16}$$

$$\frac{Sg}{Da}q_{i,t} + \frac{\hat{\tau}Sg}{Da}(u_jq_{i,j} - q_ju_{i,j}) = -q_i - \vartheta_{,i} + \frac{\hat{\tau}SgR}{Pr}u_{i,z}$$

$$+\lambda_1\Delta q_i + \lambda_2 q_{j,ji}, \tag{2.1.17}$$

where $w = u_3$ and A, λ_1, λ_2 are non-dimensional equivalents of $\hat{a}$, ξ_1 and ξ_2. Equations (2.1.14)-(2.1.17) hold on $\{(x,y) \in R^2\} \times \{z \in (0,1)\} \times \{t > 0\}$ and the boundary conditions are

$$u_in_i = 0, \qquad \vartheta = 0, \qquad \varepsilon_{ijk}n_jq_k = 0, \qquad z = 0, 1, \tag{2.1.18}$$

with $\{u_i, \vartheta, q_i, \pi\}$ satisfying a plane tiling periodicity in (x,y).

2.2 Linear instability

We now take the divergence of equations (2.1.17), put $Q = q_{i,i}$, and then analyse the linear system

$$Au_{i,t} + u_i = -\pi_{,i} + Rk_i\vartheta,$$

$$u_{i,i} = 0,$$

$$\frac{Pr}{MDa}\vartheta_{,t} = Rw - Q, \tag{2.2.1}$$

$$\frac{Sg}{Da}Q_{,t} = -Q - \Delta\vartheta + \lambda\Delta Q,$$

where we have put $\lambda = \lambda_1 + \lambda_2$. It is convenient to define P_1 and P_2 by

$$P_1 = \frac{Pr}{MDa}, \qquad P_2 = \frac{Sg}{Da}, \tag{2.2.2}$$

and then remove the π term by take curl curl to equation $(2.2.1)_1$. We then seek a time dependence like $e^{\sigma t}$, i.e. we put

$$w = w(\mathbf{x})e^{\sigma t}, \qquad \vartheta = \vartheta(\mathbf{x})e^{\sigma t}, \qquad Q = Q(\mathbf{x})e^{\sigma t},$$

and from equations (2.2.1) we have to solve the system

$$(\sigma A + 1)\Delta w = R\,\Delta^*\vartheta,$$

$$\sigma P_1 \vartheta = Rw - Q, \qquad (2.2.3)$$

$$\sigma P_2 Q = -Q - \Delta\vartheta + \lambda\Delta Q,$$

where $\Delta^* = \partial^2/\partial x^2 + \partial^2/\partial y^2$.

To analyse equations (2.2.3) we use standard methods, cf. Chandrasekhar [19]. Firstly we set $\sigma = 0$ to derive the stationary convection boundary. The foregoing equations lead to

$$\Delta w = R\,\Delta^*\vartheta,$$

$$Rw = Q, \qquad (2.2.4)$$

$$Q - \lambda\Delta Q = -\Delta\vartheta.$$

Upon eliminating ϑ and Q from equation (2.2.4), we have a fourth order ordinary differential equation of the form

$$\Delta^2 w + R^2\,\Delta^*(w - \lambda\Delta w) = 0. \qquad (2.2.5)$$

We introduce single mode solution to equation (2.2.5) to be $w = W(z)f(x,y)$ where f is a plane tiling function satisfying $\Delta^* f = -a^2 f$. The Laplace operator $\Delta = D^2 - a^2$, where $D = d/dz$ and a is a wavenumber, c.f Chandrasekhar [19], and Straughan [116].

Applying the normal mode to the equation (2.2.5) one may show

$$R^2 = \frac{\Lambda_n^2}{a^2\left[1 + \lambda\Lambda_n\right]},$$

where $\Lambda_n = n^2\pi^2 + a^2$. Then one shows $\partial R^2/\partial n^2 > 0$, so we may consider

$$R^2 = \frac{\Lambda^2}{a^2\left(1 + \lambda\Lambda\right)},$$

where Λ denotes Λ_1. Now minimizing in a^2 yields the stationary convection boundary as

$$R_{sc}^2 = \frac{4\pi^2}{(1 + \lambda\pi^2)^2}, \qquad (2.2.6)$$

together with the critical wave number a_c as given by

$$a_c^2 = \frac{\pi^2(1 + \lambda\pi^2)}{(1 - \lambda\pi^2)}. \qquad (2.2.7)$$

Clearly, equation (2.2.7) requires that $\lambda < 1/\pi^2$. Henceforth we assume the non-dimensional Guyer-Krumhansl coefficient λ satisfies this restriction, so that

$$\lambda < \frac{1}{\pi^2} \simeq 0.101321183. \qquad (2.2.8)$$

To investigate oscillatory convection we follow the Chandrasekhar [19] procedure and put $\sigma = i\sigma_1$ in (2.2.3), where $\sigma_1 \in \mathbb{R}$. This leads to the simulations equations

$$\sigma_1^2 \left[-P_1 P_2 \Lambda - A P_1 \Lambda (1 + \lambda \Lambda) \right] + \Lambda^2 = R^2 a^2 (1 + \lambda \Lambda),$$

$$\sigma_1^2 \left[A P_1 P_2 \Lambda \right] - \left[A \Lambda^2 + \Lambda P_1 (1 + \lambda \Lambda) \right] = -P_2 a^2 R^2. \qquad (2.2.9)$$

These equations in turn yield

$$R^2 = C_3 \frac{\Lambda^3}{a^2} + C_2 \frac{\Lambda^2}{a^2} + C_1 \frac{\Lambda}{a^2}, \qquad (2.2.10)$$

and

$$\sigma_1^2 = \frac{\Lambda}{P_1 P_2} - \frac{A \Lambda (1 + \lambda \Lambda)}{P_1 P_2^2} - \frac{(1 + \lambda \Lambda)^2}{P_2^2}, \qquad (2.2.11)$$

where the coefficients $C_1, \cdots, C_3$ are given by,

$$C_1 = \frac{A P_1}{P_2^2} + \frac{P_1}{P_2}, \qquad (2.2.12)$$

$$C_2 = \frac{A^2}{P_2^2} + \frac{2\lambda A P_1}{P_2^2} + \frac{\lambda P_1}{P_2}, \qquad (2.2.13)$$

$$C_3 = \frac{\lambda A^2}{P_2^2} + \frac{\lambda^2 A P_1}{P_2^2}. \qquad (2.2.14)$$

The oscillatory convection Rayleigh number R_{osc}^2 is found by minimizing R^2 in (2.2.10) over a^2 , but simultaneously requiring $\sigma_1^2 > 0$ in (2.2.11). We have not seen how to do the minimization in (2.2.10) by analytical means and do so numerically by using Maple(TM) [1]. It is straightforward to show $d^2 R^2 / db^2 > 0$ where $b = a^2$ and so since R^2 is convex in a^2 the minimum found is unique and so yields the true oscillatory convection minimum. We observe that from (2.2.11) σ_1^2 cannot be positive for all wave numbers and thus the situation is very different from the Cattaneo-Christov case studied by Straughan [117] where $\lambda = 0$ and no Guyer-Krumhansl terms are present. In fact in the numerical results section we see that

---

[1]Maple is a trademark of Waterloo Maple Inc

the Guyer-Krumhansl terms play an important role in determining the convection instability threshold.

Remark.

For the zero inertia case, $A = 0$, equation (2.2.10) may be minimized analytically. For, then

$$R^2 = \frac{P_1}{P_2} \left(\lambda \frac{\Lambda^2}{a^2} + \frac{\Lambda}{a^2} \right),$$

and so the critical wave number and oscillatory convection Rayleigh number are given by

$$a_c^2 = \frac{\pi}{\sqrt{\lambda}} \left(1 + \lambda \pi^2 \right)^{1/2},$$

$$R_{osc}^2 = \frac{P_1}{P_2} \left(2\pi\sqrt{\lambda}\sqrt{1 + \lambda\pi^2} + 1 + 2\lambda\pi^2 \right).$$

In this case σ_1^2 is found to be

$$\sigma_1^2 = \frac{\Lambda}{P_1 P_2} - \frac{(1 + \lambda\Lambda)^2}{P_2^2},$$

and using the critical value of a_c^2 , we can easily find σ_1^2 at criticality. This clearly confirms σ_1^2 cannot be positive for all wave numbers in the zero inertia case, and indeed, shows oscillatory convection will not occur unless P_2 is sufficiently large.

2.3   Numerical results

In terrestrial situations we do expect stationary convection will be the dominant mechanism of instability. To see this we note that Straughan [121] , p. 253, reports values of τ in the range $(10^{-13}s, 10^{-11}s)$ and this will yield a P_2 value relatively small as compared to P_1. From equations (2.2.10) and (2.2.11) we do not expect to witness oscillatory convection in this situation. Nevertheless, Herrera and Falcón [49] do suggest that oscillatory convection may be dominant in certain binary system stars. This is further developed for white-dwarf and neutron stars by Falcón [35]. Therefore, we believe there is reason to analyse our model for P_2 values which are much larger than those believed witnessed in mundane situations.

We report only numerical findings when oscillatory convection is dominant. We select $P_1 = 6$ and choose $P_2 = 2.8, 4$ and 10 to see the variation. Due to restriction

(2.2.8) on λ we concentrate on values of $\lambda \in [0, 0.09]$. From Figure 2.1 we see that when $P_1 = 6$, $P_2 = 10$, oscillatory convection is always dominant in that the instability curve always lies below the stationary convection one for A values $0, 0.5, 1$ and 2, at least for the chosen range of λ.

In Figure 2.2 we again see oscillatory convection is present. However, for a fixed value of A, eg. $A = 1$, we see that oscillatory convection is occuring for $\lambda < \lambda_c$ and when $\lambda > \lambda_c$ we shall witness stationary convection. (The value λ_c is the value of λ where convection switches from oscillatory to stationary.) The same behaviour is also seen for other values of A. For example, when $A = 1$, $\lambda_c = 0.060144$ as seen in Table 2.1, the transition from oscillatory to stationary convection occurs when $Ra = 15.5454$. At the transition point the wavenumber changes abruptly, e.g. when $A = 1$ we see from Table 2.1 that the oscillatory convection wavenumber is $a_{osc} = 3.12266$ whereas the stationary convection wavenumber is $a_{sta} = 6.221$. This means the cells change from wider to narrower cells as λ increases through λ_c (for fixed depth).

Table 2.1: Transition values of Ra vs. λ, for $P_1 = 6$, $P_2 = 4$.

A	Ra	a_{sta}	a_{osc}	λ
0.0	...	...	...	...
0.3	10.802	14.621	3.42257	0.09238
0.5	12.032	9.736	3.2991	0.08221
0.7	13.368	7.7625	3.21014	0.072801
1.	15.5454	6.221	3.12266	0.060144
1.3	17.8999	5.33535	3.07392	0.0491503
1.5	19.5509	4.9216	3.05745	0.04266
1.7	21.256	4.5945	3.05107	0.03676
2.	23.894	4.2134	3.05712	0.02892
2.5	28.4351	3.76198	3.1021	0.0180646
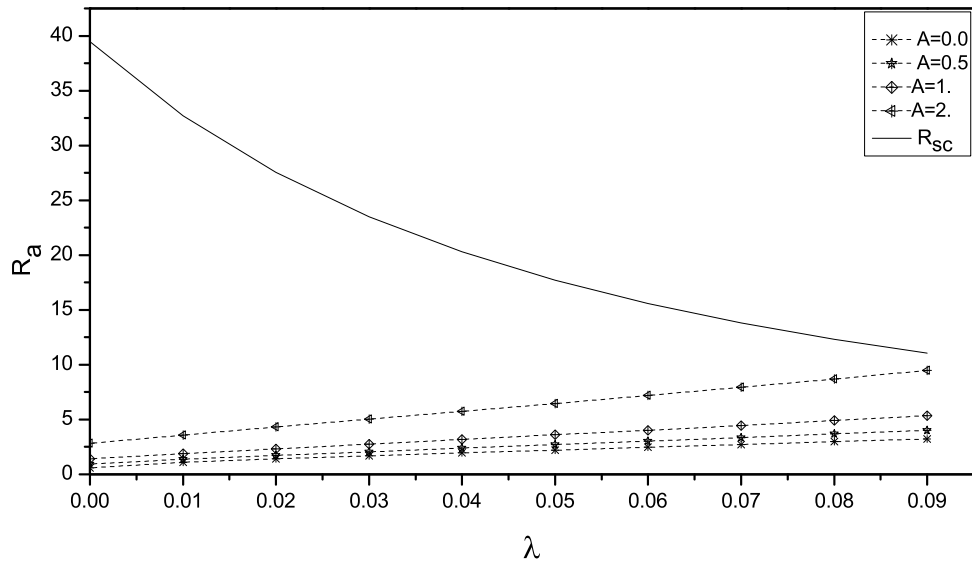
Figure 2.1: Critical values of Ra vs. λ for $P_1 = 6$, $P_2 = 10$. The upmost curve is for stationary convection. The other curves are for oscillatory convection, the lowest being when $A = 0$, increasing to $A = 2$.
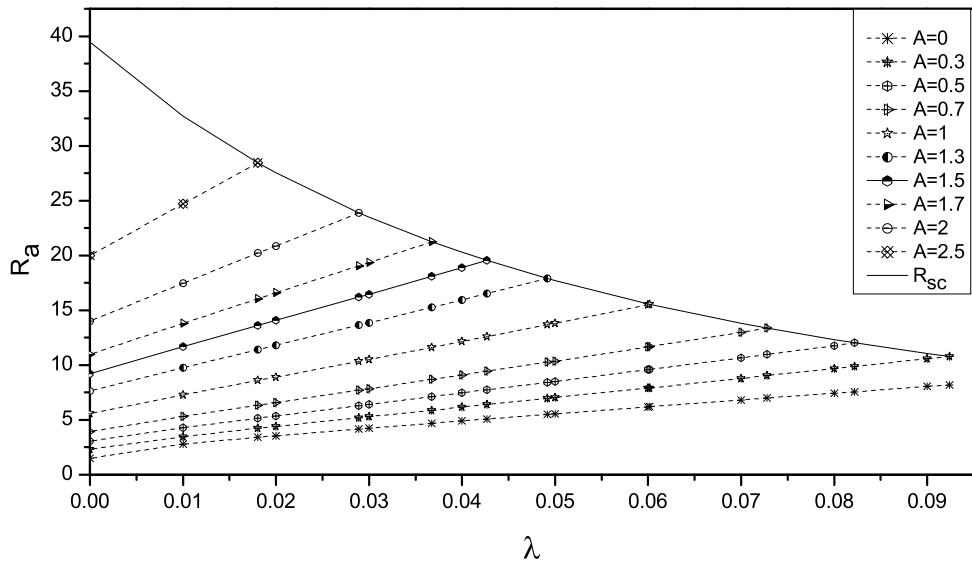
Figure 2.2: Critical values of Ra vs. λ for $P_1 = 6$, $P_2 = 4$. The upmost curve is for stationary convection. The other curves are for oscillatory convection, the lowest being when $A = 0$, increasing to $A = 2.5$.

The transition to stationary convection is very noticeable and this is where the effect of the Guyer-Krumhansl terms are playing a major role. The transition values

for $P_1 = 6$, $P_2 = 4$ are shown in figure 2.3.
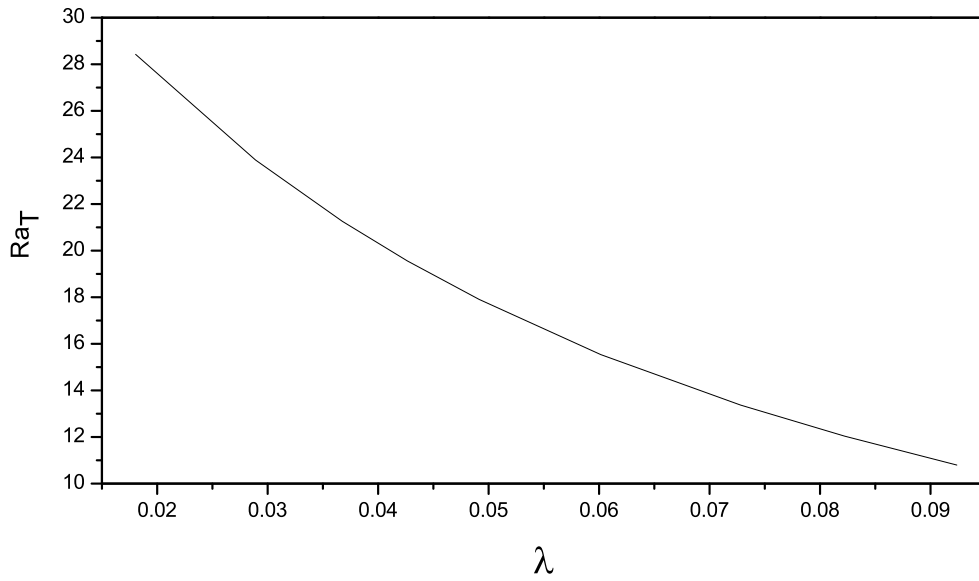
Figure 2.3: Transition values of Ra (R_{a_T}) vs. λ for $P_1 = 6$, $P_2 = 4$.

Similar findings for $P_1 = 6$, $P_2 = 2.8$ are given in Figures 2.4 and 2.5 and Table 2.2. In Figures 2.2 and 2.4 the oscillatory convection curves all are in agreement with the restriction $\sigma_1^2 > 0$. In fact, this restriction does break down but only when the Rayleigh number is larger than that on the appropriate stationary convection curve.

Table 2.2: Transition values of Ra vs. λ, for $P_1 = 6$, $P_2 = 2.8$.

A	Ra	a_{sta}	a_{osc}	λ
0.0	11.317	11.803	3.8053	0.08792
0.3	13.762	7.388	3.48698	0.07029
0.5	15.628	6.18	3.36244	0.05972
0.7	17.652	5.409	3.28131	0.050203
1.	20.9341	4.6503	3.21605	0.03782
1.3	24.4454	4.14736	3.19922	0.0274391
1.5	26.8766	3.8961	3.20874	0.0214774
1.7	29.355	3.69058	3.2328	0.016179
2.	33.12	3.4446	3.295	0.009304
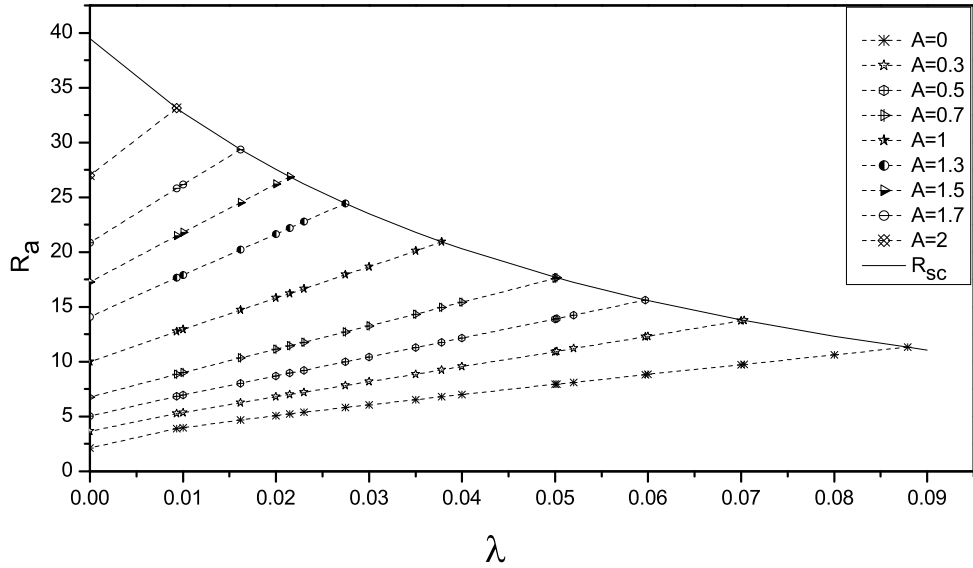
Figure 2.4: Critical values of Ra vs. λ for $P_1 = 6$, $P_2 = 2.8$. The upmost curve is for stationary convection. The other curves are for oscillatory convection, the lowest being when $A = 0$, increasing to $A = 2$.
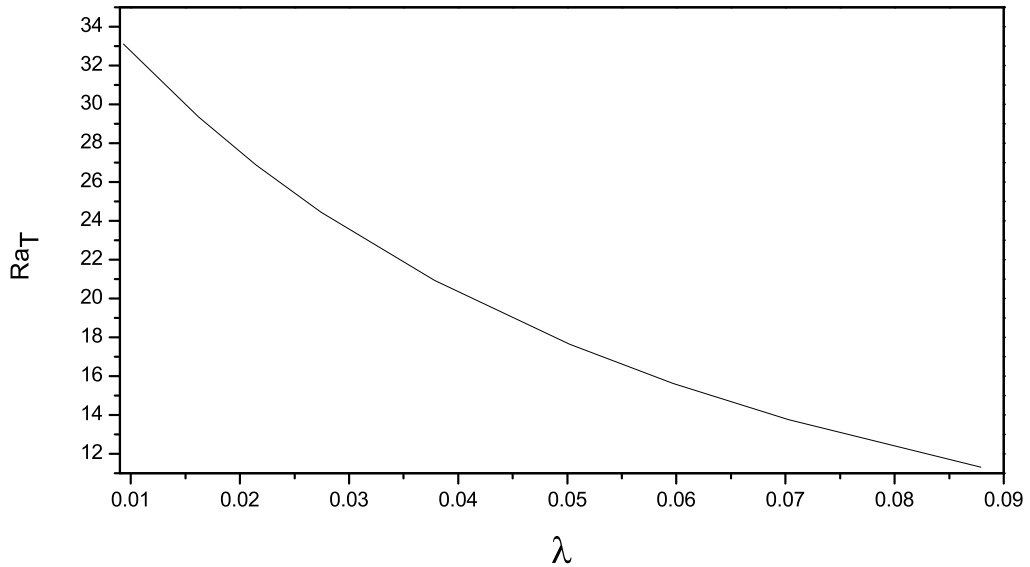
Figure 2.5: Transition values of Ra (R_{a_T}) vs. λ for $P_1 = 6$, $P_2 = 2.8$.

2.4   Further remarks

1. To check the eigenvalue results from (2.2.3) by a numerical method does not appear to be a trivial matter. The problem is that $(2.2.3)_2$ is essentially an identity, whereas $(2.2.3)_3$ contains both $\Delta\vartheta$ and ΔQ. To overcome this, we

introduce the new variable $\alpha = \vartheta - \lambda Q$, and rewriting the equation (2.2.3) in the form

$$
\begin{aligned}
\Delta w + a^2 R(\alpha + \lambda Q) &= -A\sigma\Delta w, \\
\Delta\alpha + Q &= -\sigma P_2 Q, \\
\alpha - \vartheta + \lambda Q &= 0, \\
Q - Rw &= -\sigma P_1(\alpha + \lambda Q).
\end{aligned}
\tag{2.4.1}
$$

To solve equation (2.4.1) by the D^2 Chebyshev tau numerical method, cf. Dongarra et al. [31], with details in Appendix B, we substitute $\chi = \Delta w$ and assume that

$$
w = W(\hat{z})f(x,y), \qquad \chi = \chi(\hat{z})f(x,y),
$$

$$
\vartheta = \Theta(\hat{z})f(x,y), \qquad Q = Q(\hat{z})f(x,y), \qquad \alpha = \alpha(\hat{z})f(x,y).
$$

The domain of equation (2.4.1) is transformed from $(0,1)$ to the Chebyshev domain $(-1,1)$ by setting $\hat{z} = 2z - 1$, also the functions $W, \chi, \Theta, Q, \alpha$ are expanded as series of Chebyshev polynomials. Thus for some N odd

$$
W(\hat{z}) = \sum_{n=0}^{N} W_n T_n(\hat{z}), \qquad \chi(\hat{z}) = \sum_{n=0}^{N} \chi_n T_n(\hat{z})
$$

$$
\Theta(\hat{z}) = \sum_{n=0}^{N} \Theta_n T_n(\hat{z}), \qquad Q(\hat{z}) = \sum_{n=0}^{N} Q_n T_n(\hat{z}), \qquad \alpha(\hat{z}) = \sum_{n=0}^{N} \alpha_n T_n(\hat{z}).
$$

Hence, we may write equation (2.4.1) in the form (omitting hat)

$$
\begin{aligned}
\left(4D^2 - a^2\right) W - \chi &= 0 \\
\left(4D^2 - a^2\right)\alpha + Q &= -\sigma P_2 Q \\
\chi + a^2 R\alpha + \lambda a^2 RQ &= -\sigma A\chi \\
\alpha - \Theta + \lambda Q &= 0 \\
-RW + Q &= -\sigma P_1(\alpha + \lambda Q)
\end{aligned}
\tag{2.4.2}
$$

Next we recall the boundary conditions and use the relation

$$
T_n(\pm 1) = (\pm 1)^n
$$

The appropriate boundary conditions become

$$W_0 + W_2 + \cdots + W_{N-1} = 0$$
$$W_1 + W_3 + \cdots + W_N = 0$$

(2.4.3)

With an analogous expression for α_n.

The eigenvalue problem (2.4.2) can be written as the generalized eigenvalue problem of the form $A\mathbf{x} = \sigma B\mathbf{x}$, where

$$\mathbf{x} = (W_0, \ldots, W_N, \alpha_0, \ldots, \alpha_N, \chi_0, \ldots, \chi_N, \Theta_0, \ldots, \Theta_N, Q_0, \ldots, Q_N)$$

is the $5(N+1)$ vector of unknown coefficients, and the matrices $5(N+1) \times 5(N+1)$ are given by

$$A = \begin{pmatrix} 4(D^2 - a^2)I & 0 & -I & 0 & 0 \\ BC1 & 0\cdots0 & 0\cdots0 & 0\cdots0 & 0\cdots0 \\ BC2 & 0\cdots0 & 0\cdots0 & 0\cdots0 & 0\cdots0 \\ 0 & 4(D^2 - a^2)I & 0 & 0 & I \\ 0\cdots0 & BC3 & 0\cdots0 & 0\cdots0 & 0\cdots0 \\ 0\cdots0 & BC4 & 0\cdots0 & 0\cdots0 & 0\cdots0 \\ 0 & a^2RI & I & 0 & \lambda a^2 RI \\ 0 & -I & 0 & I & -\lambda I \\ -RI & 0 & 0 & 0 & I \end{pmatrix},$$

$$B = \begin{pmatrix} 0 & 0 & 0 & 0 & 0 \\ 0\cdots0 & 0\cdots0 & 0\cdots0 & 0\cdots0 & 0\cdots0 \\ 0\cdots0 & 0\cdots0 & 0\cdots0 & 0\cdots0 & 0\cdots0 \\ 0 & 0 & 0 & 0 & -P_2 I \\ 0\cdots0 & 0\cdots0 & 0\cdots0 & 0\cdots0 & 0\cdots0 \\ 0\cdots0 & 0\cdots0 & 0\cdots0 & 0\cdots0 & 0\cdots0 \\ 0 & 0 & -AI & 0 & 0 \\ 0 & 0 & 0 & 0 & 0 \\ 0 & -P_1 I & 0 & 0 & -\lambda P_1 I \end{pmatrix},$$

Where $BC1$, $BC2$ and $BC3$, $BC4$ refer to the boundary conditions (2.4.3) on

W and α_n, respectively. The matrix system is solved by the QZ algorithm cf. Moler et al. [76], which is available in the NAG routine $F02BJF$. We find satisfactory numerical results are achieved.

2. Due to the nonlinearities present in equations (2.1.16) and (2.1.17) we cannot be sure that linear theory is correctly capturing the analysis of the onset of convection. One way of sometimes checking whether this is to employ a suitable nonlinear energy stability method. If we let V be a period cell for the perturbation in (2.1.14)-(2.1.17) and let $\|.\|$ and $(.,.)$ denote the norm and inner product on $L^2(V)$ then from equations (2.1.14)-(2.1.17) we may derive the following energy identities by multiplying (2.1.14) by u_i, (2.1.16) by ϑ, and (2.1.17) by q_i. After integrating over V we see that

$$\frac{d}{dt}\frac{A}{2}\|\mathbf{u}\|^2 \;=\; R(\vartheta, w) - \|\mathbf{u}\|^2 , \qquad (2.4.4)$$

$$\frac{d}{dt}\frac{Pr}{2MDa}\|\vartheta\|^2 \;=\; R(w, \vartheta) - (q_{i,i}, \vartheta) , \qquad (2.4.5)$$

$$\begin{aligned}
\frac{d}{dt}\frac{Sg}{2Da}\|\mathbf{q}\|^2 \;=\;& -\|\mathbf{q}\|^2 - (\vartheta_{,i}, q_i) + \frac{SgR\hat{\tau}}{Pr}(u_{i,z}, q_i) \\
& -\lambda_1 \int_V (q_{i,j} - q_{j,i})q_{i,j}dV \\
& -(\lambda_1 + \lambda_2)\|q_{i,i}\|^2 - \frac{\hat{\tau}Sg}{Da}\int_V q_i q_j u_{i,j}dV, \qquad (2.4.6)
\end{aligned}$$

cf. the calculations in Straughan [121], pp. 194–195. After integration by parts we may add (2.4.5) and (2.4.6) and remove the terms $-(q_{i,i}, \vartheta) - (\vartheta_{,i}, q_i)$. We may also integrate by parts on the third term on the right of (2.4.6) to obtain a term involving $-(u_i, q_{i,z})$ and we may rewrite the last term in (2.4.6) in terms of $\int_V q_{i,j}q_j u_i dV$ and $\int_V q_i q_{j,j} u_i dV$. The Guyer-Krumhansl terms in λ_1 and λ_2 will help us to control the derivatives of q terms.

However, it is difficult to see how to obtain unconditional nonlinear stability with the presence of the cubic nonlinear terms. Perhaps an even greater problem arises due to the (w, ϑ) terms. While there is dissipation in (2.4.4) to control the velocity terms there is no temperature dissipation in (2.4.4)-(2.4.6)and so it does not appear possible to control the (w, ϑ) terms.

At present we do not see how to overcome the above problems by an energy technique. Whether more sophisticated energy methods, such as those recently developed by Rionero [92–95, 97] , will help remains to be seen.

Chapter 3

Thermal convection in a Cattaneo-Fox porous material with Guyer-Krumhansl effects

As was mentioned in the previous chapter, it is believed that the physical mechanism of heat propagation as a temperature wave (second sound) is by phonon oscillations. Phonon oscillations undoubtedly are the subject of many recent investigations and have mundane applications in convection in a porous body. However, recently the work of Jou et al. [55], confirms that phonon oscillations play an important role in the propagation of temperature waves in nanowires.

Straughan [117] argues that heat wave effects on thermal convection in porous media may be important in some classes of real life problem. He notes that a key way of introducing finite temperature wave motion has been to use the Cattaneo law [17] for the heat flux. In thermal convection, the inclusion of the Cattaneo law was investigated by Straughan and Franchi [110], and later work followed by Lebon and Cloot [65]. Further important work using Cattaneo theory in the wave propagation is by Franchi [37]. This has also been considered further, see Puri and Jordan cf. [87,88], and work of Christov and Jordan [22]. The generalization of the Cattaneo law (see Appendix A.2) which accounts for space correlation is the well known Guyer-Krumhansl equation [42–44]. For more detail we may refer to the book of Straughan [121]. The object of this Chapter is to investigate the effect of

the Guyer-Krumhansl terms on the stability thresholds employing a Cattaneo-Fox derivative for the heat flux, rather than a Cattaneo-Christov derivative as employed in the previous chapter. The linear instability analysis is performed to find the range of the Guyer-Krumhansl values for the stationary instability threshold. This is discussed in detail throughout this chapter.

3.1   Basic equations

The flow in the porous medium is assumed to be governed by Darcy's law, as presented in Chapter 2, cf. Vadasz [131], Straughan [114],

$$\hat{a}v_{i,t} = -p_{,i} - \frac{\mu}{\mathrm{K}}v_i + k_i g \rho_0 \alpha T, \tag{3.1.1}$$

$$v_{i,i} = 0, \tag{3.1.2}$$

where $\mathbf{v}$ is the velocity field, p is the pressure, T is temperature, $\hat{a}$ is an inertia coefficient, μ is the dynamic viscosity, K is the permeability, $\mathbf{k} = (0, 0, 1)$, g is gravity, α is the thermal expansion coefficient of the fluid, and ρ_0 is the constant density assuming the Boussinesq approximation has been employed to derive (3.1.1).

The procedure to derive an energy balance equation and the heat flux in the context of the Cattaneo law may be found in the books by Straughan [121], p. 238, or Straughan [117]. In this chapter we specifically wish to consider the Cattaneo-Fox derivative rather than the Cattaneo-Christov derivative used in Chapter 2, cf. Haddad and Straughan [45]. The equation of energy balance and the constitutive equation of the heat flux using the Cattaneo-Fox derivative are established by using the same procedure as in Chapter 2, and these may be written as

$$\frac{1}{M}T_{,t} + v_i T_{,i} = -Q_{i,i}, \tag{3.1.3}$$

$$\tau Q_{i,t} + \tau_f(v_j Q_{i,j} - \tfrac{1}{2}Q_j v_{i,j} + \tfrac{1}{2}Q_j v_{j,i}) =$$
$$-Q_i - \kappa T_{,i} + \xi_1 \Delta Q_i + \xi_2 Q_{k,ki}. \tag{3.1.4}$$

Here $v_i = \varphi V_i$ (v_i is the average of the fluid velocity over the fluid and solid phases), where V_i is the fluid velocity averaged over the fluid phase. φ is the porosity, Q_i is the heat flux, and ξ_1 and ξ_2 are Guyer-Krumhansl terms, cf. Morro [77, 78]. The

coefficients M and κ are given by

$$M = \frac{(\rho_0 c_p)_f}{(\rho_0 c)_m}, \qquad \kappa = \frac{k_m}{(\rho_0 c_p)_f}.$$

Again, we let s represent the solid skeleton of the porous medium, f represent the fluid, and m refers to the porous medium. The quantities k_m, $(\rho_0 c)_m$, and τ are defined by

$$
\begin{aligned}
k_m &= \kappa_f \varphi + (1 - \varphi)\kappa_s, \\
(\rho_0 c)_m &= \varphi(\rho_0 c_p)_f + (1 - \varphi)(\rho_0 c)_s, \\
\tau &= \varphi \tau_f + (1 - \varphi)\tau_s,
\end{aligned}
$$

where c, c_p, κ, are the specific heat of solid in the porous medium, the specific heat at constant pressure in the fluid, and thermal diffusivity. The coefficients τ_f and τ_s are the relaxation times for the fluid and solid in the porous body.

We suppose the fluid saturated porous medium satisfies equations (3.1.1)-(3.1.4) and occupies the spatial domain $\Omega = \{(x, y) \in \mathbb{R}^2\} \times \{z \in (0, d)\}$, and let $\mathbf{n}$ be the unit outward so that $\mathbf{n} = (0, 0, 1)$ on $z = d$ and $\mathbf{n} = (0, 0, -1)$ on $z = 0$. The boundary conditions are

$$
\begin{aligned}
v_i n_i &= 0, \qquad \text{at } z = 0, d, \\
T &= T_L, \ z = 0; \quad T = T_U, \ z = d,
\end{aligned}
\tag{3.1.5}
$$

where T_L, T_U are constants with $T_L > T_U$. In addition the heat flux satisfies

$$\varepsilon_{ijk} n_j Q_k = 0, \qquad z = 0, d. \tag{3.1.6}$$

A steady conduction solution of system (3.1.1)-(3.1.4) in the domain Ω and satisfying boundary condition (3.1.5)-(3.1.6), is given by

$$
\begin{aligned}
\bar{v}_i &\equiv 0, \qquad \bar{T} = -\beta z + T_L, \qquad \bar{\mathbf{Q}} = (0, 0, \kappa\beta) \\
\bar{p} &= p_0 - g\rho_0 z - \frac{1}{2}\alpha\beta g\rho_0 z^2,
\end{aligned}
\tag{3.1.7}
$$

where

$$\beta = \frac{T_L - T_U}{d}.$$

To analyse the stability of (3.1.7), we perturb the steady conduction solution in such a way that

$$v_i = \bar{v}_i + u_i, \qquad T = \bar{T} + \vartheta, \qquad Q_i = \bar{Q}_i + q_i, \qquad p = \bar{p} + \pi.$$

By substituting the perturbations$(u_i, \vartheta, q_i, \pi)$ into equations (3.1.1)-(3.1.4), we obtain the system of perturbation equations

$$\hat{a}u_{i,t} = -\pi_{,i} - \frac{\mu}{K}u_i + k_i g \rho_0 \alpha \vartheta,$$

$$u_{i,i} = 0,$$

$$\frac{1}{M}\vartheta_{,t} + u_i\vartheta_{,i} = -q_{i,i} + \beta w, \tag{3.1.8}$$

$$\tau q_{i,t} + \tau_f\left(u_j q_{i,j} - \frac{1}{2}q_j u_{i,j} + \frac{1}{2}q_j u_{j,i}\right) + \tau_f\left(\frac{1}{2}\beta\kappa w_{,i} - \frac{1}{2}\beta\kappa u_{i,z}\right)$$

$$= -q_i - \kappa\vartheta_{,i} + \xi_1\Delta q_i + \xi_2 q_{k,ki}.$$

We now introduce the non-dimensional scalings for the perturbations $(u_i, \vartheta, q_i, \pi)$,

$$\mathbf{x} = d\mathbf{x}^*, \qquad \mathbf{u} = \frac{\mu d}{\rho_0 K}\mathbf{u}^*, \qquad \mathbf{q} = \kappa U\sqrt{\frac{\beta\mu}{K\rho_0\alpha g\kappa}}\mathbf{q}^*,$$

$$t = \frac{K\rho_0}{\mu}t^*, \qquad \pi = \frac{\mu U d}{K}\pi^*, \qquad \vartheta = dU\sqrt{\frac{\beta\mu}{K\rho_0\alpha g\kappa}}\vartheta^*,$$

where U is a velocity scale, although additionally we here require non-dimensional equivalents of $\hat{a}$, ξ_1 and ξ_2 by scalings

$$\hat{a} = \rho_0 a^*, \qquad \xi_1 = d\xi_1^*, \qquad \xi_2 = d\xi_2^*.$$

We require the Prandtl number $Pr = \mu/\rho_0\kappa$ and the key non-dimensional numbers

$$R = \sqrt{\frac{\alpha g d^2 \beta K\rho_0}{\mu\kappa}}, \qquad Da = \frac{K}{d^2}, \qquad Sg = \frac{\tau\mu}{\rho_0 d^2}, \qquad \hat{\tau} = \frac{\tau_f}{\tau},$$

where $R = \sqrt{Ra}$ is the square root of the Rayleigh number, Da is the Darcy number, Sg is the Straughan number, see Papanicolaou et al. [85], and $\hat{\tau}$ is a relative relaxation time.

By substituting the above variables into equations (3.1.8), we obtain the nonlin-

ear non-dimensional perturbation equations (omitting the stars)

$$Au_{i,t} = -\pi_{,i} + Rk_i\vartheta - u_i, \tag{3.1.9}$$

$$u_{i,i} = 0, \tag{3.1.10}$$

$$\frac{Pr}{Da}\left(\frac{1}{M}\vartheta_{,t} + u_i\vartheta_{,i}\right) = Rw - q_{i,i}, \tag{3.1.11}$$

$$\frac{Sg}{Da}q_{i,t} + \frac{\hat{\tau}Sg}{Da}\left(u_jq_{i,j} - \frac{1}{2}q_ju_{i,j} + \frac{1}{2}q_ju_{j,i}\right) = -q_i - \vartheta_{,i} \tag{3.1.12}$$

$$+\frac{\hat{\tau}SgR}{2Pr}(u_{i,z} - w_{,i}) + \lambda_1\Delta q_i + \lambda_2 q_{j,ji},$$

where $w = u_3$ and A, λ_1, λ_2 are non-dimensional equivalents of $\hat{a}$, ξ_1 and ξ_2. Equations (3.1.9)-(3.1.12) hold on $\{\Omega \times t > 0\}$ and the boundary conditions are

$$u_in_i = 0, \qquad \vartheta = 0, \qquad \varepsilon_{ijk}n_jq_k = 0, \qquad z = 0, 1, \tag{3.1.13}$$

with $\{u_i, \vartheta, q_i, \pi\}$ satisfying a plane tiling periodicity in (x, y).

3.2 Linear instability

We begin the linear instability analysis by removing the nonlinear terms of equations (3.1.11) and (3.1.12), take the divergence of equation (3.1.12), and then analyse the linear system.

The linear system arising from equations (3.1.9)-(3.1.12) is

$$Au_{i,t} + u_i = -\pi_{,i} + Rk_i\vartheta,$$

$$u_{i,i} = 0,$$

$$\frac{Pr}{MDa}\vartheta_{,t} = Rw - Q, \tag{3.2.1}$$

$$\frac{Sg}{Da}Q_{,t} = -Q - \Delta\vartheta - \frac{\hat{\tau}SgR}{2Pr}\Delta w + \lambda\Delta Q.$$

Here $Q = q_{i,i}$, and $\lambda = \lambda_1 + \lambda_2$. It is convenient to define P_1 and P_2 by

$$P_1 = \frac{Pr}{MDa}, \qquad P_2 = \frac{Sg}{Da}, \tag{3.2.2}$$

and then take curl curl of equation $(3.2.1)_1$ to remove π. We then assume a temporal growth rate like $e^{\sigma t}$, i.e. we write

$$w = w(\mathbf{x})e^{\sigma t}, \qquad \vartheta = \vartheta(\mathbf{x})e^{\sigma t}, \qquad Q = Q(\mathbf{x})e^{\sigma t}.$$

Upon substituting into equation (3.2.1) and setting $M = 1$, and $\hat{\tau} = 1$, we have to solve the system

$$(\sigma A + 1) \Delta w = R \Delta^* \vartheta,$$

$$\sigma P_1 \vartheta = Rw - Q, \tag{3.2.3}$$

$$\frac{P_2}{2P_1} R \Delta w + \Delta \vartheta = -(\sigma P_2 - \lambda \Delta + 1)Q,$$

where $\Delta^* = \partial^2/\partial x^2 + \partial^2/\partial y^2$ is the horizontal Laplacian operator.

3.2.1 Stationary convection

The standard methods to analyse equation (3.2.3) follows the work of Chandrasekhar [19]. To derive the stationary convection instability threshold we substitute $\sigma = 0$ into equation (3.2.3). Then replace $P_2/2P_1 = P$, and the governing system can be reduced to

$$\Delta w = R \Delta^* \vartheta,$$

$$Rw = Q, \tag{3.2.4}$$

$$(1 - \lambda \Delta)Q = -\Delta \vartheta - PR\Delta w.$$

After eliminating the variables ϑ, and Q, equation (3.2.4) can be written as

$$\Delta^2 w = -R^2 \Delta^* (\Delta w(P - \lambda) + w). \tag{3.2.5}$$

We now employ a normal mode representation w of the form $w = W(z)f(x, y)$, where f is the horizontal plan form which satisfy $\Delta^* f = -a^2 f$, a being a wave number. Also W is written as a series of terms of $\sin n\pi z$, for $n \in \mathbb{N}$ which satisfies the boundary conditions (3.1.13).

Upon substituting in equation (3.2.5), we have

$$R^2 = \frac{\Lambda_n^2}{a^2 \left[1 + \Gamma \Lambda_n\right]},$$

where $\Lambda_n = n^2 \pi^2 + a^2$, and $\Gamma = \lambda - P$. Then one may consider two cases.

Case I: when $\lambda \geq P$, ie. $\Gamma \geq 0$.

Case II: when $\lambda < P$, ie. $\Gamma < 0$.

In case II we may argue that, for any $a^2 > 0$, $\exists N$ such that, $\forall n > N$, $n^2\pi^2 + a^2 > \dfrac{1}{|\Gamma|}$. Therefore, $R^2 < 0$ for $n > N$. This suggests instability for heating from above, which is unphysical.

Hence, we only consider $\Gamma > 0$. We wish to minimize the Rayleigh number $R^2 = R^2(a^2, n^2)$. Then one shows $\partial R^2/\partial n^2 > 0$. Therefore we select $n = 1$ to obtain the lowest instability boundary. Then we have

$$R^2 = \frac{\Lambda^2}{a^2\,[1 + \Gamma\Lambda]},$$

where Λ refers to Λ_1. Then differentiating R^2 with respect to a^2 yields the stationary convection boundary as

$$R_{sc}^2 = \frac{4\pi^2}{(1 + \Gamma\pi^2)^2}\,, \tag{3.2.6}$$

and the corresponding critical wave number a_c is given by

$$a_c^2 = \frac{\pi^2(1 + \Gamma\pi^2)}{(1 - \Gamma\pi^2)}\,. \tag{3.2.7}$$

We observe that equation (3.2.7) is satisfied provided that $\Gamma < 1/\pi^2$.

We know $\Gamma = \lambda - P \geq 0$. Hence since Γ also satisfied $\Gamma < 1/\pi^2$ we find that λ must be restricted so that

$$P \leq \lambda < \frac{1}{\pi^2} + P. \tag{3.2.8}$$

3.2.2 Oscillatory convection

Again, we follow Chandrasekhar's [19] procedure. To study oscillatory convection put $\sigma = i\sigma_1$ in equation (3.2.3), where $\sigma_1 \in \mathbb{R}$. The real and imaginary parts of equation (3.2.3) yield

$$\sigma_1^2(-2PP_1^2\Lambda - AP_1\Lambda(1 + \lambda\Lambda)) + \Lambda^2 = a^2R^2(1 + \lambda\Lambda - P\Lambda),$$

and

$$\sigma_1^2(2APP_1^2\Lambda) - (A\Lambda^2 + \Lambda P_1(1 + \lambda\Lambda)) = -2PP_1a^2R^2.$$

Hence, we may solve for σ_1^2 and R^2 to find

$$\begin{aligned}
\sigma_1^2 \;=\; &\frac{-1}{2P^2P_1^2(2P_1 + A\Lambda)}[(\lambda - P)(A + \lambda P_1)\Lambda^2 \\
&+ (2\lambda P_1 - 3PP_1 + A)\Lambda + P_1],
\end{aligned} \tag{3.2.9}$$

and

$$R^2 = \frac{\beta_3 \Lambda^3}{(B_1 \Lambda + B)a^2} + \frac{\beta_2 \Lambda^2}{(B_1 \Lambda + B)a^2} + \frac{\beta_1 \Lambda}{(B_1 \Lambda + B)a^2}. \tag{3.2.10}$$

Here the coefficients β_3, β_2, β_1 are defined by

$$
\begin{aligned}
\beta_3 &= \lambda A \left(\frac{A}{2PP_1} + \frac{\lambda}{2P} \right), \\
\beta_2 &= \frac{A^2}{2PP_1} + \frac{\lambda A}{P} + \lambda P_1, \\
\beta_1 &= \frac{A}{P} + P_1,
\end{aligned} \tag{3.2.11}
$$

where

$$B = 2P_1 P, \qquad B_1 = AP.$$

It is worthy to observe that from equation (3.2.9) oscillatory convection occurs when $\sigma_1^2 > 0$. Numerical techniques are used to find R_{osc}^2 by minimizing R^2 in equation (3.2.10) over a^2, as presented in the numerical results section.

3.3 Numerical results

The numerical findings in this section are performed with $P_1 = 6$ and $P_2 = 0.6, 12, 21$, and $P_2 = 60$. We are interested in the Guyer-Krumhansl term effects on the neutral stability curve. Due to the restriction condition (3.2.8), the range of the Guyer-Krumhansl values λ which may be allowed for computed critical wave number and critical Rayleigh number are shown in Table 3.1. However, we must remember that σ_1^2 as given by equation (3.2.9) must also be positive, i.e. $\sigma_1^2 > 0$. To achieve this one find λ must be further restricted as shown in Table 3.2. We perform computations only in this range of values.

To explain the meaning of Figure 3.1, let us take an example $A = 0.01$. Then, the solution is linearly stable for R_a underneath the line with the circles on when $0.05 \leq \lambda \leq 0.051491$ as shown in Table 3.3. When R_a is above the line with the circles on and $0.05 \leq \lambda \leq 0.051491$ instability is by oscillatory convection, whereas once λ exceeds the transition value $\lambda_c = 0.051491$ instability is by stationary convection. (The value λ_c is the value of λ where convection switches from oscillatory to stationary). A similar interpretation holds for the curves where $A = 0.02$, and

Table 3.1: The ranges of the Guyer-Krumhansl coefficient, for stationary convection instability threshold.

P_2	P	λ range
0.6	0.05	$0.05 \leq \lambda < 0.1513212$
12	1.00	$1.00 \leq \lambda < 1.1013212$
21	1.75	$1.75 \leq \lambda < 1.8513212$
60	5.00	$5.00 \leq \lambda < 5.1013212$

Table 3.2: The ranges of the Guyer-Krumhansl coefficient which give $\sigma_1^2 > 0$

A	$P_2 = 0.6$	$P_2 = 12$	$P_2 = 21$	$P_2 = 60$
0.01	$0.05 \leq \lambda \leq 0.0531$	$1 \leq \lambda \leq 1.0411$	$1.75 \leq \lambda \leq 1.79475$	$5 \leq \lambda \leq 5.04842$
0.02	$0.05 \leq \lambda \leq 0.0526$	$1 \leq \lambda \leq 1.0410$	$1.75 \leq \lambda \leq 1.79468$	$5 \leq \lambda \leq 5.04839$
0.03	$0.05 \leq \lambda \leq 0.0521$	$1 \leq \lambda \leq 1.0409$	$1.75 \leq \lambda \leq 1.79461$	$5 \leq \lambda \leq 5.04836$
0.04	$0.05 \leq \lambda \leq 0.0516$	$1 \leq \lambda \leq 1.0407$	$1.75 \leq \lambda \leq 1.79453$	$5 \leq \lambda \leq 5.04834$
1.0	......	$1 \leq \lambda \leq 1.0302$	$1.75 \leq \lambda \leq 1.78755$	$5 \leq \lambda \leq 5.04550$
2.0	......	$1 \leq \lambda \leq 1.0212$	$1.75 \leq \lambda \leq 1.78108$	$5 \leq \lambda \leq 5.04263$
3.0	......	$1 \leq \lambda \leq 1.0139$	$1.75 \leq \lambda \leq 1.77544$	$5 \leq \lambda \leq 5.03990$
6.0	......	......	$1.75 \leq \lambda \leq 1.76230$	$5 \leq \lambda \leq 5.03257$
11.	......	......	......	$5 \leq \lambda \leq 5.02265$

Table 3.3: Transition values of Ra vs. λ, for $P_1 = 6$, $P_2 = 0.6$.

A	Ra	a_{sta}	a_{osc}	λ
0.01	38.340	3.1882	4.12068	0.051491
0.02	38.765	3.1705	4.12517	0.05093
0.03	39.1916	3.1531	4.12942	0.0503701
0.04	......	......	......	......

$A = 0.03$. When $A = 0.04$ the stationary curve lies below the oscillatory curve. In interpreting Figure 3.1, it must be realized that $\sigma_1^2 > 0$ for oscillatory convection and so λ is restricted as in Table 3.2.
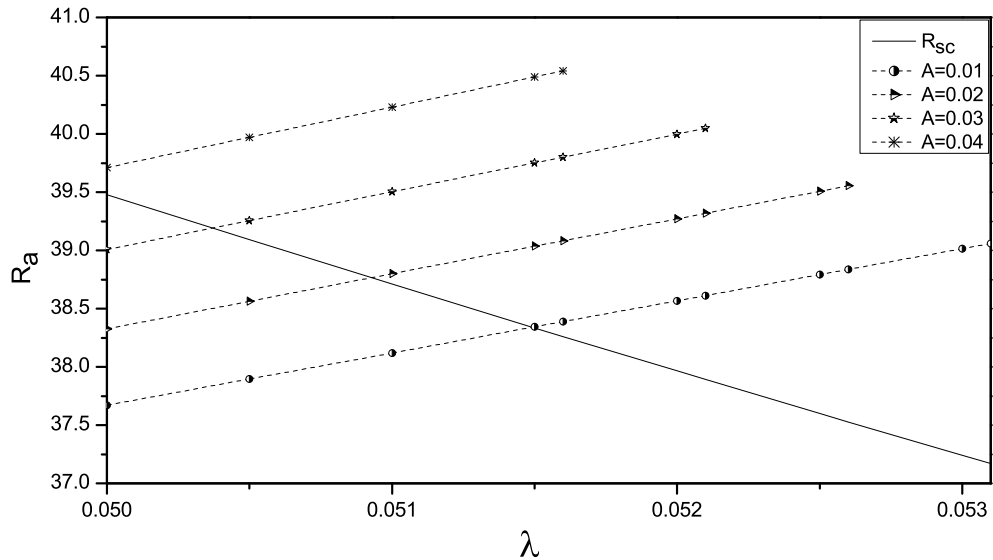
Figure 3.1: Critical Rayleigh number R_a as function of λ, with λ restricted as in table 3.1. Here $P_1 = 6$, $P_2 = 0.6$. The solid curve is for stationary convection. The other curves are for oscillatory convection, for $A = 0.01$ increasing to $A = 0.04$.

In Table 3.4, P_2 is increased to $P_2 = 12$. Here we find the transition value of R_a for $A = 0.01$ is almost the same for $A \in [0.01, 0.04]$, therefore we illustrate the oscillatory convection curves for $A = 0.01, 1, 2$, and $A = 3$ in Figure 3.2. The oscillatory convection dominates when $\lambda < \lambda_c$ and convection is by stationary when $\lambda > \lambda_c$. For $A \geq 6$, $\sigma_1^2 < 0$ as shown in Table 3.2.

Table 3.4: Transition values of Ra vs. λ, for $P_1 = 6$, $P_2 = 12$.

A	Ra	a_{sta}	a_{osc}	λ
0.01	21.4705	4.55864	3.21481	1.03607
0.02	21.491	4.5538	3.21372	1.03598
0.03	21.5290	4.5490	3.21294	1.03588
0.04	21.558	4.5443	3.21201	1.03579
1.0	24.5105	4.13981	3.17994	1.02727
2.0	27.6663	3.82589	3.17600	1.01971
3.0	30.8460	3.58510	3.17711	1.01330
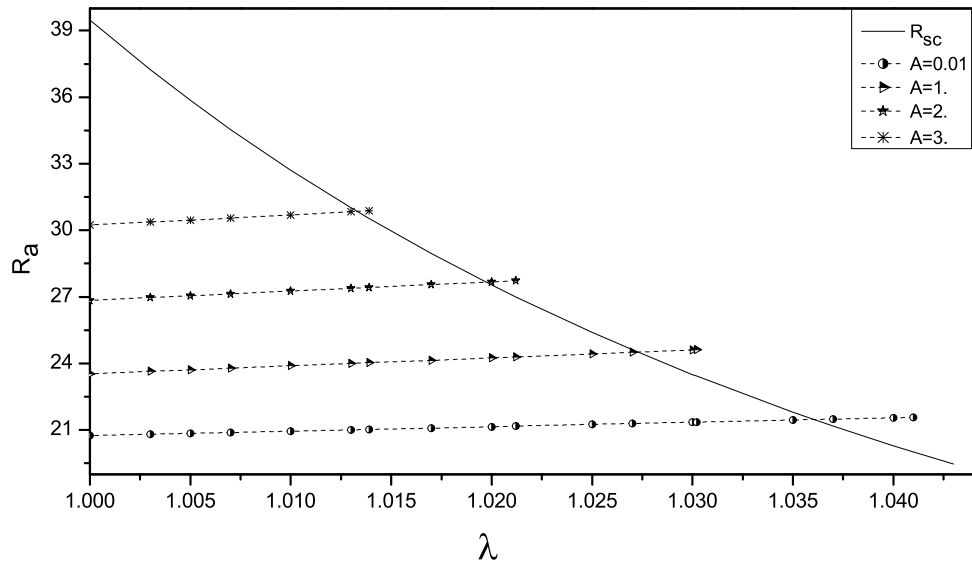
Figure 3.2: Critical Rayleigh number R_a as function of λ, with λ restricted as in table 3.2. Here $P_1 = 6$, $P_2 = 12$. The solid curve is for stationary convection. The other curves are for oscillatory convection, for $A = 0.01$ increasing to $A = 3$. The curve for $A = 0.01$ is effectively the same for $A \in [0.01, 0.04]$.

It is worth pointing out that the range of the Guyer-Krumhansl values λ for which stationary or oscillatory convection occurs depends on the value of P_2. As P_2 increases, the value of λ likewise increases. However, when P_2 increase to $P_2 = 21$, the stationary convection instability threshold occurs when $1.75 \leq \lambda < 1.8513212$ as shown in Table 3.1. Also, the range of the Guyer-Krumhansl values for $A \in [0.01, 6]$ which relate to existence of oscillatory convection are shown in Table 3.2. Figure 3.3 shows that when $A \in [0.01, 6]$, the onset of convection is more likely to be via oscillatory convection. We also observe that at the transition value λ_c, the oscillatory wave number at which R_a occurs is smaller than stationary wave number. For example, when $A = 0.01$, $\lambda_c = 1.78841$ we witness transition from oscillatory to stationary convection when $R_a = 20.7574$, the oscillatory wave number $a_{osc} = 3.18465$, whereas the stationary wave number $a_{sta} = 4.682$. This means that the convection cells change from wider to narrower cells at a transition value λ_c as seen in Table 3.5.
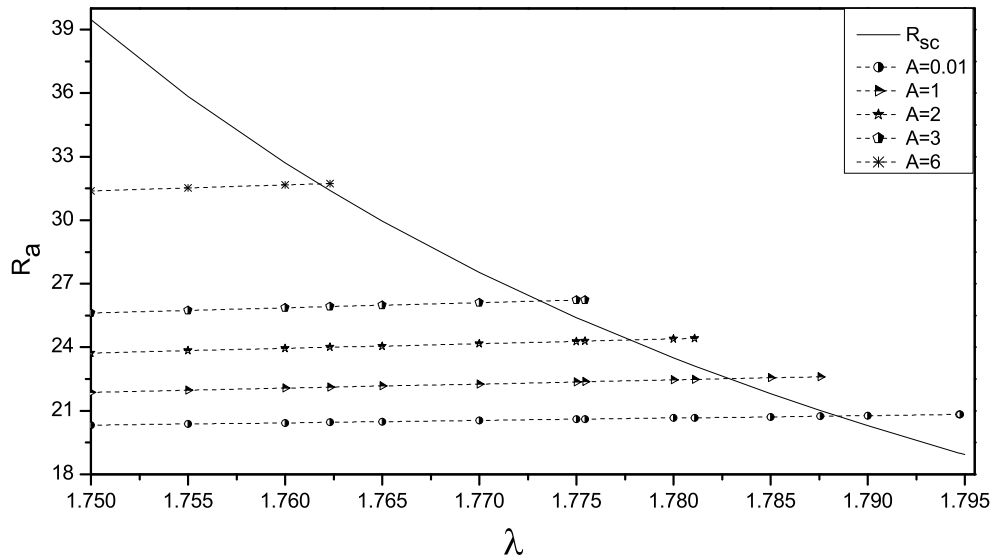
Figure 3.3: Critical Rayleigh number R_a as function of λ, with λ restricted as in table 3.2. Here $P_1 = 6$, $P_2 = 21$. The solid curve is for stationary convection. The other curves are for oscillatory convection, for $A = 0.01$ increasing to $A = 6$. The curve for $A = 0.01$ is effectively the same for $A \in [0.01, 0.04]$.

Table 3.5: Transition values of Ra vs. λ, for $P_1 = 6$, $P_2 = 21$.

A	Ra	a_{sta}	a_{osc}	λ_c
0.01	20.7574	4.682	3.18465	1.78841
0.02	20.7744	4.67894	3.18402	1.78835
0.03	20.7913	4.67587	3.18355	1.78830
0.04	20.8083	4.67280	3.18292	1.78824
1.0	22.519	4.3969	3.16244	1.78283
2.0	24.3432	4.1593	3.15864	1.77771
3.0	26.1784	3.9623	3.15816	1.77310
6.0	31.711	3.52903	3.16085	1.76173

To illustrate the effect of the Guyer-Krumhansl term λ on the oscillatory convection more, we select $P_2 = 60$, see Figure 3.4, with corresponding transition R_a, a_{sta}, a_{osc}, and λ_c values given in Table 3.6. However, in this case, we find that the oscillatory convection occurs when $A \in [0.01, 11]$. We observe that increasing P_2

had the effect of decreasing the value of R_a. This behaviour is due to the increase in the value of λ, $5 \leq \lambda < 5.1013212$ as shown in Table 3.1.
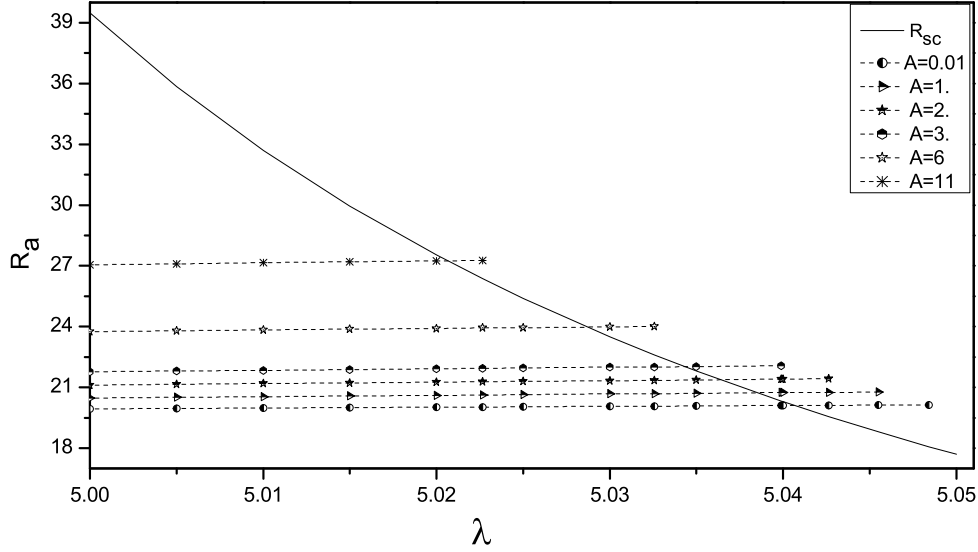
Figure 3.4: Critical Rayleigh number R_a as function of λ, with λ restricted as in table 3.2. Here $P_1 = 6$, $P_2 = 60$. The solid curve is for stationary convection. The other curves are for oscillatory convection, for $A = 0.01$ increasing to $A = 11$. The curve for $A = 0.01$ is effectively the same for $A \in [0.01, 0.04]$.

Table 3.6: Transition values of Ra vs. λ, for $P_1 = 6$, $P_2 = 60$.

A	Ra	a_{sta}	a_{osc}	λ_c
0.01	20.1053	4.80618	3.15706	5.04066
0.02	20.1113	4.80499	3.15690	5.04064
0.03	20.1170	4.8038	3.15658	5.04062
0.04	20.123	4.8026	3.15642	5.0406
1.0	20.7304	4.68693	3.14849	5.03850
2.0	21.377	4.5740	3.14659	5.03637
3.0	22.028	4.4700	3.14579	5.03432
6.0	23.9828	4.20251	3.14563	5.02868
11.0	27.247	3.86247	3.14659	5.02064

Chapter 4

Thermal instability in Brinkman porous media with Cattaneo-Christov heat flux

This chapter follows on from the two previous chapters, which investigated thermal convection of an incompressible fluid in a saturated porous medium with low porosity and for low rates of flow which are described by Darcy's model for conservation of momentum.

To investigate convection in a porous medium when the porosity of a porous medium becomes sufficiently large, the Brinkman model is employed as a balance of linear momentum. This model has been devised by Brinkman [6], who found there was a relationship between the permeability and the porosity of a porous medium. A number of writers have employed the Brinkman model to investigate convection in porous media, namely, Rudraiah et al. [99], Vasseur et al. [135], and Vasseur and Robillard [136]. Recently the Brinkman equation has been considered by Rees [90], Hill and Straughan [50], Malashetty et al. [75], Wang and Tan [140], Shivakumara et al. [104], Kelliher et al. [57], Dhananjay et al. [29], and the account in the book by Straughan [116].

The underlying motives of this chapter are to investigate the behaviour of the onset of thermal convection in a fluid saturated porous media, when the Cattaneo-Christov theory for heat flux is involved. Here we revisit Straughan's work [117] but

this time in the context of the Brinkman model, for the case of rigid-rigid and free-free boundary conditions which have been studied by Straughan [115, p. 74] and Kuznetsov and Nield [61]. From the mathematical point of view, Rayleigh [69] argues that to ease the numerical difficulties in solving the mathematical modelling in the case of fixed surfaces, one may impose an appropriate choice of boundary conditions. In order to achieve this, it would be instructive to consider two free surfaces. We then solve our system numerically and consider inertia and the Brinkman term. To this end, basic equations and appropriate steady-state solutions are presented in Section 4.1. In Section 4.2, we describe the linear instability analysis. For free surfaces, the lowest instability boundary and oscillatory convection are given in Section 4.3 and 4.4 respectively. In Section 4.5, we consider the numerical method for fixed surfaces. The D^2 Chebyshev tau method is used. In the final section, 4.6, numerical results are presented.

4.1 Basic equations

We begin our study of thermal convection in a porous medium by considering a porous medium bounded by two horizontal infinite surfaces saturated with incompressible Newtonian fluid. The fluid velocity satisfies the Brinkman equation cf. Nield and Bejan [84] and Straughan [116],

$$\hat{a}v_{i,t} = -p_{,i} + k_i g \rho_0 \alpha T - \frac{\mu}{\mathrm{K}}v_i + \hat{\lambda}\Delta v_i, \qquad (4.1.1)$$

$$v_{i,i} = 0, \qquad (4.1.2)$$

where v_i is the pore averaged velocity, p is the pressure of the fluid, T is temperature, $\hat{a}$ is an inertia coefficient, ρ_0 is the constant density, μ is the dynamic viscosity, K is the permeability, $\hat{\lambda}$ referred to as an equivalent viscosity, $\mathbf{k} = (0, 0, 1)$, g is gravity, and α is the thermal expansion coefficient of the fluid, the Boussinesq approximation is assumed to be valid.

An averaged equation for porous medium and the constitutive equation of the heat flux when the Cattaneo-Christov heat flux model coupled to an energy balance

equation has been derived in [121] or [120]

$$\frac{1}{M}T_{,t} + v_i T_{,i} = -Q_{i,i}, \tag{4.1.3}$$

$$\tau Q_{i,t} + \tau_f(v_j Q_{i,j} - Q_j v_{i,j}) = -Q_i - \kappa T_{,i}. \tag{4.1.4}$$

where Q_i is the heat flux. We have introduced $v_i = \varphi V_i$ is the pore averaged fluid velocity, where V_i is the actual velocity of the fluid in the pores. φ is the porosity. The coefficients M and κ are given by

$$M = \frac{(\rho_0 c_p)_f}{(\rho_0 c)_m}, \qquad \kappa = \frac{k_m}{(\rho_0 c_p)_f},$$

where

$$k_m = \kappa_s(1 - \varphi) + \kappa_f \varphi,$$

$$(\rho_0 c)_m = \varphi(\rho_0 c_p)_f + (\rho_0 c)_s(1 - \varphi),$$

$$\tau = \varphi \tau_f + (1 - \varphi)\tau_s.$$

Here m, s, c referring to the porous medium, solid skeleton of the porous medium, and specific heat in the porous medium. The thermal diffusivity is denoted by κ. The coefficients τ_f and τ_s are the relaxation times for the fluid and solid in the porous medium. Further, c_p is the specific heat at constant pressure in the fluid and f represent the fluid.

Let us now consider a fluid saturated porous medium that satisfies equations (4.1.1)-(4.1.4) occupying the spatial domain $\Omega = \{(x, y) \in R^2\} \times \{z \in (0, d)\}$, and let $\mathbf{n}$ is the unit outward so that $\mathbf{n} = (0, 0, 1)$ on $z = d$ and $\mathbf{n} = (0, 0, -1)$ on $z = 0$. The appropriate boundary conditions are

$$v_i = 0, \qquad \text{at } z = 0, d, \tag{4.1.5}$$

$$T = T_L, \qquad z = 0; \quad T = T_U, \ z = d, \tag{4.1.6}$$

where T_L, T_U are constants with $T_L > T_U$. In addition the heat flux satisfies

$$\varepsilon_{ijk} n_j Q_k = 0, \qquad \text{at } z = 0, d. \tag{4.1.7}$$

We seek in the instability of the conduction solution of the system (4.1.1)-(4.1.4) in the domain Ω and satisfying the boundary conditions (4.1.5)-(4.1.7), given by cf. Straughan [121, p. 193].

$$\bar{v}_i \equiv 0, \qquad \bar{T} = -\beta z + T_L, \qquad \bar{\mathbf{Q}} = (0, 0, \kappa\beta)$$
$$\bar{p} = p_0 - g\rho_0 z - \frac{1}{2}\alpha\beta g\rho_0 z^2, \tag{4.1.8}$$

where

$$\beta = \frac{T_L - T_U}{d}.$$

In order to investigate the instability of the classic steady-state solutions (4.1.8), we begin by introducing perturbation $(u_i, \vartheta, q_i, \pi)$ to the solutions (4.1.8) in such a way that

$$v_i = \bar{v}_i + u_i, \qquad T = \bar{T} + \vartheta,$$

$$\bar{Q}_i = \bar{Q}_i + q_i, \qquad \bar{p} = \bar{p} + \pi.$$

The perturbation equations arising from equations (4.1.1)-(4.1.4),are

$$\hat{a}u_{i,t} = -\pi_{,i} + k_i g\rho_0\alpha\vartheta - \frac{\mu}{\mathrm{K}}u_i + \hat{\lambda}\Delta u_i,$$

$$u_{i,i} = 0,$$
$$\frac{1}{M}\vartheta_{,t} + u_i\vartheta_{,i} = -q_{i,i} + \beta w, \tag{4.1.9}$$

$$\tau q_{i,t} + \tau_f(-\beta\kappa u_{i,z} + u_j q_{i,j} - q_j u_{i,j}) = -q_i - \kappa\vartheta_{,i}.$$

To non-dimensionalise the equation (4.1.9). We define the non-dimensional quantities by

$$\mathbf{x} = d\mathbf{x}^*, \qquad \mathbf{u} = \frac{\mu d}{\rho_0\mathrm{K}}\mathbf{u}^*, \qquad \mathbf{q} = \kappa U\sqrt{\frac{\beta\mu}{\mathrm{K}\rho_0\alpha g\kappa}}\mathbf{q}^*,$$

$$t = \frac{\mathrm{K}\rho_0}{\mu}t^*, \qquad \pi = \frac{\mu Ud}{\mathrm{K}}\pi^*, \qquad \vartheta = dU\sqrt{\frac{\beta\mu}{\mathrm{K}\rho_0\alpha g\kappa}}\vartheta^*,$$

where U is a velocity scale, we also introduce the Prandtl number $Pr = \mu/\rho_0\kappa$ and the key non-dimensional numbers

$$R = \sqrt{\frac{\alpha g d^2\beta\mathrm{K}\rho_0}{\mu\kappa}}, \qquad Da = \frac{K}{d^2}, \qquad Sg = \frac{\tau\mu}{\rho_0 d^2}, \qquad \hat{\tau} = \frac{\tau_f}{\tau},$$

where $R = \sqrt{Ra}$ is the square root of the Rayleigh number, Da is the Darcy number, Sg is the Straughan number, see Papanicolaou et al. [85], and $\hat{\tau}$ is a relative relaxation time.

Upon substituting the above variables into equations (4.1.9), we obtain the nonlinear non-dimensional perturbation equations (omitting the stars)

$$Au_{i,t} = -\pi_{,i} + Rk_i\vartheta - u_i + \lambda\Delta u_i, \tag{4.1.10}$$

$$u_{i,i} = 0, \tag{4.1.11}$$

$$\frac{Pr}{Da}\left(\frac{1}{M}\vartheta_{,t} + u_i\vartheta_{,i}\right) = Rw - q_{i,i}, \tag{4.1.12}$$

$$\frac{Sg}{Da}q_{i,t} + \frac{\hat{\tau}Sg}{Da}\left(u_jq_{i,j} - q_ju_{i,j}\right) = -q_i - \vartheta_{,i} + \frac{\hat{\tau}SgR}{Pr}u_{i,z}, \tag{4.1.13}$$

where $\lambda = K\hat{\lambda}/d^2\mu$, and A is non-dimensional equivalents of $\hat{a}$. Equations (4.1.10)-(4.1.13) hold on $\{\Omega \times t > 0\}$ and the boundary conditions are

$$u_i = 0, \qquad \vartheta = 0, \qquad \varepsilon_{ijk}n_jq_k = 0, \qquad z = 0,1, \tag{4.1.14}$$

with $\{u_i, \vartheta, q_i, \pi\}$ satisfying a plane tiling periodicity in (x,y).

4.2 Linear instability

Here we study the linear instability analysis. To this end we first remove the non-linear terms of equations (4.1.12) and (4.1.13), then follow Straughan [118] by putting $Q = q_{i,i}$ to analyse the linear system.

$$Au_{i,t} + u_i = -\pi_{,i} + Rk_i\vartheta + \lambda\Delta u_i,$$

$$u_{i,i} = 0,$$

$$\frac{Pr}{MDa}\vartheta_{,t} = Rw - Q, \tag{4.2.1}$$

$$\frac{Sg}{Da}Q_{,t} = -Q - \Delta\vartheta.$$

It is convenient to define P_1 and P_2 by

$$P_1 = \frac{Pr}{MDa}, \qquad P_2 = \frac{Sg}{Da}. \tag{4.2.2}$$

Next, we perform the curl curl of equation $(4.2.1)_1$ to remove the pressure term, retaining only the third component and therefore we seek for solutions of the form

$$w = w(\mathbf{x})\, e^{\sigma t}, \qquad \vartheta = \vartheta(\mathbf{x})\, e^{\sigma t}, \qquad Q = Q(\mathbf{x})\, e^{\sigma t}.$$

By substituting into equation (4.2.1) and removal of exponential parts, setting $M = 1$, we have to solve the system

$$-\lambda \Delta^2 w + (\sigma A + 1)\, \Delta w = R\, \Delta^* \vartheta,$$
$$\sigma P_1 \vartheta = Rw - Q, \qquad\qquad (4.2.3)$$
$$\sigma P_2 Q = -\Delta \vartheta - Q,$$

where $\Delta^* = \partial^2/\partial x^2 + \partial^2/\partial y^2$ is the horizontal Laplacian operator.

4.3 Free surfaces

To illustrate what is happening and gives the exact result of system (4.2.3), we here consider the case of the stress–free surfaces.

Let us now consider the case when instability sets in as stationary convection. We refer the reader to Chandrasekhar's book [19]. To this end, we put $\sigma = 0$ into the equation (4.2.3), which yields the following system

$$-\lambda \Delta^2 w + \Delta w = R\, \Delta^* \vartheta,$$
$$Rw = Q, \qquad\qquad (4.3.1)$$
$$\Delta \vartheta = -Q.$$

We recall that $Rw = Q = -\Delta \vartheta$, therefore equation (4.3.1) can be written as

$$-\lambda \Delta^3 w + \Delta^2 w = -R^2\, \Delta^* w. \qquad\qquad (4.3.2)$$

Assume normal mode representation w of the form

$$w = W(z) f(x, y), \qquad\qquad (4.3.3)$$

where f is the horizontal plan form which satisfies $\Delta^* f = -a^2 f$, $D = d/dz$, a is a wave number, and $\Delta = D^2 - a^2$. For two free bounded surfaces, allow to be

composed of $\sin n\pi z$, for $n \in \mathbb{N}$. Hence for $w = w_{zz} = 0$ and applying equation (4.3.3) into equation (4.3.2), we obtain

$$R^2 = \frac{\lambda\Lambda_n^3 + \Lambda_n^2}{a^2}, \tag{4.3.4}$$

where $\Lambda_n = n^2\pi^2 + a^2$. Minimization over n yields $n = 1$. In addition we can find the critical wave number a_c by (4.3.4) minimizing over a^2 which minimizes the Rayleigh number.

It now follows from equation (4.3.4)

$$2\lambda a^4 + (1 + \lambda\pi^2)a^2 - (\lambda\pi^2 + 1)\pi^2 = 0. \tag{4.3.5}$$

Which leads to

$$a_c^2 = \frac{-(1 + \lambda\pi^2) + \sqrt{(1 + \lambda\pi^2)((1 + \lambda\pi^2) + 8\lambda\pi^2)}}{4\lambda}. \tag{4.3.6}$$

Consequently, the stationary convection boundary

$$R_{sc}^2 = \frac{\left(3\lambda\pi^2 - 1 + \sqrt{(1 + \lambda\pi^2)(1 + 9\lambda\pi^2)}\right)^2}{16\lambda\left(\sqrt{(1 + \lambda\pi^2)(1 + 9\lambda\pi^2)} - (1 + \lambda\pi^2)\right)}$$
$$\times \left[3(\lambda\pi^2 + 1) + \sqrt{(1 + \lambda\pi^2)(1 + 9\lambda\pi^2)}\right]. \tag{4.3.7}$$

In equation (4.3.5) that when $\lambda \to 0$, we turn to the Darcy porous problem [117]

$$a_c^2 = \pi^2, \qquad R_{sc}^2 = 4\pi^2,$$

whereas we recover the fluid model for two free surfaces [118] as $\lambda \to \infty$

$$a_c^2 = \frac{\pi^2}{2}, \qquad R_{sc}^2 = \frac{27\pi^4}{4}.$$

Numerical results obtained for stationary convection are reported in Section 4.6.

4.4   Oscillatory convection for two free surfaces

In this Section we consider oscillatory convection for two free surfaces following the Chandrasekhar [19] method, and put $\sigma = i\sigma_1$, $\sigma_1 \in \mathbb{R}$ into equation (4.2.3). By equating real and imaginary parts, we may have the equations

$$\sigma_1^2 = \frac{1}{P_1 P_2}\left(\Lambda - \frac{P_1}{P_2} - \frac{A\Lambda}{P_2(1 + \lambda\Lambda)}\right), \tag{4.4.1}$$

and

$$R^2 = \frac{\beta_3 \Lambda^3 + \beta_2 \Lambda^2 + \beta_1 \Lambda}{a^2(B_1 \Lambda + B_2)}, \tag{4.4.2}$$

where

$$\beta_3 = \lambda^2 P_1,$$
$$\beta_2 = \frac{\lambda A P_1}{P_2} + \frac{A^2}{P_2} + 2\lambda P_1,$$
$$\beta_1 = \frac{P_1 A}{P_2} + P_1, \tag{4.4.3}$$
$$B_1 = \lambda P_2,$$
$$B_2 = P_2.$$

It should be noted that oscillatory convection requires $\sigma_1^2 > 0$. For $\lambda = 0$ and $A = 1$, we have Straughan's work in the Darcy model [117], and equations (4.4.2) and (4.4.3) consistent with that found by Straughan [118] when $\lambda = 1$ and $A = 1$, see also Straughan [121, p. 235].

Indeed, numerical techniques are used to find R_{osc}^2 by minimizing R^2 in equation (4.4.2) over a^2. Numerical results are approximated to three decimal places. However, the values of P_2 selected are such that $\sigma_1^2 > 0$ so oscillatory convection will be possible. This is explained in details in the Section 4.6.

4.5   Numerical method; fixed surfaces

In this section, the D^2 Chebyshev tau method (see Appendix B) will be used to solve equation (4.2.3), subject to the boundary conditions

$$w = w_z = \vartheta = 0, \qquad \text{at } z = 0. \tag{4.5.1}$$

This method is described in more detail in Dongarra et al. [31] and Straughan [116]. To this end, we first write $(4.2.3)_1$ as a system of second order equations by setting $\chi = \Delta w$, resetting the domain from $(0, 1)$ to $(-1, 1)$, selecting $\hat{z} = 2z - 1$. We then write (omitting the hat)

$$w = W(z)f(x, y), \qquad \chi = \chi(z)f(x, y),$$

$$\vartheta = \Theta(z)f(x, y), \qquad Q = Q(z)f(x, y).$$

Note that

$$D = \frac{d}{dz} = 2\frac{d}{d\hat{z}} \qquad and \qquad \Delta = 4D^2 - a^2.$$

Thus equation (4.2.3) may be written in the form

$$\begin{aligned}
\Delta W - \chi &= 0, \\
(\lambda\Delta - 1)\chi - a^2 R\Theta &= \sigma A\chi, \\
\Delta\Theta + Q &= -\sigma P_2 Q, \\
-Rw + Q &= -\sigma P_1\Theta.
\end{aligned} \qquad (4.5.2)$$

We now write W, χ, Θ, Q in the form of a series of Chebyshev polynomials. Truncating each sum, we have

$$W(z) = \sum_{n=0}^{N} W_n T_n(z), \qquad \chi(z) = \sum_{n=0}^{N} \chi_n T_n(z),$$

$$\Theta(z) = \sum_{n=0}^{N} \Theta_n T_n(z), \qquad Q(z) = \sum_{n=0}^{N} Q_n T_n(z).$$

Recalling the boundary conditions (4.5.1), where the relations $T_n(\pm 1) = (\pm 1)^n$, $T_n'(\pm 1) = (\pm 1)^{n-1}n^2$ are used, then

$$\begin{aligned}
BC1: & \ W_0 + W_2 + W_4 + \cdots + W_{N-1} = 0, \\
BC2: & \ W_1 + W_3 + W_5 + \cdots + W_N = 0, \\
BC3: & \ W_1 + 3^2 W_3 + 5^2 W_5 + \cdots + N^2 W_N = 0, \\
BC4: & \ 4W_2 + 4^2 W_4 + \cdots + (N-1)^2 W_{N-1} = 0, \\
BC5: & \ \Theta_0 + \Theta_2 + \Theta_4 + \cdots \Theta_{N-1} = 0, \\
BC6: & \ \Theta_1 + \Theta_3 + \Theta_5 + \cdots \Theta_N = 0.
\end{aligned}$$

Letting $\mathbf{x} = (W_0, \cdots, W_N, \chi_0, \cdots, \chi_N, \Theta_0, \cdots, \Theta_N, Q_0, \cdots, Q_N)$, equation (4.5.2) can be written in the matrix form

$$A\mathbf{x} = \sigma B\mathbf{x},$$

where A and B are $(N+1) \times (N+1)$ matrix given by

$$
A = \begin{pmatrix}
\Delta & -I & 0 & 0 \\
BC1 & 0\cdots 0 & 0\cdots 0 & 0\cdots 0 \\
BC2 & 0\cdots 0 & 0\cdots 0 & 0\cdots 0 \\
0 & \lambda\Delta - I & -a^2 R I & 0 \\
BC3 & 0\cdots 0 & 0\cdots 0 & 0\cdots 0 \\
BC4 & 0\cdots 0 & 0\cdots 0 & 0\cdots 0 \\
0 & 0 & \Delta & I \\
0\cdots 0 & 0\cdots 0 & BC5 & 0\cdots 0 \\
0\cdots 0 & 0\cdots 0 & BC6 & 0\cdots 0 \\
-RI & 0 & 0 & I
\end{pmatrix},
$$

$$
B = \begin{pmatrix}
0 & 0 & 0 & 0 \\
0\cdots 0 & 0\cdots 0 & 0\cdots 0 & 0\cdots 0 \\
0\cdots 0 & 0\cdots 0 & 0\cdots 0 & 0\cdots 0 \\
0 & AI & 0 & 0 \\
0\cdots 0 & 0\cdots 0 & 0\cdots 0 & 0\cdots 0 \\
0\cdots 0 & 0\cdots 0 & 0\cdots 0 & 0\cdots 0 \\
0 & 0 & 0 & -P_2 I \\
0\cdots 0 & 0\cdots 0 & 0\cdots 0 & 0\cdots 0 \\
0\cdots 0 & 0\cdots 0 & 0\cdots 0 & 0\cdots 0 \\
0 & 0 & -P_1 I & 0
\end{pmatrix}.
$$

We solved the above matrix system by using the QZ algorithm. Numerical results are approximated to three decimal, as presented in the next section.

4.6 Numerical results

4.6.1 Free surfaces

We report our findings for critical Rayleigh numbers R_a, wave numbers a_c, and the eigenvalues σ_1 in Tables 4.1– 4.3, respectively, with $\lambda = 0.5, 1, 2$, for fixed value of $P_1 = 6$, $A = 1, 2, 4$, and for various values of P_2 starting from the minimum

value which relates to existence of oscillatory convection. Oscillatory convection corresponds to $\sigma_1 \neq 0$, also the critical Rayleigh number R_a plotted against P_2 in the Figures 4.1–4.3.

From equation (4.3.4), the stationary convection boundary was found to be dependent on the Brinkman term λ but not on the inertia term A , while from equation (4.4.2), the oscillatory convection depends on the Brinkman term λ, inertia A, and the quantity P_2. However, as shown in Figures 4.1–4.3, the onset of thermal instability strongly depends on λ and A. One can see the increase in the Brinkman term λ leads to convection occuring more easily. It is also observed that the onset of convection is more likely to be via oscillatory convection, when λ increases with the decreasing of the inertia term A
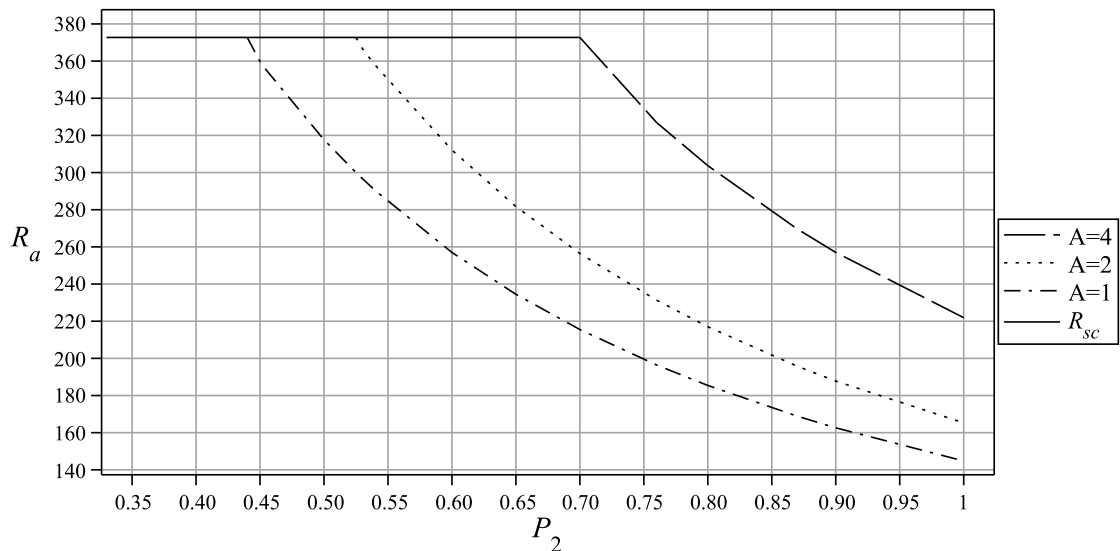
Figure 4.1: Critical values of Ra vs. P_2 for two free surfaces, with $P_1 = 6$, and $\lambda = 0.5$. The solid curve is for stationary convection. The dotted curves are for oscillatory convection, for $A = 1, 2, 4$.

To illustrate how the Brinkman term λ, the inertia term A, and beyond the quantity P_2 effect the onset of thermal instability, let us take an example. From Table 4.1 $\lambda = 0.5$, in case $A = 1$, it was found that the oscillatory convection was possible when $P_2 \geq 0.33$ and the transition of instability from stationary convection to oscillatory convection is for P_2 in the interval $P_2 \in [0.43, 0.44]$. Note that the wave

number became significantly higher at the transition, which leads to cells becoming narrower.
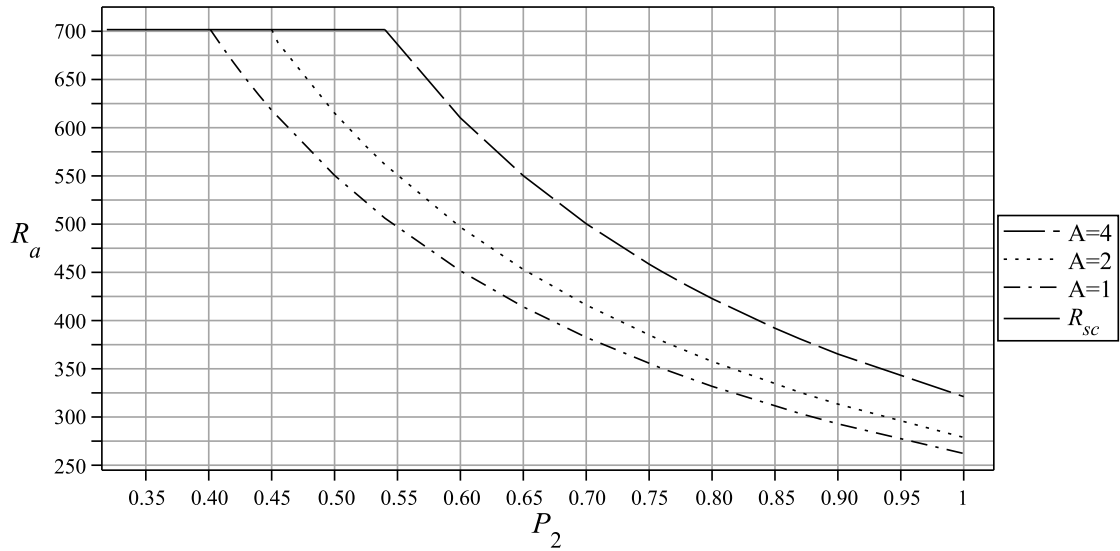
Figure 4.2: Critical values of Ra vs. P_2 for two free surfaces, with $P_1 = 6$, and $\lambda = 1$. The solid curve is for stationary convection. The dotted curves are for oscillatory convection, for $A = 1, 2, 4$.
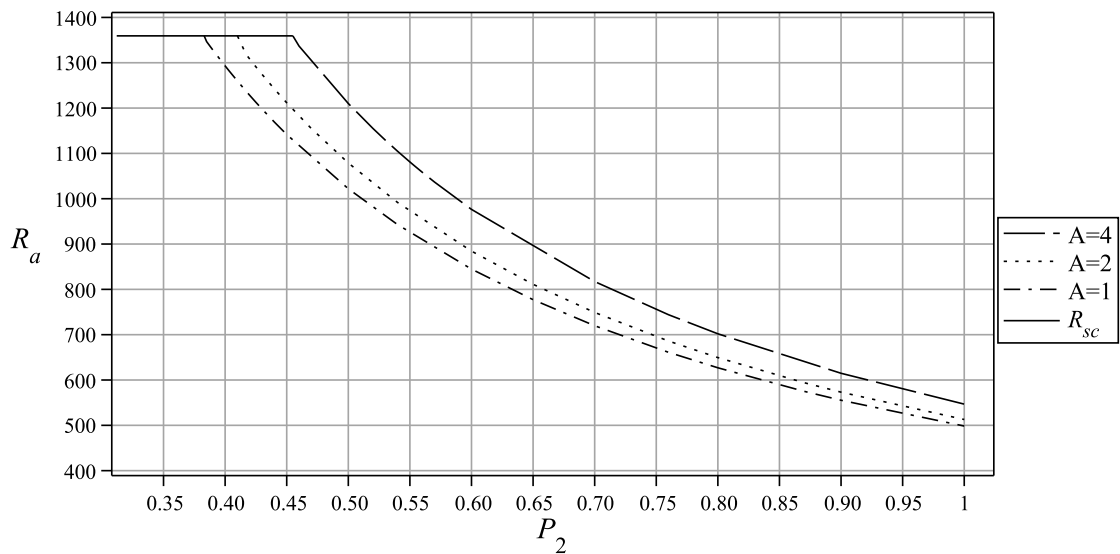
Figure 4.3: Two free surfaces. Critical values of Ra vs. P_2, with $P_1 = 6$, and $\lambda = 2$. The solid curve is for stationary convection. The dotted curves are for oscillatory convection, for $A = 1, 2, 4$.

From Figures 4.1–4.3 (and from Tables 4.1– 4.3) we observe that as A increases from $A = 1$ to $A = 2$ and then $A = 4$ the convection cells continue to become narrower, and the oscillatory convection boundary decreases below the stationary convection boundary which remains at a constant value (a different constant value for each A). It may be observed that for $A = 2$, the transition is in the interval $P_2 \in [0.5, 0.525]$, whereas when $A = 4$, the transition is in the interval $P_2 \in [0.65, 0.7]$. A similar interpretations for $\lambda = 1$ and $\lambda = 2$ are given in Table 4.2 and Table 4.3 respectively.

It is evident that, once λ increases with decrease of A, for example, when λ increases to $\lambda = 2$ in case $A = 1$, the stationary mode, however, changes earlier to the oscillatory mode in the interval $P_2 \in [0.38, 0.383]$ as seen in Table 4.3.

Table 4.1: Two free surfaces. Critical values of Rayleigh number R_a, wave number a_c vs. P_2, for $P_1 = 6$, $\lambda = 0.5$.

P_2	a_c	R_a	σ_1	a_c	R_a	σ_1	a_c	R_a	σ_1
		$A = 1$			$A = 2$			$A = 4$	
0.33–100	2.289	372.722	0	2.289	372.722	0	2.289	372.722	0
0.33	3.729	523.796	±0.034	. . .	. . .	. . .	. . .	. . .	. . .
0.3383	3.720	507.994	±0.506	. . .	. . .	. . .	. . .	. . .	. . .
0.343	3.7157	499.446	±0.624	. . .	. . .	. . .	. . .	. . .	. . .
0.3634	3.695	465.336	±0.943	4.109	609.427	±0.041	. . .	. . .	. . .
0.372	3.687	452.265	±1.032	4.095	590.063	±0.478	. . .	. . .	. . .
0.378	3.681	443.557	±1.086	4.086	577.208	±0.612	. . .	. . .	. . .
0.38	3.680	440.726	±1.102	4.083	573.036	±0.649	. . .	. . .	. . .
0.383	3.677	436.544	±1.126	4.078	566.881	±0.699	. . .	. . .	. . .
0.385	3.675	433.798	±1.141	4.075	562.845	±0.730	. . .	. . .	. . .
0.388	3.673	429.741	±1.163	4.070	556.888	±0.773	. . .	. . .	. . .
0.39	3.671	427.077	±1.176	4.067	552.981	±0.799	. . .	. . .	. . .
0.4	3.663	414.221	±1.239	4.053	534.177	±0.913	. . .	. . .	. . .
0.401	3.662	412.976	±1.244	4.051	532.361	±0.923	. . .	. . .	. . .
0.4013	3.662	412.604	±1.246	4.051	531.728	±0.926	. . .	. . .	. . .
0.40135	3.662	412.542	±1.246	4.051	531.728	±0.927	. . .	. . .	. . .
0.403	3.661	410.509	±1.255	4.049	528.763	±0.943	. . .	. . .	. . .
0.41	3.655	402.092	±1.292	4.039	516.516	±1.005	. . .	. . .	. . .
0.417	3.650	394.003	±1.324	4.029	504.780	±1.059	4.758	803.622	±0.143
0.425	3.644	385.135	±1.357	4.019	491.957	±1.114	4.741	780.229	±0.444
0.43	3.640	379.787	±1.376	4.012	484.244	±1.144	4.731	766.196	±0.548
0.44	3.634	369.511	±1.411	3.9997	469.469	±1.199	4.710	739.401	±0.702
0.45	3.627	359.761	±1.440	3.988	455.507	±1.246	4.690	714.182	±0.817
0.455	3.624	355.070	±1.454	3.982	448.811	±1.267	4.680	702.124	±0.865
0.5	3.597	317.665	±1.542	3.933	395.895	±1.405	4.599	607.727	±1.153
0.525	3.584	300.027	±1.572	3.909	371.261	±1.454	4.558	564.366	±1.248
0.54	3.577	290.334	±1.586	3.895	357.814	±1.478	4.535	540.866	±1.293
0.6	3.551	257.003	±1.618	3.847	312.099	±1.537	4.450	461.962	±1.413
0.65	3.533	234.472	±1.625	3.812	281.691	±1.559	4.389	410.406	±1.467
0.7	3.517	215.517	±1.622	3.781	256.441	±1.567	4.335	368.234	±1.496
1.	3.454	144.778	±1.526	3.654	165.276	±1.502	4.099	221.892	±1.485
4.	3.333	33.469	±0.890	3.392	34.813	±0.889	3.548	38.678	±0.893
10	3.307	13.165	±0.578	3.332	13.383	±0.577	3.400	14.017	±0.579

Table 4.2: Two free surfaces. Critical values of Rayleigh number R_a, wave number a_c vs. P_2, for $P_1 = 6$, $\lambda = 1$.

P_2	A = 1			A = 2			A = 4		
	a_c	R_a	σ_1	a_c	R_a	σ_1	a_c	R_a	σ_1
0.319–100	2.257	701.689	0	2.257	701.689	0	2.257	701.689	0
0.319	3.457	908.511	±0.094	. . .	. . .	. . .	. . .	. . .	. . .
0.321	3.456	902.078	±0.273	. . .	. . .	. . .	. . .	. . .	. . .
0.323	3.455	895.734	±0.372	. . .	. . .	. . .	. . .	. . .	. . .
0.33	3.450	874.203	±0.592	. . .	. . .	. . .	. . .	. . .	. . .
0.3383	3.445	849.957	±0.761	3.679	987.722	±0.015	. . .	. . .	. . .
0.343	3.442	836.805	±0.836	3.674	970.952	±0.371	. . .	. . .	. . .
0.3634	3.431	784.079	±1.071	3.653	904.069	±0.808	. . .	. . .	. . .
0.372	3.426	763.764	±1.142	3.644	878.453	±0.914	4.081	1160.673	±0.123
0.378	3.423	750.195	±1.185	3.638	861.391	±0.977	4.071	1135.157	±0.406
0.38	3.422	745.777	±1.199	3.637	855.845	±0.996	4.068	1126.877	±0.461
0.383	3.421	739.245	±1.218	3.634	847.652	±1.023	4.063	1114.663	±0.532
0.385	3.420	734.953	±1.231	3.632	842.274	±1.0398	4.060	1106.653	±0.573
0.388	3.418	728.607	±1.248	3.629	834.328	±1.064	4.055	1094.833	±0.628
0.39	3.417	724.435	±1.260	3.628	829.111	±1.080	4.052	1087.080	±0.661
0.4	3.413	704.267	±1.312	3.619	803.938	±1.150	4.037	1049.776	±0.799
0.401	3.412	702.310	±1.316	3.618	801.501	±1.156	4.035	1046.174	±0.811
0.4013	3.412	701.726	±1.318	3.618	800.773	±1.158	4.035	1045.098	±0.814
0.40135	3.412	701.628	±1.318	3.618	800.652	±1.159	4.035	1044.919	±0.815
0.403	3.412	698.430	±1.326	3.616	796.671	±1.1689	4.032	1039.038	±0.833
0.41	3.409	685.177	±1.356	3.611	780.197	±1.209	4.022	1014.747	±0.905
0.417	3.406	672.412	±1.383	3.605	764.366	±1.246	4.012	991.477	±0.967
0.425	3.402	658.387	±1.411	3.599	747.018	±1.283	4.001	966.055	±1.028
0.43	3.400	649.911	±1.427	3.595	736.556	±1.304	3.994	950.766	±1.062
0.44	3.397	633.591	±1.456	3.588	716.459	±1.341	3.981	921.487	±1.123
0.45	3.393	618.062	±1.481	3.581	697.395	±1.374	3.968	893.824	±1.175
0.455	3.391	610.576	±1.493	3.577	688.227	±1.389	3.962	880.560	±1.198
0.5	3.377	550.501	±1.566	3.549	615.156	±1.487	3.911	775.799	±1.350
0.525	3.370	521.931	±1.591	3.535	580.733	±1.522	3.885	727.070	±1.404
0.54	3.366	506.158	±1.602	3.528	561.823	±1.537	3.871	700.482	±1.429
0.6	3.352	451.518	±1.626	3.500	496.851	±1.575	3.819	610.168	±1.496
0.65	3.342	414.206	±1.628	3.481	452.982	±1.586	3.782	550.162	±1.522
0.7	3.334	382.560	±1.622	3.464	416.108	±1.586	3.750	500.386	±1.533
1.	3.300	262.138	±1.517	3.396	278.806	±1.499	3.614	321.136	±1.477
4.	3.239	63.027	±0.881	3.265	64.098	±0.879	3.265	64.098	±0.868
10	3.227	25.008	±0.571	3.237	25.180	±0.571	3.265	25.634	±0.571

Table 4.3: Two free surfaces. Critical values of Rayleigh number R_a, wave number a_c vs. P_2, for $P_1 = 6$, $\lambda = 2$.

P_2	$A = 1$			$A = 2$			$A = 4$		
	a_c	R_a	σ_1	a_c	R_a	σ_1	a_c	R_a	σ_1
0.312–100	2.240	1359.315	0	2.240	1359.315	0	2.240	1359.315	0
0.312	3.306	1685.793	±0.029	. . .	. . .	. . .	. . .	. . .	. . .
0.319	3.303	1646.077	±0.480	. . .	. . .	. . .	. . .	. . .	. . .
0.321	3.302	1635.069	±0.541	. . .	. . .	. . .	. . .	. . .	. . .
0.323	3.302	1624.206	±0.594	3.426	1758.158	±0.047	. . .	. . .	. . .
0.33	3.299	1587.292	±0.743	3.421	1715.748	±0.466	. . .	. . .	. . .
0.3383	3.296	1545.629	±0.876	3.416	1667.997	±0.671	. . .	. . .	. . .
0.343	3.295	1522.988	±0.938	3.413	1642.098	±0.756	3.653	1913.926	±0.087
0.3634	3.289	1431.909	±1.140	3.401	1538.288	±1.013	3.631	1781.484	±0.729
0.372	3.286	1396.683	±1.203	3.396	1498.300	±1.090	3.623	1730.772	±0.847
0.378	3.285	1373.112	±1.2415	3.393	1471.593	±1.136	3.617	1697.000	±0.915
0.38	3.284	1365.430	±1.253	3.392	1462.899	±1.150	3.615	1686.022	±0.936
0.383	3.284	1354.066	±1.271	3.391	1450.044	±1.171	3.612	1669.808	±0.965
0.385	3.283	1346.594	±1.282	3.3898	1441.598	±1.18398	3.610	1659.163	±0.984
0.388	3.282	1335.538	±1.298	3.388	1429.109	±1.203	3.607	1643.439	±1.010
0.39	3.282	1328.268	±1.308	3.387	1420.900	±1.215	3.606	1633.114	±1.027
0.4	3.280	1293.068	±1.355	3.383	1381.215	±1.2697	3.597	1583.303	±1.102
0.401	3.279	1289.650	±1.359	3.382	1377.367	±1.275	3.596	1578.482	±1.108
0.4013	3.279	1288.628	±1.360	3.382	1376.216	±1.276	3.596	1577.041	±1.110
0.40135	3.279	1288.458	±1.360	3.382	1376.025	±1.276	3.595	1576.802	±1.1108
0.403	3.279	1282.868	±1.367	3.381	1369.733	±1.285	3.594	1568.925	±1.122
0.41	3.277	1259.679	±1.395	3.378	1343.6595	±1.317	3.588	1536.332	±1.165
0.417	3.276	1237.310	±1.419	3.375	1318.548	±1.345	3.582	1505.018	±1.203
0.425	3.274	1212.696	±1.445	3.372	1290.961	±1.375	3.576	1470.703	±1.242
0.43	3.273	1197.802	±1.459	3.3697	1274.291	±1.392	3.572	1450.012	±1.264
0.44	3.271	1169.081	±1.485	3.366	1242.195	±1.422	3.564	1410.271	±1.304
0.45	3.269	1141.702	±1.508	3.362	1211.658	±1.449	3.557	1372.579	±1.339
0.455	3.268	1128.485	±1.518	3.360	1196.9401	±1.461	3.554	1354.454	±1.355
0.5	3.260	1021.977	±1.584	3.345	1078.848	±1.539	3.525	1210.043	±1.458
0.525	3.257	971.041	±1.605	3.338	1022.706	±1.566	3.510	1142.044	±1.495
0.54	3.255	942.8397	±1.615	3.334	991.718	±1.578	3.502	1104.699	±1.512
0.6	3.247	844.683	±1.633	3.319	884.398	±1.604	3.474	976.441	±1.553
0.65	3.242	777.229	±1.633	3.309	811.143	±1.608	3.454	889.892	±1.566
0.7	3.238	719.736	±1.625	3.301	749.034	±1.603	3.437	817.179	±1.567
1.	3.221	498.404	±1.514	3.266	512.8697	±1.503	3.366	546.757	±1.486
4.	3.191	122.217	±0.876	3.203	123.134	±0.875	3.2299	125.314	±0.874
10	3.185	48.695	±0.568	3.189	48.842	±0.568	3.201	49.193	±0.567

4.6.2   Fixed surfaces

In this section, we display our numerical results in Tables 4.4–4.6, respectively, with $\lambda = 0.5, 1, 2$ for varying value of P_2, and for fixed value of $P_1 = 6$. These results are obtained by using using D^2 Chebyshev tau method coupled with QZ algorithm. The critical Rayleigh numbers and the critical wave numbers for the oscillatory mode correspond to $\sigma_1 \neq 0$. Figures 4.4–4.6 represent the critical Rayleigh numbers R_a against the quantity P_2.

In Figure 4.4–4.6, we display the effects of the Brinkman term λ, with inertia term A on thermal instability R_a. For $A = 1$ and $A = 4$, once λ increased will advance the oscillatory convection and the transition from stationary to oscillatory mode will occur earlier at small value of P_2.
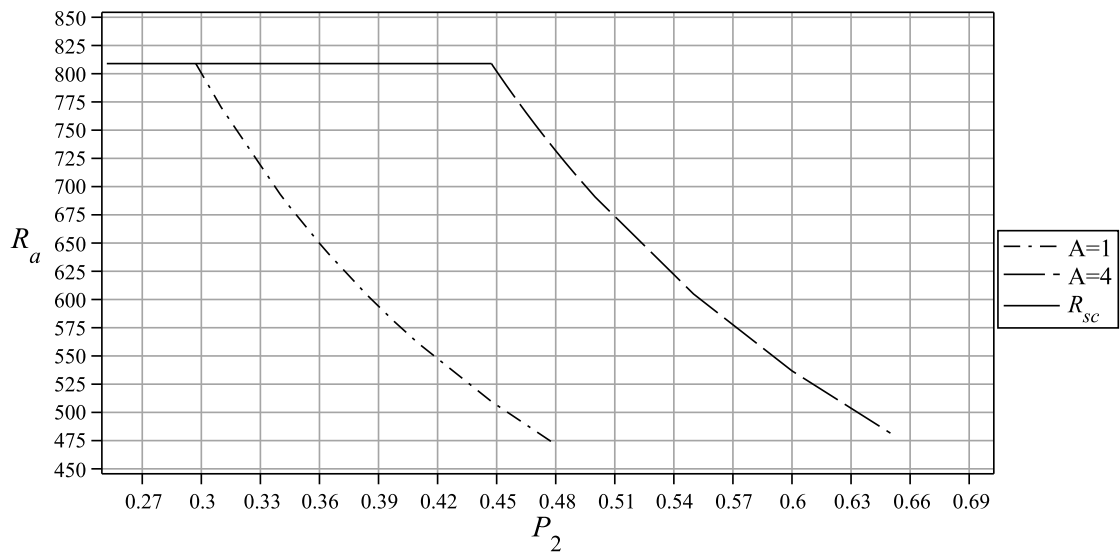
Figure 4.4: Two fixed surfaces. Critical values of Ra vs. P_2 , with $P_1 = 6$, and $\lambda = 0.5$. The solid curve is for stationary convection. The dotted curves are for oscillatory convection, for $A = 1, 4$.
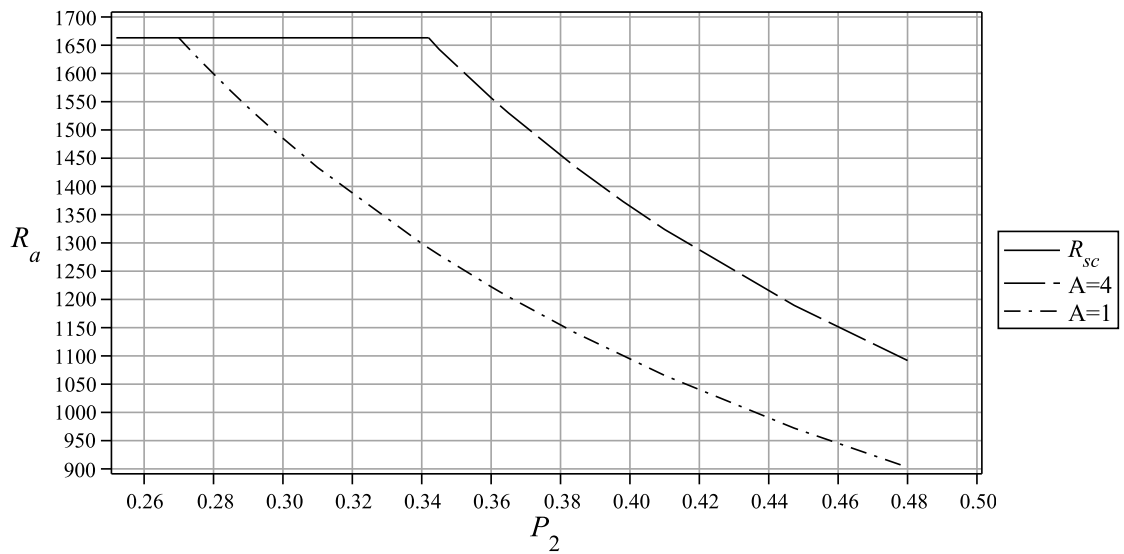
Figure 4.5: Two fixed surfaces. Critical values of Ra vs. P_2, with $P_1 = 6$, and $\lambda = 1$. The solid curve is for stationary convection. The dotted curves are for oscillatory convection, for $A = 1, 4$.
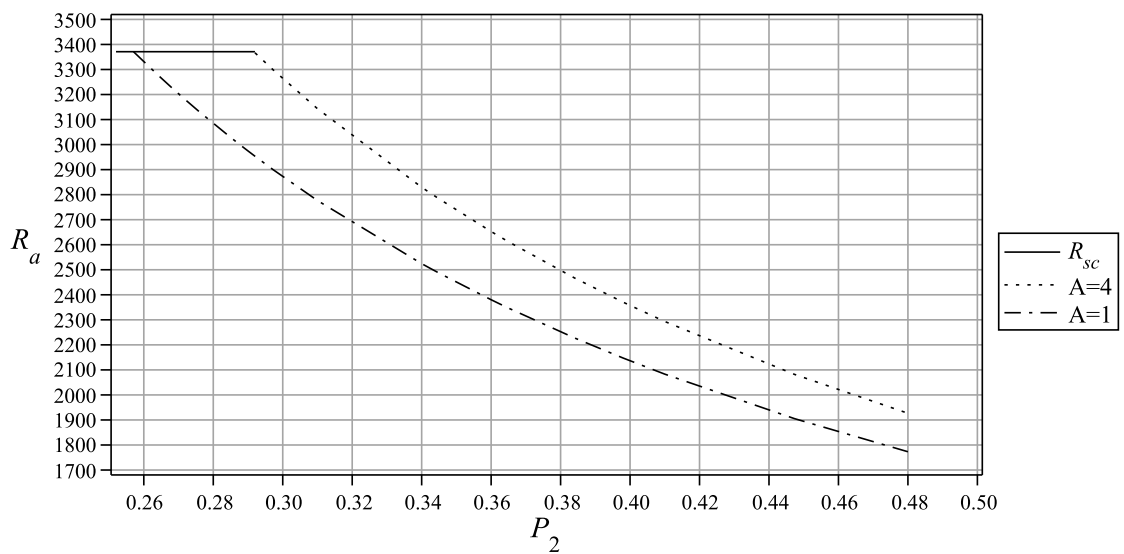
Figure 4.6: Two fixed surfaces. Critical values of Ra vs. P_2, with $P_1 = 6$, and $\lambda = 2$. The solid curve is for stationary convection. The dotted curves are for oscillatory convection, for $A = 1, 4$.

Tables 4.4–4.6 demonstrate the effects of the Brinkman term λ increasing from $\lambda = 0.5$ to $\lambda = 2$ with inertia term A on the dominant mode of instability and the transition within the interval P_2.

Table 4.6 confirms the effects of increase λ to $\lambda = 2$, the transition from stationary to oscillatory mode occurs at smaller value of P_2. For example, when $A = 1$ the transition is for P_2 in the interval $P_2 \in [0.25703, 0.25704]$ and the cells become narrower due to the intense increasing of the critical wave number at the transition from stationary to oscillatory convection.

Table 4.4: Two fixed surfaces. Critical values of Rayleigh number R_a, wave number a_c vs. P_2, for $P_1 = 6$, $\lambda = 0.5$.

P_2	a_c	R_a	σ_1	a_c	R_a	σ_1
		$A = 1$			$A = 4$	
0.255–0.48	3.07	808.958	0	3.07	808.958	0
0.255	4.9	966.540	± 1.728	. . .	. . .	. . .
0.2568	4.89	958.594	± 1.743	. . .	. . .	. . .
0.25702	4.89	957.631	± 1.747	. . .	. . .	. . .
0.25703	4.89	957.588	± 1.747	. . .	. . .	. . .
0.25704	4.89	957.543	± 1.747	. . .	. . .	. . .
0.264	4.89	928.046	± 1.859	. . .	. . .	. . .
0.2676	4.89	913.476	± 1.910	. . .	. . .	. . .
0.2688	4.89	908.719	± 1.926	. . .	. . .	. . .
0.27	4.88	904.010	± 1.927	. . .	. . .	. . .
0.272	4.88	896.266	± 1.952	. . .	. . .	. . .
0.285	4.87	848.939	± 2.078	. . .	. . .	. . .
0.288	4.87	838.705	± 2.105	. . .	. . .	. . .
0.29	4.87	832.016	± 2.122	. . .	. . .	. . .
0.292	4.87	825.431	± 2.138	. . .	. . .	. . .
0.2972	4.87	808.780	± 2.178	. . .	. . .	. . .
0.31	4.86	770.473	± 2.250	. . .	. . .	. . .
0.34	4.84	693.313	± 2.360	5.31	1208.491	± 0.999
0.342	4.84	688.707	± 2.365	5.3	1197.939	± 1.024
0.345	4.84	681.910	± 2.375	5.3	1182.415	± 1.091
0.36	4.84	649.818	± 2.413	5.28	1109.888	± 1.323
0.365	4.83	639.773	± 2.414	5.27	1087.450	± 1.377
0.384	4.83	604.245	± 2.445	5.24	1009.133	± 1.55
0.398	4.82	580.465	± 2.4534	5.23	957.639	± 1.660
0.41	4.82	561.508	± 2.463	5.21	917.134	± 1.723
0.4473	4.81	509.696	± 2.468	5.17	808.983	± 1.875
0.4474	4.81	509.570	± 2.470	5.17	808.725	± 1.875
0.48	4. 8	471.491	± 2.457	5.14	731.730	± 1.956
1.2	4.73	177.179	± 1.902	4.88	219.363	± 1.816
1.8	4.71	116.433	± 1.610	4.82	135.249	± 1.567
2.8	4.7	74.076	± 1.321	4.77	81.874	± 1.300
4	4.69	51.562	± 1.117	4.74	55.389	± 1.106
10	4.69	20.461	± 0.720	4.71	21.075	± 0.717

Table 4.5: Two fixed surfaces. Critical values of Rayleigh number R_a, wave number a_c vs. P_2, for $P_1 = 6$, $\lambda = 1$.

P_2	A = 1			A = 4		
	a_c	R_a	σ_1	a_c	R_a	σ_1
0.255–0.31	3.1	1663.124	0	3.1	1663.124	0
0.31–0.41	. . .	. . .	. . .	3.1	1663.124	0
0.255	4.83	1769.049	±2.122	5.14	2431.432	±0.767
0.2568	4.83	1755.612	±2.143	5.13	2408.837	±0.829
0.25702	4.83	1753.983	±2.145	5.13	2406.102	±0.841
0.25703	4.83	1753.909	±2.145	5.13	2405.978	±0.841
0.25704	4.83	1753.835	±2.145	5.13	2405.854	±0.842
0.264	4.83	1703.834	±2.217	5.12	2322.264	±1.104
0.2676	4.83	1679.068	±2.250	5.12	2281.134	±1.220
0.2688	4.83	1670.972	±2.261	5.12	2267.728	±1.255
0.27	4.83	1662.953	±2.271	5.12	2254.469	±1.289
0.272	4.83	1649.756	±2.287	5.11	2232.692	±1.321
0.285	4.83	1568.812	±2.377	5.1	2100.265	±1.581
0.288	4.82	1551.243	±2.3833	5.09	2071.788	±1.616
0.29	4.82	1539.746	±2.394	5.09	2053.203	±1.649
0.292	4.82	1528.419	±2.405	5.09	2034.931	±1.680
0.2972	4.82	1499.729	±2.431	5.08	1988.836	±1.739
0.31	4.81	1433.480	±2.473	5.07	1883.277	±1.878
0.34	4.81	1298.927	±2.552	5.04	1673.544	±2.083
0.342	4.81	1290.847	±2.556	5.04	1661.132	±2.095
0.345	4.81	1278.914	±2.561	5.04	1642.840	±2.112
0.36	4.8	1222.399	±2.572	5.03	1556.866	±2.176
0.365	4.8	1204.652	±2.577	5.02	1530.092	±2.188
0.384	4.8	1141.657	±2.5901	5.01	1435.925	±2.244
0.398	4.8	1099.292	±2.594	5.0	1373.372	±2.273
0.41	4.8	1065.399	±2.588	4.99	1323.786	±2.291
0.4473	4.79	972.206	±2.578	4.97	1189.569	±2.329
0.4474	4.79	971.978	±2.578	4.97	1189.244	±2.329
0.48	4.8	902.947	±2.553	4.96	1091.881	±2.344
1.2	4.75	351.355	±1.931	4.82	381.383	±1.889
1.8	4.74	232.807	±1.628	4.79	246.382	±1.607
2.8	4.74	149.01	±1.335	4.77	154.628	±1.324
4	4.74	104.062	±1.130	4.76	106.817	±1.124
10	4.73	41.488	±0.725	4.74	41.929	±0.724

Table 4.6: Two fixed surfaces. Critical values of Rayleigh number R_a, wave number a_c vs. P_2, for $P_1 = 6$, $\lambda = 2$,

P_2		$A = 1$			$A = 4$	
	a_c	R_a	σ_1	a_c	R_a	σ_1
0.255–0.31	3.1	3371.034	0	3.1	3371.034	0
0.31–0.345	. . .	. . .	. . .	3.1	3371.034	0
0.255	4.8	3398.990	±2.295	4.96	3939.830	±1.848
0.2568	4.8	3374.232	±2.311	4.96	3907.569	±1.878
0.25702	4.8	3371.231	±2.313	4.96	3903.661	±1.881
0.25703	4.8	3371.095	±2.313	4.96	3903.484	±1.881
0.25704	4.8	3370.958	±2.313	4.96	3903.306	±1.882
0.264	4.8	3278.704	±2.371	4.95	3783.539	±1.968
0.2676	4.8	3232.940	±2.397	4.95	3724.361	±2.014
0.2688	4.8	3217.968	±2.406	4.95	3705.048	±2.029
0.27	4.8	3203.134	±2.414	4.95	3685.923	±2.043
0.272	4.8	3178.713	±2.427	4.95	3654.474	±2.066
0.285	4.8	3028.622	±2.499	4.94	3462.227	±2.171
0.288	4.8	2995.978	±2.512	4.94	3420.651	±2.205
0.29	4.8	2974.598	±2.516	4.94	3393.475	±2.220
0.292	4.79	2953.529	±2.519	4.94	3366.721	±2.235
0.2972	4.79	2900.112	±2.539	4.93	3299.055	±2.260
0.31	4.79	2776.506	±2.579	4.93	3143.371	±2.335
0.34	4.79	2524.352	±2.637	4.91	2829.461	±2.434
0.342	4.79	2509.161	±2.639	4.91	2810.909	±2.439
0.345	4.79	2486.715	±2.642	4.91	2783.264	±2.448
0.36	4.79	2380.249	±2.654	4.9	2652.719	±2.473
0.365	4.79	2346.759	±2.657	4.9	2611.841	±2.482
0.384	4.78	2227.655	±2.654	4.89	2467.280	±2.501
0.398	4.78	2147.354	±2.653	4.89	2370.490	±2.514
0.41	4.78	2082.995	±2.6498	4.88	2293.319	±2.514
0.4473	4.78	1905.489	±2.630	4.87	2082.327	±2.514
0.4474	4.78	1905.054	±2.630	4.87	2081.813	±2.514
0.48	4.78	1773.039	±2.604	4.87	1926.687	±2.507
1.2	4.76	700.833	±1.946	4.8	725.523	±1.927
1.8	4.76	466.038	±1.639	4.78	477.022	±1.627
2.8	4.76	299.063	±1.342	4.77	303.605	±1.336
4	4.76	209.146	±1.136	4.77	211.372	±1.132
10	4.75	83.549	±0.728	4.76	83.905	±0.728

Part II. Thermal convection with anisotropic permeability

There has been much recent interest in the study of thermal convection in porous media due to the great importance of many applications in engineering and geophysics, see e.g. Nield and Bejan [84], Straughan [116, 121], and references therein. However, many materials, possess a pronounced anisotropy in permeability, or in thermal diffusivity. Thus, the effect of anisotropy on thermal convection in porous media is currently a subject receiving a particular interest. To this end, this part draws attention to the modelling of thermal convection problems which allow to the permeability to be an anisotropic tensor.

Thermal convection in anisotropic porous media has been investigated by many researchers. For example, Castinel and Combarnous [16], investigated the Rayleigh-Benard instability in porous media with anisotropic permeability. Later, Epherre [32] considered convection in a porous medium with anisotropy in the thermal diffusivity. Other publications, such as Kvernold and Tyvand [64], and Tyvand [126], were concerned with the effects of anisotropy with respect to permeability and thermal diffusivity, at the onset of thermal convection. Storesletten [109] considered natural convection in a horizontal fluid saturated porous layer with anisotropic thermal diffusivity, whereas the permeability was isotropic. Straughan and Walker [111] developed linear and nonlinear energy stability analysis for penetrative convection in anisotropic porous media with permeability transversely isotropic with respect to an inclined axis. Subsequently, Payne et al. [86] studied structural stability for the problem of penetrative convection in anisotropic porous media which arises out of Straughan and Walker the work of [111]. The onset of convection in an inclined

anisotropic porous layer has been considered also by Rees and Postelnicu [91].

The layout of this Part is as follows. In Chapter 5 we consider a model for thermal convection in a saturated porous material of the Darcy type incorporating fluid inertia. We investigate how the changes in the vertical direction of permeability tensor affect the stability of the system. The optimal results are achieved, by using an energy method, that the nonlinear critical Rayleigh numbers coincide with those of the linear analysis. Analogous unconditional stability results are also derived when we ignore the inertia term and the layer of a saturated porous medium is rotating about an axis orthogonal to the planes bounding the layer in Chapter 6. The work in these chapters, respectively, has been published in Haddad [48] and submitted for publication. The influence of the inclusion of the inertia term on the onset of thermal convection is considered for this model in Chapter 7.

Chapter 5

Thermal convection in a Darcy porous medium with anisotropic spatially varying permeability

In this chapter, we analyse the effect of anisotropic permeability at the onset of convection in porous Darcy media incorporating fluid inertia. We focus our attention on the case of a permeability tensor $\mathbf{K} = diag\left\{K_{\mathrm{II}}, K_{\mathrm{II}}, K_{\perp}(z)\right\}$, i.e. the case in which the permeability varies in the vertical direction, while the thermal diffusivity is constant. Our aim is to analyse the linear instability and the nonlinear stability to obtain conditions for global nonlinear stability, we show that the growth rate σ is real and as a result the convection is by stationary convection.

It is worth mentioning that the effects of anisotropy, of both permeability and thermal diffusivity, have raised much interest recently. See for example Carr and de Putter [15], who introduced an internal heat sink model which allowed for penetrative convection in a porous medium with horizontal isotropic permeability, Capone et al. [7, 9], studied the effect of anisotropic constant thermal diffusivity and the variable permeability in the vertical direction for problems of convection and penetrative convection in a Darcy porous medium. The same authors, in [9], and [11] analysed the effect of variable diffusivity and variable permeability in the vertical direction.

The chapter is organized as follows. In the Section 5.1 we present the equations

for thermal convection in a fluid saturated anisotropic porous medium, and we present also the non-dimensionalised perturbation equations. The linear stability and the non-linear stability problems are the subject of Section 5.2 and Section 5.3 respectively. In section 5.4 we employ both the compound matrix method and the D^2 Chebyshev tau method (see Appendix B) to solve the eigenvalue problem. In the Section 5.5 numerical results are reported.

5.1 Governing equations

We consider a layer of porous media heated from below and bounded by two horizontal planes $z = 0$ and $z = d$. Further, we suppose the fluid saturated porous medium occupying the three dimensional layer $\{(x, y) \in R^2\} \times \{z \in (0, d)\}$. We are interested in the situation in which the permeability is an anisotropic tensor K_{ij}. The governing equations incorporating fluid inertia and adopting the Boussineq approximation for thermal convection in an anisotropic porous medium of Darcy type may be found in Straughan [116], and are

$$\hat{a} K_{ij} v_{j,t} = - K_{ij} p_{,j} - \mu v_i + K_{ij} k_j g \rho_0 \alpha T \tag{5.1.1}$$

$$v_{i,i} = 0, \tag{5.1.2}$$

$$T_{,t} + v_i T_{,i} = \kappa \Delta T, \tag{5.1.3}$$

where $\mathbf{v}$ is the velocity field, p is the pressure, T is temperature, $\hat{a}$ is an inertia coefficient, μ is the dynamic viscosity, κ is the thermal diffusivity, g is gravity, $\mathbf{k} = (0, 0, 1)$, α is the thermal expansion coefficient of the fluid, and ρ_0 is the constant density coefficient.

In this chapter we are particulary interested in the case in which the vertical permeability depends on the depth z, isotropic constant permeability in the horizontal directions. In this case the permeability tensor has the form

$$K_{ij} = diag \left\{ K_{\mathrm{II}}, K_{\mathrm{II}}, K_\perp(z) \right\},$$

where K_{II} is a positive constant, and $K_\perp(z) = 1/m_0 h(z)$. Here $m_0 > 0$, $h(z) > h_0 > 0$ is a linear or an exponential function.

We assume that the fluid is saturated by a Darcy porous medium and we add the boundary conditions

$$\mathbf{n} \cdot \mathbf{v} = 0, \qquad \text{at } z = 0, d,$$
$$T = T_L, \ z = 0; \quad T = T_U, \ z = d, \tag{5.1.4}$$

where T_L, T_U are constants with $T_L > T_U$, and $\mathbf{n}$ is the unit outward normal to the boundary, so $\mathbf{n} = (0, 0, 1)$ on $z = d$ and $\mathbf{n} = (0, 0, -1)$ on $z = 0$.

The steady solution whose stability is under investigation is

$$\bar{v}_i \equiv 0, \qquad \bar{T} = -\beta z + T_L,$$
$$\bar{p} = p_0 - g\rho_0 z - \frac{1}{2}\alpha\beta g\rho_0 z^2, \tag{5.1.5}$$

with p_0 is the pressure at the surface $z = 0$, $\beta = (T_L - T_U)/d$.

To study stability and linear instability we introduce perturbations (u_i, ϑ, π) to the solutions (5.1.5) in such a way that

$$v_i = \bar{v}_i + u_i, \qquad T = \bar{T} + \vartheta, \qquad p = \bar{p} + \pi.$$

The nonlinear perturbation equations arising from equations (5.1.1)-(5.1.3), are

$$\hat{a}K_{ij}u_{j,t} = -K_{ij}\pi_{,j} - \mu u_i + K_{ij}k_j g\rho_0\alpha\vartheta,$$
$$u_{i,i} = 0, \tag{5.1.6}$$
$$\vartheta_{,t} + u_i\vartheta_{,i} = \beta w + \kappa\Delta\vartheta,$$

where $w = u_3$. We introduce an inverse permeability tensor M_{ij} which satisfies

$$M_{ij}K_{jk} = \delta_{ik}.$$

Then $M_{ij} = m_0 m_{ij}$, with $m_{ij} = diag\{\xi, \xi, h(z)\}$, $\xi = 1/m_0 K_{\mathrm{II}}$.

In terms of the inverse permeability tensor M_{ij}, equations (5.1.6) are equivalent to

$$\hat{a}u_{i,t} = -\pi_{,i} - \mu m_0 m_{ij}u_j + k_i g\rho_0\alpha\vartheta,$$
$$u_{i,i} = 0, \tag{5.1.7}$$
$$\vartheta_{,t} + u_i\vartheta_{,i} = \beta w + \kappa\Delta\vartheta.$$

To non-dimensionalise equations (5.1.7). We define the non-dimensional quantities by

$$x_i = dx_i^*, \qquad u_i = Uu_i^*, \qquad t = \mathcal{T}t^*, \qquad \pi = P\pi^*, \qquad \vartheta = T^\# \vartheta^*,$$

where the inertia, time, velocity, pressure, and temperature scales are chosen as

$$a_0 = \frac{\hat{a}\kappa}{m_0 \mu d^2}, \qquad \mathcal{T} = \frac{d^2}{\kappa}, \qquad U = \frac{\kappa}{d},$$

$$P = m_0 d\mu U, \qquad T^\# = U\sqrt{\frac{m_0 d^2 \beta \mu}{\kappa \rho_0 g \alpha}}.$$

The Rayleigh number $R = \sqrt{Ra}$ is introduced as

$$R = \sqrt{\frac{d^2 \rho_0 g \alpha \beta}{m_0 \mu \kappa}}.$$

Omitting all stars, the nonlinear non-dimensional perturbation equations are

$$a_0 u_{i,t} = -\pi_{,i} - m_{ij}u_j + Rk_i\vartheta,$$

$$u_{i,i} = 0, \tag{5.1.8}$$

$$\vartheta_{,t} + u_i\vartheta_{,i} = Rw + \Delta\vartheta,$$

where

$$h(z) = 1 - qz, \;\; \text{or} \;\; h(z) = e^{qz}, \;\; q > 0 \tag{5.1.9}$$

and the corresponding boundary conditions are given by

$$n_i u_i = \vartheta = 0, \qquad \text{at } z = 0, 1, \tag{5.1.10}$$

with $\{u_i, \vartheta, \pi\}$ satisfying a plane tiling periodicity in (x, y).

5.2 Linearized instability and the principle of exchange of stabilities

In order to study the linear instability, we first linearize equations (5.1.8), then follow Chandrasekhar [19] by imposing a temporal growth rate like $e^{\sigma t}$ for solutions of the form

$$\mathbf{u}(\mathbf{x}, t) = \mathbf{u}(\mathbf{x})\, e^{\sigma t}, \qquad \vartheta(\mathbf{x}, t) = \vartheta(\mathbf{x})\, e^{\sigma t}, \qquad \pi(\mathbf{x}, t) = \pi(\mathbf{x})\, e^{\sigma t}.$$

The linearized equations arising from (5.1.8) are

$$a_0 \sigma u_i = -\pi_{,i} - m_{ij} u_j + R k_i \vartheta,$$

$$u_{i,i} = 0 \tag{5.2.1}$$

$$\sigma \vartheta_{,t} = R w + \Delta \vartheta,$$

In general σ is a complex number. We now show that $\sigma \in \mathbb{R}$, and so the strong principle of exchange of stabilities holds. To this end, let V be a period cell for the solution (u_i, ϑ, π), and let u_i^*, ϑ^* be the complex conjugate of u_i, ϑ respectively. Multiplying equation $(5.2.1)_1$ by u_i^* and equation $(5.2.1)_3$ by ϑ^* and integrate over the periodic cell V to obtain

$$\sigma a_0 \|\mathbf{u}\|^2 = -(m_{ij} u_j, u_i^*) + R(\vartheta, w^*), \tag{5.2.2}$$

$$\sigma \|\vartheta\|^2 = R(w, \vartheta^*) - \|\nabla \vartheta\|^2, \tag{5.2.3}$$

where $(.,.)$ and $\|.\|$ denote the inner product and norm on the complex Hilbert space $L^2(V)$.

After addition of equations (5.2.2) and (5.2.3), we obtain

$$\sigma(a_0 \|\mathbf{u}\|^2 + \|\vartheta\|^2) = -(m_{ij} u_j, u_i^*) - \|\nabla \vartheta\|^2 + R[(\vartheta, w^*) + (w, \vartheta^*)]. \tag{5.2.4}$$

Since $\sigma = \sigma_r + i\sigma_i$, equating the imaginary part of equation (5.2.4) yields

$$\sigma_i(a_0 \|\mathbf{u}\|^2 + \|\vartheta\|^2) = 0.$$

Hence, $\sigma_i = 0$ and so $\sigma \in \mathbb{R}$ which implies that the linearized equations (5.2.1) satisfy the strong principle of exchange of stabilities. Therefore, convection sets in as stationary convection (and it is sufficient to take $\sigma = 0$ in equations (5.2.1)). After removing π by taking curl curl of equation $(5.2.1)_1$, we have the system to determine the marginal region

$$\xi w_{,zz} + h(z) \Delta^* w - R \Delta^* \vartheta = -\sigma a_0 \Delta w,$$

$$R w + \Delta \vartheta = \sigma \vartheta, \tag{5.2.5}$$

where $\Delta^* = \partial^2/\partial x^2 + \partial^2/\partial y^2$ is the horizontal Laplacian operator.

The associated boundary conditions are

$$w = 0, \qquad \vartheta = 0, \qquad \text{at } z = 0, 1.$$

In Section 5.4 we will apply the D^2 Chebyshev tau method and the compound matrix method to compute eigenvalues.

5.3 Nonlinear stability analysis

In this section, nonlinear energy stability analysis is examined to give a threshold in which the system is stable. To this end, we return to the nonlinear non–dimensional perturbation equations (5.1.8) with boundary conditions (5.1.10). We multiply equation $(5.1.8)_1$ by u_i and equation $(5.1.8)_3$ by ϑ and integrate each over V to find

$$\frac{a_0}{2}\frac{d}{dt}\|\mathbf{u}\|^2 = -\left(m_{ij}u_j, u_i\right) + R\left(\vartheta, w\right), \tag{5.3.1}$$

$$\frac{1}{2}\frac{d}{dt}\|\vartheta\|^2 = -\|\nabla\vartheta\|^2 + R\left(\vartheta, w\right). \tag{5.3.2}$$

Let $\lambda > 0$ be a parameter to be chosen. We form $\lambda(5.3.1) + (5.3.2)$, and then we derive an energy identity of form

$$\frac{dE}{dt} = RI - D, \tag{5.3.3}$$

where

$$E(t) = \frac{1}{2}(\lambda a_0 \|\mathbf{u}\|^2 + \|\vartheta\|^2), \tag{5.3.4}$$

$$I = (1 + \lambda)(\vartheta, w), \tag{5.3.5}$$

$$D = \lambda\left(m_{ij}u_j, u_i\right) + \|\nabla\vartheta\|^2. \tag{5.3.6}$$

Define R_E by

$$\frac{1}{R_E} = \max_{\mathcal{H}}\frac{I}{D}, \tag{5.3.7}$$

where $\mathcal{H}$ is the space of admissible functions given by

$$\mathcal{H} = \{u_i, \vartheta | u_i \in L^2(V), \vartheta \in H^1(V), u_{i,i} = 0, u_i, \vartheta \text{ are periodic in } x, y\}.$$

From (5.3.3) provided $R < R_E$, one can show

$$\frac{dE}{dt} \leq -D\left(\frac{R_E - R}{R_E}\right). \tag{5.3.8}$$

Since $m_{ij} = diag\{\xi, \xi, h(z)\}$, and $\xi > 0$, $h(z) > h_0 > 0$, it follows that m_{ij} is positive definite. Hence

$$\left(m_{ij}u_j, u_i\right) \geq \xi_0 \|\mathbf{u}\|^2 \ where \ \xi_0 = min\{\xi, h_0\},$$

and since by Poincaré inequality on D

$$D \geq \lambda \xi_0 \|\mathbf{u}\|^2 + \pi^2 \|\vartheta\|^2,$$

it follows that $D \geq \hat{\mu} E(t)$, where $\hat{\mu} = min\,\{2\pi^2, 2\xi_0/a_0\}$.

Put $c = (R_E - R)/R_E > 0$, then from inequality (5.3.8), if $R < R_E$,

$$\frac{dE}{dt} \leq -c\hat{\mu}E(t),$$

which implies

$$E(t) \leq E(0)e^{-c\hat{\mu}t}.$$

Thus $E(t)$ tends to 0 as $t \to \infty$. Therefore $\|\vartheta(t)\| \to 0$ and $\|\mathbf{u}(t)\| \to 0$. Hence global nonlinear stability of the conduction solution is satisfied provided $R < R_E$.

We now aim to solve the maximisation problem (5.3.7). We do this by deriving the Euler–Lagrange equations and maximising in the coupling parameter λ to determine the nonlinear stability threshold R_E (see Section (1.4)). The maximum problem (5.3.7) is

$$\frac{1}{R_E} = \max_{\mathcal{H}} \frac{(1+\lambda)(\vartheta, w)}{\lambda(m_{ij}u_j, u_i) + \|\nabla\vartheta\|^2}.$$

It is convenient to put $\hat{u}_i = \sqrt{\lambda}u_i$, then the foregoing equation becomes (dropping the hat)

$$\frac{1}{R_E} = \max_{\mathcal{H}} \frac{g(\lambda)(\vartheta, w)}{(m_{ij}u_j, u_i) + \|\nabla\vartheta\|^2},$$

where

$$g(\lambda) = \frac{1+\lambda}{\sqrt{\lambda}}.$$

The Euler-Lagrange equations for this maximum are derived by using the calculus of variations technique as follows.

Let $\hat{h}_i, \eta$ be arbitrary, fixed $C^2(0,1)$ functions which satisfy the boundary conditions $\hat{h}_i(0) = \hat{h}_i(1) = 0$, $\eta(0) = \eta(1) = 0$.

We now consider solution of the form $u_i + \varepsilon\hat{h}_i$ and $\vartheta + \varepsilon\eta$ where ε is a constant. The maximum occurs at $\varepsilon = 0$, so

$$\frac{d}{d\varepsilon}\left(\frac{I}{D}\right)\Big|_{\varepsilon=0} = \frac{1}{D}\left(\frac{dI}{d\varepsilon} - \frac{I}{D}\frac{dD}{d\varepsilon}\right)\Big|_{\varepsilon=0},$$

$$= \frac{1}{D}\left(\frac{dI}{d\varepsilon} - \frac{1}{R_E}\frac{dD}{d\varepsilon}\right)\Big|_{\varepsilon=0}.$$

This yields

$$R_E \left.\frac{dI}{d\varepsilon}\right|_{\varepsilon=0} - \left.\frac{dD}{d\varepsilon}\right|_{\varepsilon=0} = 0. \tag{5.3.9}$$

Here we include the constraint $u_{i,i} = 0$ by way of a Lagrange multiplier $2\pi(x)$,

$$\left.\frac{dI}{d\varepsilon}\right|_{\varepsilon=0} = \left.\frac{d}{d\varepsilon} \int_V \left(g(\lambda)(\vartheta + \varepsilon\eta)(w + \varepsilon\hat{h}_3) - 2\pi(u_{i,i} + \varepsilon\hat{h}_{i,i}) \right) dV \right|_{\varepsilon=0},$$

$$= \left.\int_V \left(g(\lambda) \left(\eta(w + \varepsilon\hat{h}_3) + \hat{h}_3(\vartheta + \varepsilon\eta) \right) - 2\hat{h}_{i,i}\pi \right) dV \right|_{\varepsilon=0},$$

and

$$\left.\frac{dD}{d\varepsilon}\right|_{\varepsilon=0} = \left.\frac{d}{d\varepsilon} \int_V \left(m_{ij}(u_j + \varepsilon\hat{h}_j)(u_i + \varepsilon\hat{h}_i) + (\nabla(\vartheta + \varepsilon\eta))^2 \right) dV \right|_{\varepsilon=0},$$

$$= \left.\int_V \left(m_{ij} \left(\hat{h}_j(u_i + \varepsilon\hat{h}_i) + \hat{h}_i(u_j + \varepsilon\hat{h}_j) \right) + 2\left(\nabla(\vartheta + \varepsilon\eta)\nabla\eta\right) \right) dV \right|_{\varepsilon=0}.$$

Further, after some integrations by parts and using the boundary conditions, we have

$$\left.\frac{dI}{d\varepsilon}\right|_{\varepsilon=0} = \int_V \left(g(\lambda) \left(\eta w + \hat{h}_3\vartheta \right) - 2\hat{h}_i\pi_{,i} \right) dV,$$

$$\left.\frac{dD}{d\varepsilon}\right|_{\varepsilon=0} = \int_V \left(2m_{ij}u_j\hat{h}_j - \eta\Delta\vartheta \right) dV.$$

Since $\hat{h}_i$ and η were chosen arbitrary functions, hence from equation (5.3.9) we must have

$$R_E \frac{g(\lambda)}{2}\vartheta k_i - m_{ij}u_j = \pi_{,i},$$

$$u_{i,i} = 0, \tag{5.3.10}$$

$$R_E \frac{g(\lambda)}{2}w + \Delta\vartheta = 0.$$

We now wish to investigate the optimal value of λ which maximise R_E. For this one now uses the parametric differentiation method. Thus let $g(\lambda)/2 = \zeta$, and let $(R_E^1, u_i^1, \vartheta^1, \pi^1)$ be a solution to the eigenvalue problem arising from equation (5.3.10) on V for $\lambda = \lambda^1 > 0$, and likewise let $(R_E^2, u_i^2, \vartheta^2, \pi^2)$ be a solution for $\lambda = \lambda^2 > 0$, $\lambda^1 \neq \lambda^2$.

Now multiply equation $(5.3.10)_1$ by u_i^1 holding for $\lambda = \lambda^2$. Likewise, multiply $(5.3.10)_1$ by u_i^2 holding for $\lambda = \lambda^1$ and then integrate over V to find

$$R_E^2 \zeta^2 \left(\vartheta^2, w^1\right) - \left(m_{ij} u_j^2, u_i^1\right) = 0, \tag{5.3.11}$$

$$R_E^1 \zeta^1 \left(\vartheta^1, w^2\right) - \left(m_{ij} u_j^1, u_i^2\right) = 0. \tag{5.3.12}$$

Similarly, multiply equation $(5.3.10)_3$ by ϑ^1 holding for $\lambda = \lambda^2$ and by ϑ^2 holding for $\lambda = \lambda^1$, after integration over V we have

$$R_E^2 \zeta^2 \left(w^2, \vartheta^1\right) - \left(\nabla \vartheta^2, \nabla \vartheta^1\right) = 0, \tag{5.3.13}$$

$$R_E^1 \zeta^1 \left(w^1, \vartheta^2\right) - \left(\nabla \vartheta^1, \nabla \vartheta^2\right) = 0. \tag{5.3.14}$$

Next, combine (5.3.11) - (5.3.12) + (5.3.13) - (5.3.14) to obtain

$$\left(R_E^2 \zeta^2 - R_E^1 \zeta^1\right) \left[\left(w^1, \vartheta^2\right) + \left(w^2, \vartheta^1\right)\right] = 0.$$

Now, we write $(R_E^2 \zeta^2 - R_E^1 \zeta^1) = (R_E^2 \zeta^2 - R_E^2 \zeta^1) + (R_E^2 \zeta^1 - R_E^1 \zeta^1)$, and recall $\lambda^1 \neq \lambda^2$, divide by $\lambda^2 - \lambda^1 \neq 0$. Thus we have

$$\left[\frac{R_E^2 \left(\zeta^2 - \zeta^1\right)}{\lambda^2 - \lambda^1} + \frac{\zeta^1 \left(R_E^2 - R_E^1\right)}{\lambda^2 - \lambda^1}\right] \left[\left(w^1, \vartheta^2\right) + \left(w^2, \vartheta^1\right)\right] = 0.$$

Take the limit $\lambda^2 \to \lambda^1$, this leads to

$$\left[R_E \frac{\partial \zeta}{\partial \lambda} + \zeta \frac{\partial R_E}{\partial \lambda}\right] (w, \vartheta) = 0. \tag{5.3.15}$$

Here R_E^1, ζ^1, w^1, and ϑ^1 are replaced by R_E, ζ, w, and ϑ.

Then by multiplying equation $(5.3.10)_1$ by u_i and equation $(5.3.10)_3$ by ϑ and integrating over V. It follows that

$$\zeta R_E \left(\vartheta, w\right) = \left(m_{ij} u_j, u_i\right), \quad \zeta R_E \left(w, \vartheta\right) = \|\nabla \vartheta\|^2. \tag{5.3.16}$$

After adding these equations and substituting into the equation (5.3.15) and recalling $g(\lambda) = 2\zeta$, one may deduce

$$\left[\frac{\|\nabla \vartheta\|^2 + (m_{ij} u_j, u_i)}{g R_E}\right] \left[g \frac{\partial R_E}{\partial \lambda} + R_E \frac{\partial g}{\partial \lambda}\right] = 0. \tag{5.3.17}$$

The maximum value of R_E satisfies $\partial R_E / \partial \lambda = 0$, and so $\partial g / \partial \lambda = 0$ gives the best value of λ. Thus the optimal value of λ is $\lambda = 1$.

Upon substituting $\lambda = 1$ into equations (5.3.10), we arrive at the eigenvalue problem

$$R_E \vartheta k_i - m_{ij} u_j = \pi_{,i},$$

$$u_{i,i} = 0, \tag{5.3.18}$$

$$R_E w + \Delta \vartheta = 0.$$

These equations (5.3.18) are exactly the same as those of linear instability theory arising from equations (5.2.1) with $\sigma = 0$. Thus, we have an optimum result that the critical Rayleigh number for global nonlinear stability R_E^2 is exactly the same as the critical Rayleigh number of linear theory R_L^2. Therefore, no subcritical instabilities can arise. Indeed this is due to the fact that the operator attached to the linear theory is symmetric, see Straughan [115], and Falsaperla et al. [36]

The numerical results, which employ the D^2 Chebyshev tau method and the compound matrix method as the eigenvalue solver, confirm that the stationary convection is the dominate mode.

5.4   Numerical methods

In this Section, we seek to solve system (5.3.18), or equivalently system (5.2.1) for the lowest eigenvalue $R_E = R_L$. To do this we take curl curl of equation $(5.3.18)_1$, this leads to equations (5.2.5) with $R = R_E$ and $\sigma = 0$ as presented in section 5.2. Therefore, we consider in turn equations (5.2.5) for R.

Assuming a normal mode with the representations for w, and ϑ of the form

$$\vartheta = \Theta(z) f(x, y), \qquad w = W(z) f(x, y),$$

where f satisfied $\Delta^* f = -a^2 f$, a is being the wave number. Hence, equation (5.2.5) can be written as

$$\left(D^2 - \frac{h(z)}{\xi} a^2 \right) W + \frac{R}{\xi} a^2 \Theta = -\sigma(D^2 - a^2)W,$$

$$(D^2 - a^2)\Theta + RW = \sigma \Theta, \tag{5.4.1}$$

where $D = d/dz$. In the numerical program we actually take $\sigma = 0$. This system is

solved numerically subject to the boundary conditions

$$W = \Theta = 0, \qquad \text{at } z = 0, 1 \tag{5.4.2}$$

5.4.1 The D^2 Chebyshev tau method

In this section, we present D^2 Chebyshev tau method to solve system (5.4.1)-(5.4.2) for the eigenvalue σ with R given, cf. Dongarra et al. [31]. To this end, we begin by resetting the domain from $(0, 1)$ to $(-1, 1)$, selecting $\hat{z} = 2z - 1$.

By introducing the function χ in such way that $\chi = (4D^2 - a^2)W$, we may alternatively write equations (5.4.1) in the form (omitting the hat)

$$
\begin{aligned}
(4D^2 - a^2)W - \chi &= 0, \\
(4D^2 - a^2)\Theta + RW &= \sigma\Theta, \\
\chi + \left(a^2 - \frac{H(z)}{\xi}a^2\right)W + \frac{R}{\xi}a^2\Theta &= -\sigma\chi,
\end{aligned}
\tag{5.4.3}
$$

where $H(z) = h((z+1)/2)$ and now $z \in (-1, 1)$.

Next, we write W, Θ, χ in the form of a series of Chebyshev polynomials, truncating each sum, we have

$$W(z) = \sum_{n=0}^{N} W_n T_n(z), \qquad \chi(z) = \sum_{n=0}^{N} \chi_n T_n(z), \qquad \Theta(z) = \sum_{n=0}^{N} \Theta_n T_n(z).$$

Recalling the boundary conditions (5.4.2), where the relation $T_n(\pm 1) = (\pm 1)^n$ is used, then

$$
\begin{aligned}
BC1: & \quad W_0 + W_2 + W_4 + \cdots + W_{N-1} = 0, \\
BC2: & \quad W_1 + W_3 + W_5 + \cdots + W_N = 0, \\
BC3: & \quad \Theta_0 + \Theta_2 + \Theta_4 + \cdots \Theta_{N-1} = 0, \\
BC6: & \quad \Theta_1 + \Theta_3 + \Theta_5 + \cdots \Theta_N = 0.
\end{aligned}
$$

In this way we find the D^2 Chebyshev tau method requires solution of the $(N+1) \times (N+1)$ matrix equation

$$A\mathbf{x} = \sigma B\mathbf{x}, \tag{5.4.4}$$

where $\mathbf{x} = (W_0, \cdots, W_N, \Theta_0, \cdots, \Theta_N, \cdots, \chi_0, \cdots, \chi_N)$, and A and B are given by

$$A = \begin{pmatrix} 4D^2 - a^2 I & 0 & -I \\ BC1 & 0 \cdots 0 & 0 \cdots 0 \\ BC2 & 0 \cdots 0 & 0 \cdots 0 \\ RI & 4D^2 - a^2 I & 0 \\ 0 \cdots 0 & BC3 & 0 \cdots 0 \\ 0 \cdots 0 & BC4 & 0 \cdots 0 \\ (I - \dfrac{H(z)}{\xi})a^2 & \dfrac{R}{\xi}a^2 I & I \end{pmatrix},$$

$$B = \begin{pmatrix} 0 & 0 & 0 \\ 0 \cdots 0 & 0 \cdots 0 & 0 \cdots 0 \\ 0 \cdots 0 & 0 \cdots 0 & 0 \cdots 0 \\ 0 & I & 0 \\ 0 \cdots 0 & 0 \cdots 0 & 0 \cdots 0 \\ 0 \cdots 0 & 0 \cdots 0 & 0 \cdots 0 \\ 0 & 0 & -I \end{pmatrix}.$$

The eigenvalues of the generalised eigenvalue problem (5.4.4) are found efficiently using the QZ algorithm.

5.4.2 The compound matrix method

To solve equations (5.4.1) with $\sigma = 0$ by the compound matrix method, cf. Straughan [112], we let $\mathbf{U}(z) = (W, W', \Theta, \Theta')^T$, and then suppose $\mathbf{U}_1(z)$ and $\mathbf{U}_2(z)$ are independent solutions of (5.4.1) with values at $z = 0$ of $\mathbf{U}_1(0) = (0, 1, 0, 0)^T$, and $\mathbf{U}_2(0) = (0, 0, 0, 1)^T$. The two initial value problems thereby obtained are then integrated numerically between 0 and 1, and the solution found by writing it as a linear combination of the two solution so obtained, say $\mathbf{U}(z) = \alpha \mathbf{U}_1 + \beta \mathbf{U}_2$. Then the correct boundary conditions $W = \Theta = 0$ at $z = 1$ are imposed which require

$$det \begin{pmatrix} W_1 & W_2 \\ \Theta_1 & \Theta_2 \end{pmatrix} = 0.$$

The variables $y_1, \cdots, y_6$ are formed from 2×2 minors of the 4×2 solution matrix whose columns are $\mathbf{U}_1(z)$ and $\mathbf{U}_2(z)$. Thus

$$y_1 = W_1 W_2' - W_2 W_1', \qquad y_2 = W_1 \Theta_2 - W_2 \Theta_1,$$

$$y_3 = W_1 \Theta_2' - W_2 \Theta_1', \qquad y_4 = W_1' \Theta_2 - W_2' \Theta_1,$$

$$y_5 = W_1' \Theta_2' - W_2' \Theta_1', \qquad y_6 = \Theta_1 \Theta_2' - \Theta_2 \Theta_1'.$$

Differentiation the variables $y_1, \ldots, y_6$ and using equations (5.4.1) with $\sigma = 0$, we arrive at the differential equations for the compound matrix variables

$$y_1' = -\frac{R}{\xi} a^2 y_2, \qquad y_2' = y_3 + y_4,$$

$$y_3' = a^2 y_2 + y_5, \qquad y_4' = \frac{a^2}{\xi} h(z) y_2 + y_5,$$

$$y_5' = R y_1 + \frac{a^2}{\xi} h(z) y_3 + a^2 y_4 - \frac{R}{\xi} a^2 y_6,$$

$$y_6' = R y_2.$$

This system was integrated numerically subject to the initial conditions $y_5(0) = 1$, and the final condition $y_2(1) = 0$. The eigenvalue R was varied until these conditions were satisfied to some predefined accuracy. Keeping $a^2 > 0$ fixed, a golden section search was employed to numerically find

$$Ra = \min_{a^2} R^2(a^2). \tag{5.4.5}$$

The numerical results are explained in detail in the next section.

5.5   Numerical results and discussion

As stated in section 5.4, the eigenvalue problem has been solved by using the compound matrix method and D^2 Chebyshev tau method. The two sets of results concur perfectly. To achieve the precision used in the tables, we have chosen to display the results obtained via D^2 Chebyshev tau method. In the present analysis, Tables 5.1 and 5.2 display the numerical results for critical Rayleigh number Ra and wave number a_c, respectively, with the functions $h(z) = 1 - qz$, and $h(z) = e^{qz}$, for varying value of ξ, and $q = 0, 0.2, 0.5$. We also include two Figures representing the

critical Rayleigh numbers Ra against the quantity of q, for $\xi = 0.25$ increasing to $\xi = 1.5$.

The results shown in Tables 5.1 and 5.2 demonstrate that, for a fixed value of q, the the critical Rayleigh numbers Ra increases with increasing the anisotropy parameter ξ. This means the system becomes more stable as ξ increases. It is also observed that the anisotropy parameter leads to some very interesting behaviour, in that as ξ increases the wave number becomes considerably larger, which leads to cells becoming narrower.

Table 5.1: Critical values of Rayleigh number Ra, and wave number a_c vs. ξ, with $h(z) = 1 - qz$, for $q = 0, 0.2, 0.5$.

	$q = 0$		$q = 0.2$		$q = 0.5$	
ξ	a_c	Ra	a_c	Ra	a_c	Ra
0.25	2.221	22.207	2.281	20.713	2.387	18.417
0.5	2.642	28.762	2.712	27.059	2.839	24.425
0.75	2.924	34.366	3.002	32.502	3.142	29.609
1.0	3.14	39.478	3.230	37.479	3.38	34.367
1.25	3.322	44.276	3.41	42.156	3.576	38.852
1.5	3.477	48.850	3.57	46.621	3.736	43.143

It is expected that when $\xi = 1$, $q = 0$, and then $a_c = \pi^2$, $Ra = 4\pi^2$, which is the Darcy result cf. Straughan [115]. We may also consider different values of q as shown in Figures 5.1 and 5.2.

In Figure 5.1, it is evident that for $h(z) = 1 - qz$, the effects of increasing q destabilize the system. This indicates that the thermal convection occurs more easily. However, it appears that, for large values of the anisotropy parameter ξ the system becomes more stable when q is smaller. The opposite behaviour is seen when $h(z) = e^{qz}$ as shown in Figure 5.2.
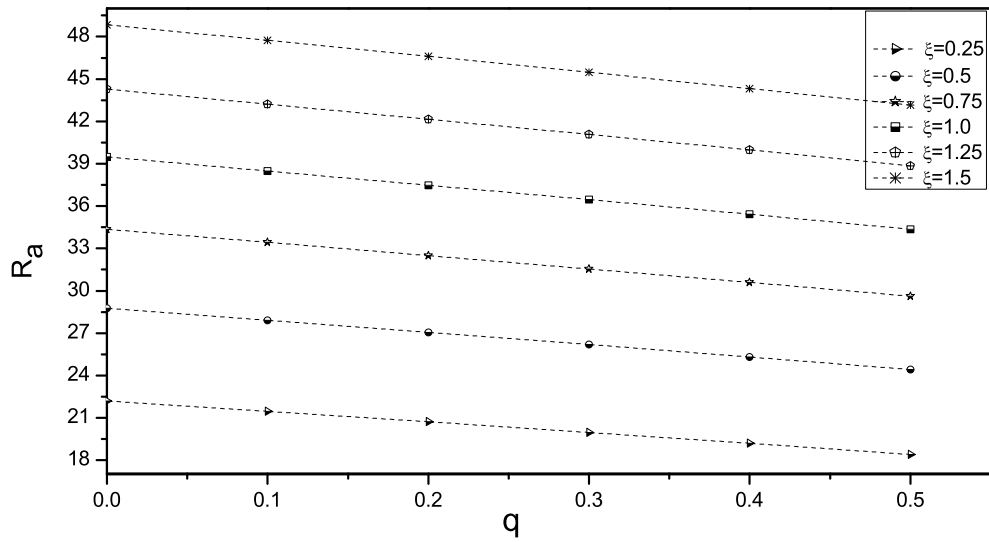
Figure 5.1: Critical Rayleigh number Ra as function of q, with $h(z) = 1 - qz$. For $\xi = 0.25$ increasing to $\xi = 1.5$.
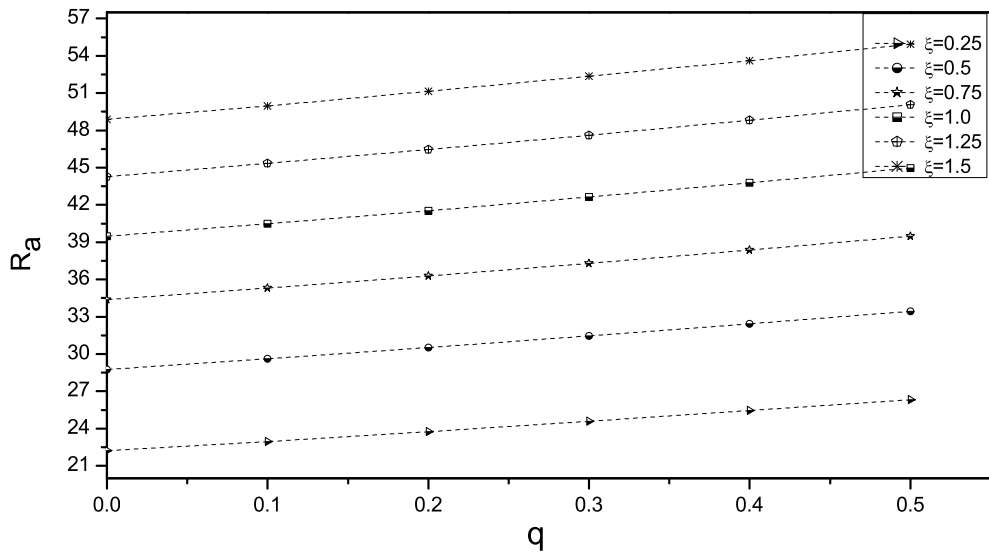
Figure 5.2: Critical Rayleigh number Ra as function of q, with $h(z) = e^z$. For $\xi = 0.25$ increasing to $\xi = 1.5$.

Table 5.2: Critical values of Rayleigh number Ra, and wave number a_c vs. ξ, with $f(z) = e^{qz}$, for $q = 0, 0.2, 0.5$.

ξ	$q = 0$		$q = 0.2$		$q = 0.5$	
	a_c	Ra	a_c	Ra	a_c	Ra
0.25	2.221	22.207	2.167	23.753	2.091	26.334
0.5	2.642	28.762	2.577	30.520	2.485	33.451
0.75	2.924	34.366	2.852	36.287	2.749	39.484
1.0	3.14	39.478	3.064	41.536	2.953	44.956
1.25	3.322	44.276	3.240	46.453	3.122	50.071
1.5	3.477	48.850	3.391	51.136	3.267	54.931

Chapter 6

Thermal convection in a rotating anisotropic fluid saturated Darcy porous medium

Having already studied the effect of permeability anisotropy on the onset of convection in a Darcy porous medium incorporating fluid inertia as presented in Chapter 5 we are now going to estimate what could be the result when we take into account the rotation of a layer of saturated porous medium about an axis orthogonal to the planes bounding the layer.

Thermal convection in a rotating porous medium is an active topic of research since it has many applications including geophysics, chemical engineering, and food processing, see e.g. Vadasz [129], Nield and Bejan [84], and references therein. Indeed, thermal convection involving the rotating of the layer of saturated porous medium is a subject receiving attention and being studied extensively by many researchers. For instance, Vadasz [128–131]. In particular, he investigated the effect of the coriolis force on thermal convection when the Darcy model is extended including the time-derivative term in the momentum equation [131]. A comprehensive review of thermal convection in a rotating porous medium are given by Vadasz [132]. Vadasz and Govender [133] also considered the influence of gravity and centrifugal forces on the onset of convection in a rotating porous layer. Straughan [114] presented an analysis of the nonlinear stability problem for convection in a rotating

porous medium. He showed that the global nonlinear stability boundary is exactly the same as the linear instability when the inertia is absent.

It is important to note that the above mentioned studies assumed that the fluid saturated body is an isotropic porous medium. However, the effect of anisotropy combined with the rotation effect on thermal instability has been the contribution of Alex and Patil [2], who investigated thermal instability subject to the centrifugal acceleration and the anisotropy effect as in the case of both Darcy and Brinkman rotating porous media. Govender [40], considered the Vadasz paper 1994, but included the anisotropy effects for both permeability and thermal diffusivity. Later, Malashetty and Swamy [70], also performed linear instability and weakly nonlinear theory to investigate the anisotropy effects on the onset of convection in a rotating porous medium. They found that by increasing an anisotropy parameter for both permeability and thermal diffusivity leads to advance oscillatory convection. The same authors, in [71] employed the linear instability to investigate the effect both of the thermal modulation and the rotation on the onset of the stationary convection boundary. Govender and Vadasz [41] also deal with the effect that thermal diffusivity and permeability anisotropy have on the thermal convection in a rotating porous medium with a thermal non-equilibrium model.

Recently, Vanishree and Siddheshwar [137] performed linear instability for an anisotropic porous medium with a temperature dependent viscosity. They found that the onset of convection in a rotating porous medium is qualitatively similar to that in a non-rotating one. Additionally, the linear instability and nonlinear stability in an anisotropic porous medium were analysed by Kumar and Bhadauria [60] who considered a viscoelastic fluid in a rotating anisotropic porous medium, Saravanan and Brindha [100] deal with the onset of centrifugal convection in the Brinkman model, and Gaikwad and Begum [39] considered the onset of double-diffusive reaction convection in an anisotropic porous medium.

In this Chapter we consider the system of equations which is essentially the same as that given in Vadasz [131], but we allow for the symmetric permeability tensor to be anisotropic. In particular, we consider the permeability as discussed in chapter 5 where it varies in the vertical direction, but now we consider the vertical

direction with constant permeability rather than variable permeability. The goal of this chapter is to investigate the effect of anisotropy with rotation on the stability thresholds using linear instability and nonlinear stability methods. Here we will ignore the inertia term in the momentum equation. More precisely, when the values of Vadasz number tend to be large [131]. We show that the critical Rayleigh number of the linear theory is the same as the critical Rayleigh number of the nonlinear theory. We observe that energy methods are very much in vogue in the current hydrodynamical stability literature, cf. Capone and Rionero [13], Hill and Carr [52, 53], Capone et al. [10, 11], and Capone and De Luca [12]. The next chapter investigate including the inertia term in detail.

6.1 Governing equations

As in Chapter 5 we consider a layer of porous media heated from below and bounded by two horizontal planes $z = 0$ and $z = d$, with gravity acting in the vertical direction of z-axis. We assume an incompressible Newtonian fluid is contained the layer and occupies the spatial domain $\{(x, y) \in \mathbb{R}^2\} \times \{z \in (0, d)\}$. Further, we suppose that the layer rotates about z-axis.

The governing equations incorporating fluid inertia for thermal convection in an anisotropic rotating porous media of Darcy type may be written as, cf. Malashetty, and Swamy [70],

$$a_0 v_{j,t} = -p_{,j} - \mu M_{ij} v_i + g\rho_0 \alpha T k_j - \frac{2}{\varphi} \left(\mathbf{\Omega} \times v \right)_j \tag{6.1.1}$$

$$v_{i,i} = 0, \tag{6.1.2}$$

$$T_{,t} + v_i T_{,i} = \kappa \Delta T, \tag{6.1.3}$$

Here $\mathbf{v}$, t, p, T are velocity field, time, pressure, and temperature respectively, and μ, κ, g, α, ρ_0, φ are dynamic viscosity, thermal diffusivity, gravity, thermal expansion coefficient of the fluid, constant density coefficient, and porosity respectively, and $\mathbf{\Omega}$ is the angular velocity vector with $\mathbf{k} = (0, 0, 1)$, $a_0 = \hat{a}/\varphi$ is an inertia coefficient, $\hat{a}$ is constant and φ is porosity.

The permeability tensor is assumed to be of the form

$$M_{ij} = diag\left\{1/k_x, 1/k_x, 1/k_z\right\},$$

where k_x, k_z is a constant. The boundary conditions for the problem are

$$\mathbf{n} \cdot \mathbf{v} = 0, \qquad \text{at } z = 0, d,$$
$$T = T_L, \ z = 0; \quad T = T_U, \ z = d, \tag{6.1.4}$$

where T_L, T_U are constants with $T_L > T_U$, and $\mathbf{n}$ is the unit outward normal to the boundary, so $\mathbf{n} = (0, 0, 1)$ at $z = d$ and $\mathbf{n} = (0, 0, -1)$ at $z = 0$.

Again, when no motion occurs and the temperature gradient is constant throughout the layer, the basic steady state solution $(\bar{\mathbf{v}}, \bar{p}, \bar{T})$ of the system has the same solution as in Chapter 5. This is given by

$$\bar{v}_i \equiv 0, \qquad \bar{T} = -\beta z + T_L,$$
$$\bar{p} = p_0 - g\rho_0 z - \frac{1}{2}\alpha\beta g\rho_0 z^2, \tag{6.1.5}$$

with p_0 is the pressure at the surface $z = 0$, $\beta = (T_L - T_U)/d$.

Letting $v_i = \bar{v}_i + u_i$, $T = \bar{T} + \vartheta$, $p = \bar{p} + \pi$, the nonlinear perturbation equations arising from equations (6.1.1)-(6.1.3), are

$$a_0 u_{j,t} = -\pi_{,j} - \mu M_{ij} u_i + k_j g\rho_0 \alpha\vartheta - \frac{2}{\varphi}(\mathbf{\Omega} \times u)_j,$$
$$u_{i,i} = 0, \tag{6.1.6}$$
$$\vartheta_{,t} + u_i\vartheta_{,i} = \beta w + \kappa\Delta\vartheta,$$

where $w = u_3$.

The perturbation equations are non-dimensionalised with the non-dimensionalisation scalings as follows

$$x_i = dx_i^*, \qquad u_i = Uu_i^*, \qquad t = \mathcal{T}t^*, \qquad \pi = P\pi^*, \qquad \vartheta = T^\#\vartheta^*,$$

$$U = \frac{\kappa}{d}, \qquad \mathcal{T} = \frac{d^2}{\kappa}, \qquad P = \frac{d\mu U}{k_x}, \qquad T^\# = U\sqrt{\frac{d^2\beta\mu}{\kappa\rho_0 g\alpha k_x}},$$

$$V_a = \frac{\varphi Pr}{\hat{a} Da}, \qquad R = \sqrt{\frac{d^2 \rho_0 g \alpha \beta k_x}{\mu \kappa}}, \qquad \tilde{T} = \frac{2\Omega k_x}{\mu \varphi},$$

where $Ra = R^2$ is the Rayleigh number, $Ta = \tilde{T}^2$ is the Taylor number, Va is the Vadasz number, and Pr is the Prandtl number, with $Da = k_x/d^2$ being the Darcy number.

Omitting all stars, the nonlinear non-dimensional perturbation equations are

$$\frac{1}{V_a} u_{i,t} = -\pi_{,i} + R k_i \vartheta - \tilde{T}(\mathbf{k} \times \mathbf{u})_i - m_{ij} u_j,$$
$$u_{i,i} = 0, \tag{6.1.7}$$
$$\vartheta_{,t} + u_i \vartheta_{,i} = R w + \Delta \vartheta.$$

Here $m_{ij} = diag\{1, 1, \xi\}$, where $\xi = k_x/k_z$ is the anisotropy parameter. The corresponding boundary conditions are

$$n_i u_i = \vartheta = 0, \qquad \text{at } z = 0, 1, \tag{6.1.8}$$

with $\{u_i, \vartheta, \pi\}$ satisfying a plane tiling periodicity in (x, y).

6.2 The principle of exchange of stabilities ignoring inertia term

As stated in the Vadasz paper [131] the values of Vadasz for many porous media applications in a real life are large. To this end, we let $Va \to \infty$ in the equation (6.1.7) to be

$$-\pi_{,i} + R k_i \vartheta - \tilde{T}(\mathbf{k} \times \mathbf{u})_i - m_{ij} u_j = 0,$$
$$u_{i,i} = 0, \tag{6.2.1}$$
$$\vartheta_{,t} + u_i \vartheta_{,i} = R w + \Delta \vartheta.$$

We now take curl of equation $(6.2.1)_1$ and curl curl of the same equation to find

$$R(\vartheta_{,y} \delta_{i1} - \vartheta_{,x} \delta_{i2}) + \tilde{T} \frac{\partial u_i}{\partial z} - \varepsilon_{ijk} m_{kq} u_{q,j} = 0, \tag{6.2.2}$$

and

$$m_{ir} \Delta u_r - m_{jr} u_{r,ji} + \tilde{T} \frac{\partial \omega_i}{\partial z} = R(k_i \Delta^* \vartheta - \vartheta_{,xz} \delta_{i1} - \vartheta_{,yz} \delta_{i2}), \tag{6.2.3}$$

where $\Delta^* = \partial^2/\partial x^2 + \partial^2/\partial y^2$ is the horizontal Laplacian operator, and ω_i is the vorticity.

Upon taking the third component of the foregoing equations, we obtain

$$m_{3r}\Delta u_r - m_{jr}u_{r,j3} + \tilde{T}\omega_{3,z} = R\,\Delta^*\,\vartheta,$$
$$\tilde{T}w_{,z} - \varepsilon_{3jk}m_{kq}u_{q,j} = 0, \tag{6.2.4}$$
$$\vartheta_{,t} + w\vartheta_{,z} = Rw + \Delta\vartheta.$$

We now consider the linearised equations of (6.2.4) by removing the nonlinear term of equation $(6.2.4)_3$, and therefore we seek for solutions of the form

$$\mathbf{u}\,(\mathbf{x},t) = \mathbf{u}\,(\mathbf{x})\,e^{\sigma t}, \quad \vartheta\,(\mathbf{x},t) = \vartheta\,(\mathbf{x})\,e^{\sigma t}.$$

By substituting into equations (6.2.4) and removal of exponential parts, we have to solve the system

$$m_{3r}\Delta u_r - m_{jr}u_{r,j3} + \tilde{T}\omega_{3,z} = R\,\Delta^*\,\vartheta,$$
$$\tilde{T}w_{,z} - \varepsilon_{3jk}m_{kq}u_{q,j} = 0, \tag{6.2.5}$$
$$\sigma\vartheta = Rw + \Delta\vartheta.$$

The corresponding boundary conditions are

$$w = \vartheta = 0\,, \qquad \text{at } z = 0,1. \tag{6.2.6}$$

In order to show that $\sigma \in \mathbb{R}$, and so the principle of exchange of stabilities holds, we consider a three dimensional period cell V for solution to equation (6.2.5) and assume momentarily that σ, u_i, and ϑ are complex. Then multiply equation $(6.2.5)_1$ by w^* (the complex conjugate of w) and integrate over V to obtain

$$\int_V (m_{3r}\Delta u_r - m_{jr}u_{r,j3})w^*dV + \int_V \tilde{T}\omega_{3,z}w^*dV = \int_V R\,\Delta^*\,\vartheta w^*dV, \tag{6.2.7}$$

since $m_{ij} = diag\,\{1,1,\xi\}$, so one may rewrite the first term in (6.2.7) as shown below

$$\begin{aligned}
m_{3r}\Delta u_r - m_{jr}u_{r,j3} &= m_{33}\Delta u_3 - m_{11}u_{1,13} - m_{22}u_{2,23} - m_{33}u_{3,33} \\
&= \xi(u_{3,11} + u_{3,22} + u_{3,33}) - u_{1,13} - u_{2,23} - \xi u_{3,33} \\
&= \xi(u_{3,11} + u_{3,22}) - (u_{1,1} + u_{2,2})_{,3}\,.
\end{aligned}$$

Recalling $u_{1,1} + u_{2,2} = -u_{3,3}$, we have

$$m_{3r}\Delta u_r - m_{jr}u_{r,j3} = \xi\,\Delta^*\,w + w_{,zz}. \tag{6.2.8}$$

Making use of equation $(6.2.5)_2$

$$
\begin{aligned}
\tilde{T}w_{,z} &= \varepsilon_{3jk}m_{kq}u_{q,j} \\
&= \varepsilon_{321}m_{11}u_{1,2} + \varepsilon_{312}m_{22}u_{2,1} \\
&= -u_{,y} + v_{,x}.
\end{aligned}
\tag{6.2.9}
$$

Furthermore, we now make use of vorticity equation

$$
\omega_i = \nabla \times u_i = \varepsilon_{ijk}u_{k,j} \equiv \left(w_{,y} - v_{,z}, u_{,z} - w_{,x}, v_{,x} - u_{,y} \right),
\tag{6.2.10}
$$

and so

$$
\omega_3 = v_{,x} - u_{,y}.
\tag{6.2.11}
$$

Then we form the combination of equation (6.2.9) and equation (6.2.11) to find

$$
\omega_3 = \tilde{T}w_{,z}.
\tag{6.2.12}
$$

After differentiating equation (6.2.12) with respect to z and expressing $w_{,zz} = \Delta w - \Delta^* w$, we employ the results and equation (6.2.8) into equation (6.2.7) to obtain

$$
\int_V \left(1 + \tilde{T}^2\right)\Delta w w^* dV - \int_V \left(1 - \xi + \tilde{T}^2\right) \Delta^* w w^* dV = \int_V R\,\Delta^*\vartheta w^* dV,
$$

and hence we arrive at

$$
-\left(1 + \tilde{T}^2\right)\|\nabla w\|^2 + \left(1 - \xi + \tilde{T}^2\right)\|\nabla^* w\|^2 = -R(\nabla^* w, \nabla^* \vartheta),
\tag{6.2.13}
$$

where $\nabla^* \equiv (\partial/\partial x, \partial/\partial y, 0)$, $(.,.)$ and $\|.\|$ denote the inner product and norm on the complex Hilbert space $L^2(V)$.

By applying the horizontal Laplacian operator Δ^* to equation $(6.2.5)_3$, multiplying by ϑ^* (the complex conjugate of ϑ)and again integrating, we find

$$
\sigma\|\nabla^*\vartheta\|^2 = R(\nabla^* w, \nabla^*\vartheta) + \|\nabla^*\nabla\vartheta\|^2.
\tag{6.2.14}
$$

Next, addition of equations (6.2.13) and (6.2.14). It follows that

$$
\sigma\|\nabla^*\vartheta\|^2 = \left(1 + \tilde{T}^2\right)\|\nabla w\|^2 - \left(1 - \xi + \tilde{T}^2\right)\|\nabla^* w\|^2 + \|\nabla^*\nabla\vartheta\|^2.
\tag{6.2.15}
$$

Since $\sigma = \sigma_r + i\sigma_i$, equating the imaginary part of equation (6.2.15) yields

$$\sigma_i \left\| \nabla^* \vartheta \right\|^2 = 0.$$

Thus, $\sigma_i = 0$ and so $\sigma \in \mathbb{R}$ which implies that the linearized equations (6.2.5) satisfy the strong principle of exchange of stabilities. As such the instability set in as stationary convection.

6.3   Linear instability analysis

In this section, we seek to find the critical Rayleigh number of linear theory follows the work of Chandrasekhar [19]. To this end, we set $\sigma = 0$ into equation (6.2.5). We further employ equation (6.2.8), and the governing system can be reduced to

$$\xi \, \Delta^* w + w_{,zz} + \tilde{T} \omega_{3,z} = R \, \Delta^* \vartheta,$$
$$\omega_{3,z} - \tilde{T} w_{,zz} = 0, \tag{6.3.1}$$
$$Rw + \Delta\vartheta = 0,$$

where differentiating equation (6.2.12) with respect to z has been employed.

We now eliminate $\omega_{3,z}$ from equations $(6.3.1)_1$ and $(6.3.1)_2$, therefore system (6.3.1) can be written as follows

$$\xi \, \Delta^* w + \left(1 + \tilde{T}^2 \right) w_{,zz} = R \, \Delta^* \vartheta,$$
$$Rw + \Delta\vartheta = 0. \tag{6.3.2}$$

To proceed we assume a normal mode representation for w, and ϑ of the form

$$w = W(z)f(x,y), \qquad \vartheta = \Theta(z)f(x,y),$$

where $f(x,y)$ is the horizontal planform which satisfies $\Delta^* f = -a^2 f$, a being a wave number. With $D = d/dz$, we arrive at the following system

$$\left((1 + \tilde{T}^2)D^2 - \xi a^2 \right) W = -a^2 R\Theta,$$
$$\left(D^2 - a^2 \right) \Theta = -RW. \tag{6.3.3}$$

The corresponding boundary conditions are

$$W = \Theta = 0, \qquad \text{at } z = 0, 1. \tag{6.3.4}$$

The variable Θ is eliminated from equation (6.3.3) to yield the fourth order differential equation

$$\left[(1 + \tilde{T}^2)(D^2 - a^2)D^2 - \xi a^2(D^2 - a^2)\right]W = a^2 R^2 W. \tag{6.3.5}$$

In view of the boundary conditions (6.3.4) and from equation (6.3.3), one obtains

$$D^2 W = 0, \qquad \text{at } z = 0, 1.$$

Applying these boundary conditions to equation (6.3.5), it turns out that

$$D^4 W = 0, \qquad \text{at } z = 0, 1. \tag{6.3.6}$$

Further differentiation of equation (6.3.5) yields

$$D^{(2n)} W = 0, \qquad \text{at } z = 0, 1, \quad \text{for } n = 0, 1, 2, ...$$

Thus, we may select $W = \sin n\pi z$, for $n \in \mathbb{N}$. Upon substituting in equation (6.3.5), we have

$$\left[(1 + \tilde{T}^2)(n^2\pi^2 + a^2)n^2\pi^2 + \xi a^2(n^2\pi^2 + a^2)\right] = a^2 R^2,$$

which leads to

$$R_L^2 = \frac{\left(1 + \tilde{T}^2\right)\pi^2 n^2 \Lambda_n}{a^2} + \xi\Lambda_n, \tag{6.3.7}$$

where $\Lambda_n = n^2\pi^2 + a^2$. Minimizing over n yields $n = 1$. Then differentiating R^2 with respect to a^2 yields the stationary convection boundary

$$R_{L(sc)}^2 = \pi^2 \left(\sqrt{\xi} + \sqrt{1 + \tilde{T}^2}\right)^2, \tag{6.3.8}$$

and the corresponding critical wave number a_c is given by

$$a_{L(c)}^2 = \pi^2 \sqrt{\frac{1 + \tilde{T}^2}{\xi}}. \tag{6.3.9}$$

It is worth observing that as $\tilde{T}^2 = 0$, and $\xi = 1$, we recover the result for Darcy porous problem [115]

$$a_{L(c)}^2 = \pi^2, \qquad R_{L(sc)}^2 = 4\pi^2.$$

6.4 Nonlinear stability analysis

In this section, we commence deriving further boundary conditions which will be used to continue with the nonlinear stability analysis. To obtain these we observe from equation (6.2.2) and equation (6.2.10),

$$\omega_1 = (1 - \xi)\, w_{,y} + \tilde{T} u_{,z} + R\vartheta_{,y}, \qquad \omega_2 = (\xi - 1)\, w_{,x} + \tilde{T} v_{,z} - R\vartheta_{,x}. \qquad (6.4.1)$$

One may then deduce from the boundary conditions (6.2.6),

$$\omega_1 = \tilde{T} u_{,z}, \,, \qquad \omega_2 = \tilde{T} v_{,z}, \qquad z = 0, 1. \qquad (6.4.2)$$

In addition, from equation (6.2.10),we also find at the boundaries

$$\omega_1 = -v_{,z}, \qquad \omega_2 = u_{,z}, \qquad z = 0, 1. \qquad (6.4.3)$$

One may then deduce from equations (6.4.2) and (6.4.3),

$$u_{,z} = v_{,z} = 0, \qquad \text{at } z = 0, 1, \qquad (6.4.4)$$

and hence

$$\omega_1 = \omega_2 = 0, \qquad \text{at } z = 0, 1, \qquad (6.4.5)$$

and again we find from equation (6.2.10) and equation (6.2.12) that

$$\tilde{T} w_{,zz} = v_{,xz} - u_{,yz}. \qquad (6.4.6)$$

It follows from (6.4.4) that

$$w_{,zz} = 0, \qquad \text{at } z = 0, 1. \qquad (6.4.7)$$

Since $w \equiv \vartheta \equiv 0$ at $z = 0, 1$, we obtain from equation $(6.2.5)_3$

$$\vartheta_{,zz} = 0, \qquad \text{at } z = 0, 1. \qquad (6.4.8)$$

Then differentiating equation $(6.2.1)_3$ an even numbers of times with respect to z, we find

$$\vartheta_{,t}^{(2n)} + \sum_{s=0}^{2n} \binom{2n}{s} u_i^{(s)} \vartheta_{,i}^{(2n-s)} = Rw^{(2n)} + \Delta\vartheta^{(2n)},$$

where we have used the General Leibniz Rule.

Further, we may rewrite the foregoing equation as shown below,

$$\vartheta_{,t}^{(2n)}+\sum_{s=0}^{2n}\binom{2n}{s}\left[u^{(s)}\vartheta_{,x}^{(2n-s)}+v^{(s)}\vartheta_{,y}^{(2n-s)}+w^{(s)}\vartheta^{(2n-s+1)}\right]=Rw^{(2n)}+\Delta^*\vartheta^{(2n)}+\vartheta^{(2n+2)}.$$

Now, setting $n=1$, we have

$$\vartheta_{,t}^{(2)}+\sum_{s=0}^{2}\binom{2}{s}\left[u^{(s)}\vartheta_{,x}^{(2-s)}+v^{(s)}\vartheta_{,y}^{(2-s)}+w^{(s)}\vartheta^{(3-s)}\right]=Rw^{(2)}+\Delta^*\vartheta^{(2)}+\vartheta^{(4)}.$$

$$(6.4.9)$$

Thus, employing (6.2.6), (6.4.4), (6.4.7), and (6.4.8) yields

$$\vartheta^{(4)}=0,\qquad\text{at }z=0,1.\tag{6.4.10}$$

We next differentiate equation (6.4.1), an even numbers of times with respect to z, to find

$$\omega_{1,zz}=\tilde{T}u_{,zzz},\qquad\omega_{2,zz}=\tilde{T}v_{,zzz},\qquad\text{at }z=0,1.\tag{6.4.11}$$

In addition, we also differentiate equation (6.4.3), an even number of times with respect to z, we have

$$\omega_{1,zz}=-v_{,zzz},\qquad\omega_{2,zz}=u_{,zzz},\qquad\text{at }z=0,1.\tag{6.4.12}$$

Therefore, from (6.4.11) and (6.4.12), we obtain

$$u_{,zzz}=0,\qquad v_{,zzz}=0,\qquad\text{at }z=0,1.\tag{6.4.13}$$

By further differentiation of (6.4.6), an even number of times with respect to z, we find

$$w^{(4)}=0\qquad\text{at }z=0,1.\tag{6.4.14}$$

The above process may be repeated to derive the general boundary conditions

$$w^{(2n)}=0,\qquad\vartheta^{(2n)}=0,\qquad\text{at }z=0,1,\qquad\text{for }n\in\mathbb{N},\tag{6.4.15}$$

which hold for the solution of the nonlinear problem.

We aim now to study nonlinear energy stability and find a stability threshold. Again, we let V be a period cell for a disturbance to (6.2.1), and let $\|.\|$ and $(.,.)$

be the norm and inner product on $L^2(V)$. The energy identities are derived by multiplying the vertical component of equation (6.2.3) by w, upon use of (6.2.8) and (6.2.12) with $i = 3$, and also use some integrations by parts, with the aid of boundary conditions one may show

$$\xi \|\nabla^* w\|^2 + \left(1 + \tilde{T}^2\right) \|w_{,z}\|^2 = R\left(\nabla^* \vartheta, \nabla^* w\right). \tag{6.4.16}$$

Next, multiply $(6.2.1)_3$ by ϑ and integrate over V to find

$$\frac{1}{2}\frac{d}{dt} \|\vartheta\|^2 = R\left(w, \vartheta\right) - \|\nabla\vartheta\|^2. \tag{6.4.17}$$

By adding λ (6.4.16) to (6.4.17), for $\lambda > 0$ a parameter to be chosen, thus we may derive an energy identity of form

$$\frac{dE}{dt} = RI - D, \tag{6.4.18}$$

where

$$E(t) = \frac{1}{2} \|\vartheta\|^2, \tag{6.4.19}$$

$$I = \left(w, \vartheta\right) + \lambda\left(\nabla^* \vartheta, \nabla^* w\right), \tag{6.4.20}$$

$$D = \|\nabla\vartheta\|^2 + \lambda\left(\xi \|\nabla^* w\|^2 + \left(1 + \tilde{T}^2\right) \|w_{,z}\|^2\right). \tag{6.4.21}$$

Define R_E by

$$\frac{1}{R_E} = \max_{\mathcal{H}} \frac{I}{D}, \tag{6.4.22}$$

where $\mathcal{H}$ is the space of admissible functions given by

$$\mathcal{H} = \{u_{,i}, \vartheta | u_i \in L^2(V), \vartheta \in H^1(V), u_{i,i} = 0, u_i, \vartheta \text{ are periodic in } x, y\}.$$

Therefore, from equation (6.4.18) we deduce

$$\frac{dE}{dt} \leq -D\left(\frac{R_E - R}{R_E}\right). \tag{6.4.23}$$

Then, from the Poincaré's inequality on D we have

$$D \geq \pi^2 \|\vartheta\|^2.$$

Provided $R < R_E$, put $c = 1 - R/R_E > 0$ and then from (6.4.23) we have

$$\frac{dE}{dt} \leq -2\pi^2 c E(t).$$

This yields

$$E(t) \leq E(0)e^{-2\pi^2 ct}.$$

Thus $E(t)$ tends to 0 as $t \to \infty$ at least exponentially. Therefore $\|\vartheta(t)\| \to 0$ at least exponentially.

To obtain decay of $\mathbf{u}$, we multiply equation (6.2.1) by u_i and integrate over V to obtain

$$(m_{ij}u_j, u_i) = R(\vartheta, w). \tag{6.4.24}$$

We may observe that

$$(m_{ij}u_j, u_i) \geq \hat{\mu}\|\mathbf{u}\|^2,$$

where

$$\hat{\mu} = \min\{1, \xi\}.$$

From (6.4.24) it now follows that

$$\hat{\mu}\|\mathbf{u}\|^2 \leq R(\vartheta, w),$$

and then with use of the arithmetic geometric mean inequality, one shows

$$\begin{aligned}
\hat{\mu}\|\mathbf{u}\|^2 &\leq \frac{R}{2\hat{\alpha}}\|\vartheta\|^2 + \frac{R\hat{\alpha}}{2}\|w\|^2 \\
&\leq \frac{R}{2\hat{\alpha}}\|\vartheta\|^2 + \frac{R\hat{\alpha}}{2}\|\mathbf{u}\|^2,
\end{aligned}$$

for $\hat{\alpha} > 0$ to be chosen.

If we now pick $\hat{\alpha} = \hat{\mu}/R$, then we show

$$0 < \|\mathbf{u}\|^2 \leq \frac{R^2}{\hat{\mu}^2}\|\vartheta\|^2,$$

which implies $\|\mathbf{u}\|^2$ must also decay at least exponentially. Hence, the global non-linear stability criterion is determined by (6.4.22).

To determine R_E we have to derive the Euler-Lagrange equations and maximising in the coupling parameter λ. To do this we must find the stationary point of I/D, we use the calculus of variations technique (see Section (1.4)). From a similar procedure

to that leading to (1.4.10), the Euler-Lagrange equations arising from (6.4.22) are determined from

$$R_E \delta I - \delta D = 0. \tag{6.4.25}$$

For all $h_i \in \mathcal{H}$, and $\eta \in \mathcal{H}$. We have that

$$\delta D = \frac{d}{d\varepsilon} \int_V \left[(\nabla(\vartheta + \eta\varepsilon))^2 + \lambda\xi \left(\nabla^*(w + h_3\varepsilon)\right)^2 + \lambda\left(1 + \tilde{T}^2\right)(w_{,z} + h_{3,z}\varepsilon)^2 \right] dV \Bigg|_{\varepsilon=0},$$

$$= \int_V \left[2\nabla(\vartheta + \eta\varepsilon)\nabla\eta + 2\lambda\xi \nabla^*(w + h_3\varepsilon)\nabla^* h_3 + 2\lambda\left(1 + \tilde{T}^2\right)(w_{,z} + h_{3,z}\varepsilon)h_{3,z} \right] dV \Bigg|_{\varepsilon=0},$$

and

$$\delta I = \frac{d}{d\varepsilon} \int_V \left[(w + \varepsilon h_3)(\vartheta + \varepsilon\eta) + \lambda\nabla^*(\vartheta + \eta\varepsilon)\nabla^*(w + h_3\varepsilon) - (u_{i,i} + \varepsilon h_{i,i})\pi(x) \right] dV \Bigg|_{\varepsilon=0},$$

$$= \int_V \left[(w + \varepsilon h_3)\eta + h_3(\vartheta + \varepsilon\eta) + \lambda\nabla^*(\vartheta + \eta\varepsilon)\nabla^* h_3 + \nabla^*(w + h_3\varepsilon)\nabla^*\eta - h_{i,i}\pi(x) \right] dV \Bigg|_{\varepsilon=0},$$

where we have included the constraint $u_{i,i} = 0$ by way of a Lagrange multiplier $2\pi(x)$, and ε is a positive constant.

Further, after some integrations by parts and using the boundary conditions we find that

$$\delta D = \int_V \left[-2\eta\Delta\vartheta + 2\lambda h_3 \left(-\xi\Delta^* w - \left(1 + \tilde{T}^2\right)w_{,zz} \right) \right] dV,$$

$$\delta I = \int_V \left[\eta(w - \lambda\Delta^* w) + h_i \left(\delta_{i3}(\vartheta - \lambda\Delta^*\vartheta) - \pi_{,i} \right) \right] dV.$$

Since h_i and η were chosen arbitrary functions, hence from equation (6.4.25) we obtain the Euler-Lagrange equations

$$R_E k_i(\vartheta - \lambda\Delta^*\vartheta) + 2\lambda k_i \left(\xi\Delta^* w + \left(1 + \tilde{T}^2\right)w_{,zz} \right) = \pi_{,i}, \tag{6.4.26}$$

$$R_E(w - \lambda\Delta^* w) + 2\Delta\vartheta = 0, \tag{6.4.27}$$

where $\pi(\mathbf{x})$ is a Lagrange multiplier. We now eliminate π by performing taking curl curl of equation $(6.4.26)_1$, and then consider the third component of the resulting

equation. To do this, we look at each terms of $(6.4.26)_1$ and simplify as follows,

for the first term let $\hat{A} = k_i \left(1 - \lambda \Delta^*\right) \vartheta$, then we have

$$\begin{aligned}
\text{curl}(\hat{A})_i &= \varepsilon_{ijk} \hat{A}_{k,j} \\
&= \varepsilon_{ijk} \left(\delta_{k3} \left(1 - \lambda \Delta^*\right) \vartheta_{,j}\right) \\
&= \varepsilon_{ij3} \left(1 - \lambda \Delta^*\right) \vartheta_{,j} \\
&= \delta_{i1} \left(1 - \lambda \Delta^*\right) \vartheta_{,y} - \delta_{i2} \left(1 - \lambda \Delta^*\right) \vartheta_{,x},
\end{aligned}$$

and

$$\begin{aligned}
\text{curlcurl}(\hat{A})_i &= \text{curl} \left[\delta_{i1} \left(1 - \lambda \Delta^*\right) \vartheta_{,y} - \delta_{i2} \left(1 - \lambda \Delta^*\right) \vartheta_{,x}\right]_i \\
&= \varepsilon_{ijk} \left[\left(1 - \lambda \Delta^*\right) \left(\delta_{k1} \vartheta_{,y} - \delta_{k2} \vartheta_{,x}\right)\right]_{,j} \\
&= \left(1 - \lambda \Delta^*\right) \left(\varepsilon_{ij1} \vartheta_{,yj} - \varepsilon_{ij2} \vartheta_{,xj}\right) \\
&= \left(1 - \lambda \Delta^*\right) \left(\delta_{i2} \vartheta_{,yz} - \delta_{i1} \vartheta_{,xz} - \delta_{i3} \Delta^* \vartheta\right). \qquad (6.4.28)
\end{aligned}$$

For the second term we put $\hat{B} = k_i \left(\xi \Delta^* w + \left(1 + \tilde{T}^2\right) w_{,zz}\right)$ to find

$$\begin{aligned}
\text{curl}(\hat{B})_i &= \varepsilon_{ijk} \hat{B}_{k,j} \\
&= \varepsilon_{ijk} \left(\delta_{k3} \left(\xi \Delta^* w + \left(1 + \tilde{T}^2\right) w_{,zz}\right)_{,j}\right) \\
&= \varepsilon_{ij3} \left(\xi \Delta^* w_{,j} + \left(1 + \tilde{T}^2\right) w_{,zzj}\right) \\
&= \delta_{i1} \left(\xi \Delta^* w_{,y} + \left(1 + \tilde{T}^2\right) w_{,zzy}\right) - \delta_{i2} \left(\xi \Delta^* w_{,x} + \left(1 + \tilde{T}^2\right) w_{,zzx}\right),
\end{aligned}$$

and

$$\begin{aligned}
&\text{curlcurl}(\hat{B})_i = \\
&\varepsilon_{ijk} \delta_{k1} \left(\xi \Delta^* w_{,y} + \left(1 + \tilde{T}^2\right) w_{,zzy}\right)_{,j} - \varepsilon_{ijk} \delta_{k2} \left(\xi \Delta^* w_{,x} + \left(1 + \tilde{T}^2\right) w_{,zzx}\right)_{,j} \\
&= \varepsilon_{ij1} \left(\xi \Delta^* w_{,yj} + \left(1 + \tilde{T}^2\right) w_{,zzyj}\right) - \varepsilon_{ij2} \left(\xi \Delta^* w_{,xj} + \left(1 + \tilde{T}^2\right) w_{,zzxj}\right) \\
&= \delta_{i1} \left(\xi \Delta^* w_{,xz} + \left(1 + \tilde{T}^2\right) w_{,zzzx}\right) + \delta_{i2} \left(\xi \Delta^* w_{,yz} + \left(1 + \tilde{T}^2\right) w_{,zzzy}\right) \\
&\quad - \delta_{i3} \Delta^* \left(\xi \Delta^* w + \left(1 + \tilde{T}^2\right) w_{,zz}\right).
\end{aligned}$$

$$(6.4.29)$$

Now, taking $i = 3$ in (6.4.28) and (6.4.29), we arrive at

$$R_E \left(\lambda \Delta^* - 1\right) \Delta^* \vartheta - 2\lambda \Delta^* \left(\xi \Delta^* w + \left(1 + \tilde{T}^2\right) w_{,zz}\right) = 0, \qquad (6.4.30)$$

$$R_E \left(w - \lambda \Delta^* w\right) + 2\Delta \vartheta = 0. \qquad (6.4.31)$$

We again use a normal mode representation, as for the linear stability analysis, $\vartheta = \Theta(z)f(x,y)$, $w = W(z)f(x,y)$. This leave us to solve the eigenvalue problem

$$R_E \left(1 + \lambda a^2\right) \Theta + 2\lambda \left[\left(1 + \tilde{T}^2\right) D^2 - \xi a^2\right] W = 0$$
$$R_E \left(1 + \lambda a^2\right) W + 2 \left(D^2 - a^2\right) \Theta = 0. \tag{6.4.32}$$

This system would have to be solved for R_E subject to the boundary conditions (6.3.4). Further, we observe that W and Θ satisfy the boundary conditions

$$W^{(2n)} = 0, \qquad \Theta^{(2n)} = 0, \qquad \text{at } z = 0, 1, \qquad \text{for } n \in \mathbb{N}. \tag{6.4.33}$$

By eliminating Θ we obtain a forth order equation in W,

$$4\lambda \left(1 + \tilde{T}^2\right) \left(D^2 - a^2\right) D^2 W - 4\lambda \xi a^2 \left(D^2 - a^2\right) W = R_E^2 \left(1 + \lambda a^2\right)^2 W. \tag{6.4.34}$$

Hence, $W(z)$ may be written in the form

$$W = \sin n\pi z, \qquad n = 1, 2, \cdots .$$

After some calculations, following the method in section 6.3, one may find

$$R_E^2 = 4\lambda \frac{\pi^2 n^2 \left(1 + \tilde{T}^2\right) \left(\pi^2 n^2 + a^2\right) + \xi a^2 \left(\pi^2 n^2 + a^2\right)}{\left(1 + \lambda a^2\right)^2}. \tag{6.4.35}$$

For any fixed wave number a^2 the minimum with respect to n^2 of $R_E^2 \left(a^2, n^2\right)$ is obtained for $n = 1$. Then

$$R_E^2 = 4\lambda \frac{\pi^2 \left(1 + \tilde{T}^2\right) \left(\pi^2 + a^2\right) + \xi a^2 \left(\pi^2 + a^2\right)}{\left(1 + \lambda a^2\right)^2}. \tag{6.4.36}$$

Let us now select $\lambda = 1/a^2$, and then

$$R_E^2 = \frac{\pi^2 \left(\pi^2 + a^2\right) \left(1 + \tilde{T}^2\right)}{a^2} + \xi \left(\pi^2 + a^2\right). \tag{6.4.37}$$

This is exactly the same equation (6.3.7) for linear instability problem. This is, in a sense, the best possible threshold for the onset of linear unconditional stability. Thus, the minimum of R_E^2 with respect to a^2 is identical to the minimum of R_L^2 with respect to a^2, and hence no subcritical instabilities can arise. Although this result is undoubtedly due to the fact that the operator attached to the linear theory is symmetric in this case, cf. Straughan [115], and Falsaperla et al. [36].

6.5 Numerical results

The aim of this Chapter was to investigate how the inclusion of the Taylor number $\tilde{T}^2$ effects the thermal instability threshold in an anisotropic porous medium. The results of different values of the anisotropy parameter ξ and the Taylor number $\tilde{T}^2$ are presented in Tables 6.1 and 6.2, and are presented graphically in Figures 6.1 and 6.2.

Table 6.1 and Figure 6.1 present the values of $R^2_{L(sc)} = R_c$, the critical Rayleigh number for both the onset of linear instability and for the nonlinear stability. This shows that the effect of increasing the Taylor number $\tilde{T}^2$ always results in an increase in the critical Rayleigh number R_c, so that rotation stabilize the system. Furthermore, the effect of increasing the anisotropy parameter ξ is seen also to increase the critical Rayleigh number R_c. This means when the rate of rotation, and ξ increases, the stability becomes more pronounced. For example, for $\xi = 3$ and $\tilde{T}^2 = 5$ we see from Table 6.1 that the critical Rayleigh number is $R_c = 172.573$, whereas when $\xi = 10$ and $\tilde{T}^2 = 25$ the critical Rayleigh number is $R_c = 673.591$.

Table 6.2 and Figure 6.2 present the values of $a_{L(c)} = a_c$, the critical wave number for both the onset of linear instability and for the nonlinear stability. It can be observed that for a fixed values of the anisotropy parameter ξ, the effect of increasing the Taylor number $\tilde{T}^2$ is to increase the wave number. For example, for $\xi = 3$ and $\tilde{T}^2 = 5$ we see from Table 6.2 that the critical wave number is $a_c = 3.736$, whereas when $\tilde{T}^2 = 25$ for the same anisotropy parameter $\xi = 3$ the critical wave number is $a_c = 5.390$. It is also observed that increasing the anisotropy parameter ξ had the effect of decreasing the value of wave number. However, as soon as the value of the Taylor number $\tilde{T}^2$ increases one can observe the critical wave number also increases which corresponds to the narrow convection cells.

Table 6.1: Critical values of Rayleigh number R_c, vs. ξ, for $\tilde{T}^2 = 5, 10, 15, 20, 25$.

|	R_c				
ξ	$\tilde{T}^2 = 5$	$\tilde{T}^2 = 10$	$\tilde{T}^2 = 15$	$\tilde{T}^2 = 20$	$\tilde{T}^2 = 25$
1.	117.438	183.903	246.740	307.588	367.130
2.	147.335	220.890	289.315	354.926	418.690
3.	172.573	251.568	324.280	393.546	460.550
4.	195.398	278.979	355.306	427.653	497.389
5.	216.682	304.304	383.815	458.876	531.019
6.	236.871	328.145	410.535	488.051	562.370
7.	256.230	350.864	435.901	515.674	591.993
8.	274.932	372.693	460.194	542.068	620.249
9.	293.097	393.795	483.611	567.457	647.388
10.	310.813	414.288	506.293	592.006	673.591
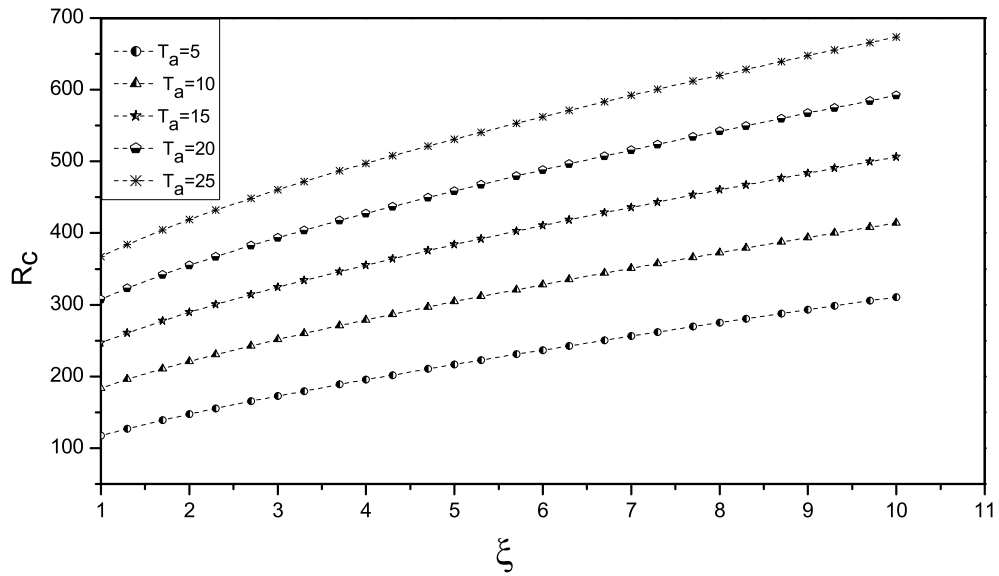
Figure 6.1: Critical Rayleigh number R_c as function of ξ, for $\tilde{T}^2 = 5$ increasing to $\tilde{T}^2 = 25$.

Table 6.2: Critical values of wave number a_c, vs. ξ, for $\tilde{T}^2 = 5, 10, 15, 20, 25$.

ξ	a_c				
	$\tilde{T}^2 = 5$	$\tilde{T}^2 = 10$	$\tilde{T}^2 = 15$	$\tilde{T}^2 = 20$	$\tilde{T}^2 = 25$
1.	4.917	5.721	6.283	6.725	7.094
2.	4.135	4.811	5.284	5.655	5.965
3.	3.736	4.347	4.774	5.110	5.390
4.	3.477	4.046	4.443	4.755	5.016
5.	3.288	3.826	4.202	4.497	4.744
6.	3.142	3.656	4.015	4.297	4.533
7.	3.023	3.517	3.863	4.135	4.361
8.	2.924	3.402	3.736	3.999	4.218
9.	2.839	3.303	3.628	3.883	4.096
10.	2.765	3.217	3.533	3.782	3.989
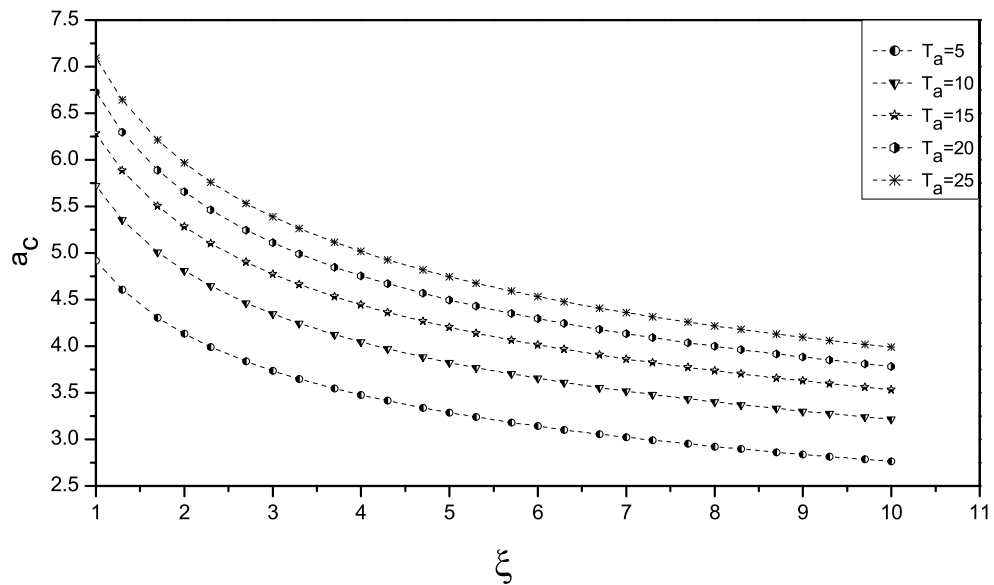
Figure 6.2: Critical wave number a_c as function of ξ, for $\tilde{T}^2 = 5$ increasing to $\tilde{T}^2 = 25$.

Chapter 7

Rotating anisotropic fluid saturated Darcy porous medium with inertia

In the previous Chapter we investigated the combined effects of the Taylor number and the anisotropy parameter on the stability threshold for the thermal convection problem of Darcy model. Our analysis, by using the energy method, emphasized that the subcritical instabilities are not possible when the inertia term is neglected. In this Chapter we will employ the linear instability method to find instability boundaries for our previous problem in Chapter 6, but this time we are interested in the effect of inclusion of the inertia term in the momentum equation on the onset of convection.

It is noteworthy that the paper of Vadasz [131] has concerned with how the presence of fluid inertia term in the momentum equation influences the onset of thermal convection in a fluid saturated porous medium of Darcy type. In particular, he found the onset of convection may be by oscillatory when the inertia term is considered. Recently, the work of Capone and Rionero [13] confirms that the inertia term plays an important role on the onset of convection instability in a rotating porous media. They revisited the Vadasz paper [131] and they found that, by using an auxiliary method, new behaviours for the Rayleigh number stability thresholds

which are complementary to the Vadasz results. Further recent interesting work on the effect of the inclusion of the inertia term, is also due to Straughan [123], who incorporated such an anisotropic inertia term in Darcy's equation to study the onset of thermosolutal convection in a microfludic porous medium. His results reveals that including an anisotropic inertia has a significant role in the thermal instability threshold.

In this Chapter we will work with the complete system (6.1.1)-(6.1.3) which includes inertia, considered in Chapter 6. To this end, the fully nonlinear non–dimensional perturbation equations and the linear instability analysis are represented in Section 7.1. In Sections 7.1.1 and 7.1.2, we study, respectively, the stationary convection and the oscillatory convection. Section 7.2 is devoted to the numerical results.

It is found that the inertia term has no effect on the stationary convection instability boundary.

7.1 Governing equations and linear instability analysis

To study the linear instability analysis, once more we consider the fully nonlinear nondimensional system for the perturbation equations for the velocity, u_i, pressure, π, and temperature, ϑ, of (6.1.7),

$$\frac{1}{V_a} u_{i,t} = -\pi_{,i} + Rk_i\vartheta - \tilde{T}(\mathbf{k} \times \mathbf{u})_i - m_{ij}u_j,$$

$$u_{i,i} = 0, \tag{7.1.1}$$

$$\vartheta_{,t} + u_i\vartheta_{,i} = Rw + \Delta\vartheta,$$

and with the corresponding boundary conditions,

$$n_i u_i = \vartheta = 0, \quad z = 0, 1. \tag{7.1.2}$$

Here the square root of the Rayleigh number, R, the square root of the Taylor number, $\tilde{T}$, and the Vadasz number, V_a, are the nondimensional variables as defined in

Chapter 6. Again $m_{ij} = diag\{1, 1, \xi\}$, where ξ is the anisotropy parameter as given in Chapter 6.

To proceed with the linear instability, we follow the same procedure to that using in the Chapter 6, by performing taking the curl of equation $(7.1.1)_1$ and curl curl of the same equation. After taking the third component we arrive at the system of the form

$$-V_a^{-1}\Delta w_{,t} = -R\Delta^*\vartheta + \tilde{T}\omega_{3,z} + m_{3r}\Delta u_r - m_{jr}u_{r,j3},$$

$$V_a^{-1}\omega_{3,t} = \tilde{T}w_{,z} - \varepsilon_{3jk}m_{kq}u_{q,j}, \qquad (7.1.3)$$

$$\vartheta_{,t} + w\vartheta_{,z} = Rw + \Delta\vartheta.$$

Applying equations (6.2.8), (6.2.9), and (6.2.11) in Chapter 6 to (7.1.3), we have

$$-V_a^{-1}\Delta w_{,t} = -R\Delta^*\vartheta + \tilde{T}\omega_{3,z} + \xi\Delta^*w + w_{,zz},$$

$$V_a^{-1}\omega_{3,t} = \tilde{T}w_{,z} - \omega_3, \qquad (7.1.4)$$

$$\vartheta_{,t} + w\vartheta_{,z} = Rw + \Delta\vartheta.$$

We now consider the linearised equations of (7.1.4) by removing the nonlinear term of equation $(7.1.4)_3$. We then assume a temporal growth rate like $e^{\sigma t}$, i.e. we write

$$w = w(\mathbf{x})\,e^{\sigma t}, \quad \vartheta = \vartheta(\mathbf{x})\,e^{\sigma t}, \quad \omega_3 = \omega_3(\mathbf{x})\,e^{\sigma t}.$$

Upon substituting into equation (7.1.4), we have to solve the system

$$-V_a^{-1}\sigma\Delta w = -R\Delta^*\vartheta + \tilde{T}\omega_{3,z} + \xi\Delta^*w + w_{,zz},$$

$$V_a^{-1}\sigma\omega_3 = \tilde{T}w_{,z} - \omega_3, \qquad (7.1.5)$$

$$\sigma\vartheta = Rw + \Delta\vartheta.$$

After eliminating the variable ω_3 from equations $(7.1.5)_1$ and $(7.1.5)_2$, and then assuming a normal mode with the representation for w, and ϑ of the form $w = W(z)f(x,y)$, and $\vartheta = \Theta(z)f(x,y)$ where $f(x,y)$ is the horizontal planform which satisfies $\Delta^*f = -a^2f$, a being a wave number. The system (7.1.5) can be written as

$$-\sigma V_a^{-1}(1 + \sigma V_a^{-1})(D^2 - a^2)W - \left(\tilde{T}^2 + (1 + \sigma V_a^{-1})\right)D^2W =$$

$$-a^2\xi(1 + \sigma V_a^{-1})W + a^2R(1 + \sigma V_a^{-1})\Theta, \qquad (7.1.6)$$

$$(D^2 - a^2)\Theta = \sigma\Theta - RW, \qquad (7.1.7)$$

where $D = d/dz$. This system is solved subject to the boundary conditions

$$W = \Theta = 0, \qquad \text{at } z = 0, 1. \tag{7.1.8}$$

7.1.1 Stationary convection

In this section, we consider the case when instability sets in as stationary convection. Again we use the standard method to analyse equations (7.1.6), and (7.1.7) follows the work of Chandrasekhar [19]. To this end, we put $\sigma = 0$ into equations (7.1.6), and (7.1.7). Then we eliminate the variable W to obtain a single equation in Θ

$$\left(D^2 - \xi a^2\right)\left(D^2 - a^2\right)\Theta + \tilde{T}^2 D^2 \left(D^2 - a^2\right)\Theta = a^2 R^2 \Theta. \tag{7.1.9}$$

We now apply the boundary conditions (7.1.8) into equation (7.1.7) to deduce

$$D^2\Theta = 0, \qquad \text{at } z = 0, 1.$$

Then from (7.1.9) we have

$$\left(1 + \tilde{T}^2\right) D^4 \Theta = 0.$$

Since $\tilde{T}^2 \geq 0$. This leads to the further boundary condition

$$D^4 \Theta = 0, \qquad \text{at } z = 0, 1.$$

By differentiating equation (7.1.9), an even number of times with respect to z. Then employing the foregoing boundary condition to find

$$D^6 \Theta = 0, \qquad \text{at } z = 0, 1.$$

Further differentiation of equation (7.1.9) yields

$$D^{(2n)} \Theta = 0, \qquad \text{at } z = 0, 1, \quad \text{for } n = 0, 1, 2, \dots \tag{7.1.10}$$

Thus, we may select $\Theta = \sin n\pi z$, for $n \in \mathbb{N}$. Upon substituting in equation (7.1.9) we have, with $\Lambda_n = n^2\pi^2 + a^2$,

$$R_{sta}^2 = \frac{\left(1 + \tilde{T}^2\right)\pi^2 n^2 \Lambda_n}{a^2} + \xi\Lambda_n. \tag{7.1.11}$$

This equation is exactly the same equation (6.3.7) in Chapter 6 of linear instability method. It follows straightaway from equation (7.1.11), that the stationary convection for the case of presence inertia term occurs for the same critical Rayleigh number $R_{L(sc)}^2$ (6.3.8) and the same critical wave number $a_{L(c)}^2$ (6.3.9).

7.1.2 Oscillatory convection

The aim of this section is to consider the instability by oscillatory convection. To this end, we put $\sigma = i\sigma_1$, $\sigma_1 \in \mathbb{R}$ into equations (7.1.6), and (7.1.7). After eliminating the variable W , the real and imaginary parts yield

$$\sigma_1^2 \left[-V_a^{-1} \left(D^2 - a^2 \right) + V_a^{-2} \left(D^2 - a^2 \right)^2 - V_a^{-1} \left(D^2 - \xi a^2 \right) \right] \Theta =$$
$$-a^2 R^2 \Theta + \left(D^2 - \xi a^2 \right) \left(D^2 - a^2 \right) \Theta + \tilde{T}^2 D^2 \left(D^2 - a^2 \right) \Theta$$

and

$$-\sigma_1^2 V_a^{-2} \left(D^2 - a^2 \right) \Theta \ = V a^{-1} \left(D^2 - a^2 \right)^2 \Theta + V_a^{-1} \left(D^2 - \xi a^2 \right) \left(D^2 - a^2 \right) \Theta$$
$$- \left(D^2 - \xi a^2 \right) \Theta - \tilde{T}^2 D^2 \Theta - V_a^{-1} a^2 R^2 \Theta.$$

On considering the boundary condition (7.1.10), allow Θ to be composed of $sin\, n\pi z$, for $n \in \mathbb{N}$, we may solve for σ_1 and R^2 to find

$$\sigma_1^2 = \frac{\pi^2 V_a^2 \tilde{T}^2 \left(\Lambda - V_a \right)}{\Lambda^2 + V_a \beta} - V_a^2, \tag{7.1.12}$$

and

$$R_{os}^2 = \frac{(\Lambda + \beta)}{a^2} \left[\frac{\pi^2 V_a^2 \tilde{T}^2}{\Lambda^2 + V_a \beta} + \Lambda + V_a \right]. \tag{7.1.13}$$

Here $\beta = \pi^2 + \xi a^2$, and $\Lambda = n^2 \pi^2 + a^2$. Minimization over n yields $n = 1$. The critical Rayleigh number R_{osc}^2 and the corresponding critical wave number a_{osc}^2 are obtained by minimising R_{os}^2 in equation (7.1.13) over a^2. Setting $\partial^2 R / \partial a^2 = 0$, we may arrive at the following equation.

$$Ba^{12} + 2\chi Ba^{10} + \left(B\chi^2 + 2\alpha\xi \right) a^8 + \left(2\alpha\chi \left(\xi - 1 \right) - 2BV_a^2 \pi^2 \tilde{T}^2 \right) a^6$$
$$+ \left(B\alpha^2 - V_a^2 \pi^2 \tilde{T}^2 \left(B\chi + 6\pi^2 \right) - 2\alpha \left(\chi^2 + 2\alpha \right) \right) a^4$$
$$-4\chi \left(\alpha^2 + \pi^4 V_a^2 \tilde{T}^2 \right) a^2 - 2\alpha \left(\alpha^2 + \pi^4 V_a^2 \tilde{T}^2 \right) = 0, \tag{7.1.14}$$

where

$$B = 1 + \xi, \quad \alpha = \pi^2 \left(\pi^2 + V_a \right), \quad \chi = 2\pi^2 + V_a \xi.$$

Equation (7.1.14) is solved numerically by using the Maple(TM) [1] which gives the critical wave number a_{osc}^2. The oscillatory convection Rayleigh number R_{osc}^2 is then

---

[1]Maple is a trademark of Waterloo Maple Inc.

determined by substituting a_{osc}^2 into equation (7.1.13), but simultaneously requiring $\sigma_1^2 > 0$ in equation (7.1.12). It is evident that σ_1^2 cannot be positive for all wave number unless the Taylor number $\tilde{T}^2$ and the Vadasz number V_a are satisfying the following conditions

$$\tilde{T}^2 > \frac{(\Lambda^2 + V_a\beta)}{\pi^2 (\Lambda - V_a)}, \quad \text{and} \quad V_a < \Lambda. \tag{7.1.15}$$

Numerical results obtained for the stationary convection and the oscillatory convection are reported in the next section.

7.2   Numerical results

In this section we describe how the inclusion of the inertia term A together with the Taylor number $\tilde{T}^2$ and the anisotropy parameter ξ effects the onset of thermal convection. In Table 7.1 we present the results of the linear instability analysis for the critical Rayleigh number Ra, the stationary wave number a_{sta}, and the oscillatory wave number a_{osc}. We also represent the critical Rayleigh number Ra as a function of ξ for different values of Vadasz number $\gamma = V_a/\pi^2$ and $\tilde{T}^2 = 5, 10, 25$, and 120. The values of the anisotropy parameter ξ and the Vadasz number V_a are selected so that the condition (7.1.15) is taken into account. It is noteworthy that the stationary convection, see equation (6.3.8) depends on the Taylor number $\tilde{T}^2$ and the anisotropy parameter ξ. However, as show in Figures 7.1–7.4 increasing $\tilde{T}^2$ as well as ξ increases the stationary convection boundary R_{sc}.

Figure 7.1 shows when the small value of the Taylor number $\tilde{T}^2 = 5$ and the Vadasz number $\gamma = 0.3, 0.5$, and 0.7 the stationary convection is dominant when the values of ξ below a transition value ξ_c ($\xi < \xi_c$), and the convection is by oscillatory when $\xi > \xi_c$. As γ increases the onset of convection is more likely to be by stationary convection. For example, for $\gamma = 0.3, \xi_c = 0.0204$, the transition from the stationary mode to the oscillatory mode occurs when $Ra = 66.331$, whereas when $\gamma = 0.7$, $\xi_c = 0.3589$, the transition occurs when $Ra = 91.726$ as seen in Table 7.1.

In Figure 7.2, $\tilde{T}^2$ is increased to $\tilde{T}^2 = 10$. Here we observe that an increase in the value of ξ advances the oscillatory convection for $\xi < \xi_c$. However, as γ increases the transition from the oscillatory convection to the stationary convection occurs

sooner. For example, when $\gamma = 0.8$, $\xi_c = 8.8911$ as seen in Table 7.1, the convection switchs to the stationary convection when $Ra = 391.527$, whereas when $\gamma = 1.5$, $\xi_c = 1.6773$, the transition occurs when $Ra = 209.908$.
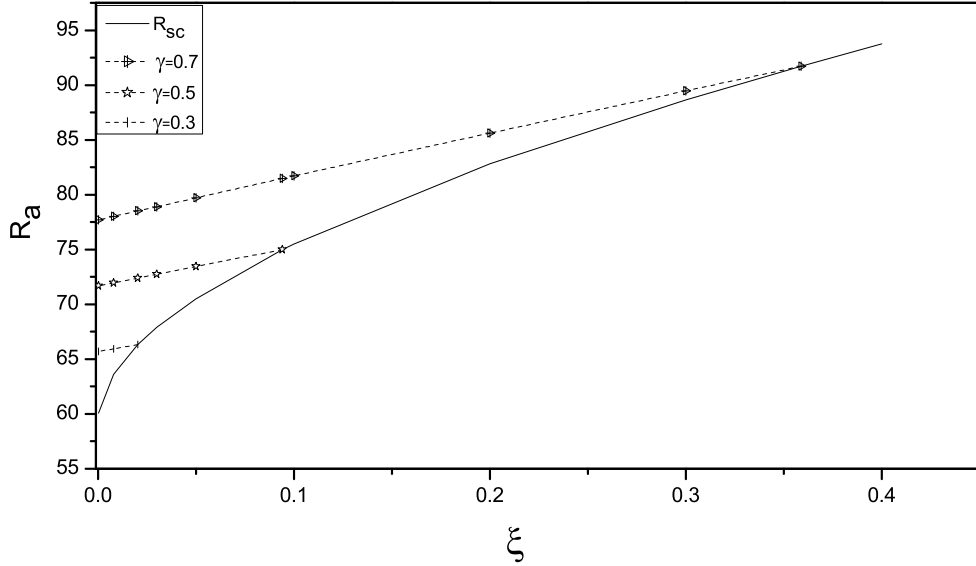

Figure 7.1: Critical values of Ra vs. ξ for $\tilde{T}^2 = 5$. The solid curve is for stationary convection. The other curves are for oscillatory convection, for $\gamma = 0.3, 0.5, 0.7$.
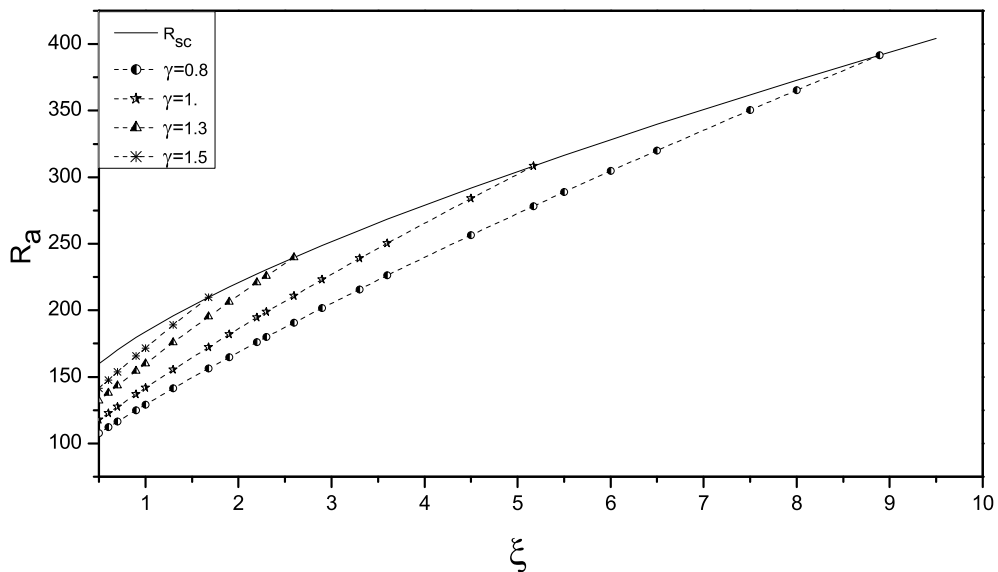

Figure 7.2: Critical values of Ra vs. ξ for $\tilde{T}^2 = 10$. The solid curve is for stationary convection. The other curves are for oscillatory convection, for $\gamma = 0.8, 1., 1.3, 1.5$.

Figure 7.3 confirms the effect of increasing the Taylor number $\tilde{T}^2$ on the onset of

the convection. We find that when $\tilde{T}^2$ is further increased to $\tilde{T}^2 = 25$, the instability is by oscillatory convection rather than stationary convection. We also find that the critical Rayleigh numbers Ra are greater in the case of $\tilde{T}^2 = 25$ than the case of $\tilde{T}^2 = 10$ (see Table 7.1). For example, for fixed value of $\gamma = 1.5$ in case $\tilde{T}^2 = 10$, the critical Rayleigh number $Ra = 209.9084$ at $\xi_c = 1.6773$, whereas when $\tilde{T}^2 = 25$, the critical Rayleigh number $Ra = 642.276$ at $\xi_= 8.8088$.

The effects of increasing the anisotropy parameter ξ are shown in Figure 7.4. It is interesting to mention that, by increasing $\tilde{T}^2$ from $\tilde{T}^2 = 25$ to $\tilde{T}^2 = 120$, one needs large values of the anisotropy parameter for instability, and so as a result, an increasing value of Ra. Therefore, an increase in the anisotropy parameter ξ in the vertical direction with an increase in the Taylor number $\tilde{T}^2$ has the effect of stabilizing the system. This is also due to the influence of the Vadasz number γ. Since $\pi^2 \gamma = V_a$ and the inertia coefficient is V_a^{-1}, this means increasing inertia is a destabilizing effect.

It is worth pointing out that if the Vadasz number $\gamma \leq 1$, the oscillatory wave number is smaller than the stationary wave number, which means the cells become narrower when the convection changes from the oscillatory convection to the stationary convection. For $\gamma > 1$ the situation reverses and cells become wider.

Figure 7.3: Critical values of Ra vs. ξ for $\tilde{T}^2 = 25$. The solid curve is for stationary convection. The other curves are for oscillatory convection, for $\gamma = 1.5, 1.7, 1.75, 2, 2.5$.
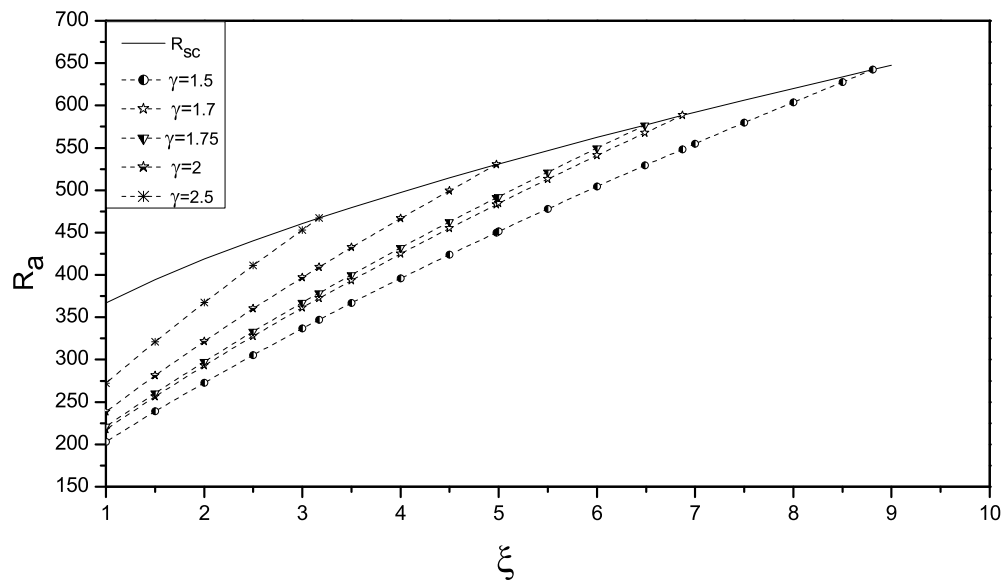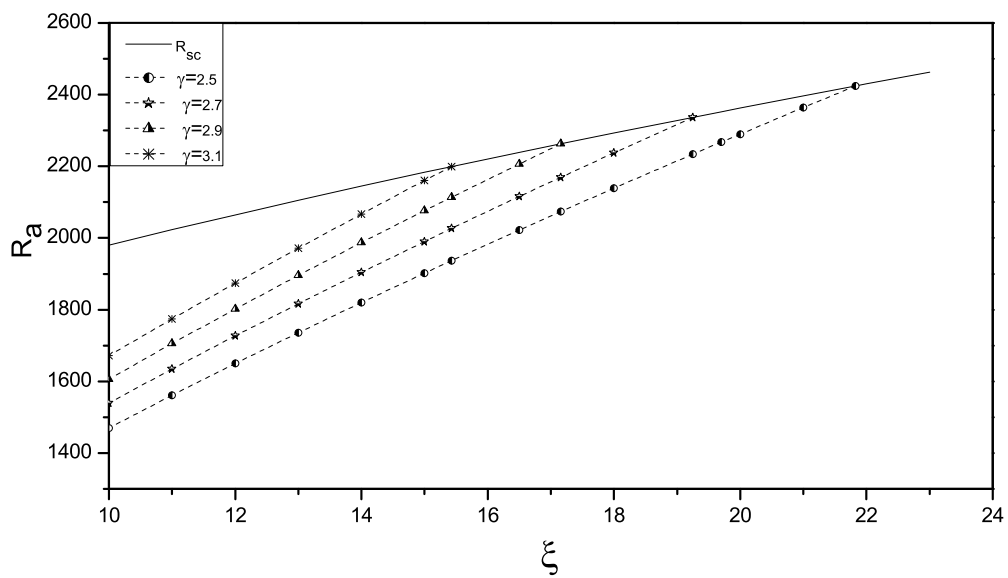

Figure 7.4: Critical values of Ra vs. ξ for $\tilde{T}^2 = 120$. The solid curve is for stationary convection. The other curves are for oscillatory convection, for $\gamma = 2.5, 2.7, 2.9, 3.1$.

Table 7.1: Transition values of Ra vs. ξ, for $\tilde{T}^2 = 5, 10, 25, 120$.

γ	$\tilde{T}^2$	ξ	Ra	a_{sta}	a_{osc}
0.3	5	0.0204	66.331	13.005	4.108
0.5	5	0.0941	74.981	8.877	4.337
0.7	5	0.3589	91.726	6.353	4.411
0.8	10	8.8911	391.527	3.3133	3.1986
1.	10	5.1704	308.459	3.7942	3.7837
1.3	10	2.5975	239.714	4.5067	4.5947
1.5	10	1.6773	209.908	5.0274	5.1029
1.5	25	8.8088	642.276	4.1178	4.5256
1.7	25	6.8702	588.233	4.3818	4.9387
1.75	25	6.4868	576.981	4.4451	5.0835
2.	25	4.9771	530.280	4.7495	5.5180
2.5	25	3.1699	467.094	5.3166	6.3948
2.5	120	21.8230	2423.940	4.8208	6.0447
2.7	120	19.2491	2336.840	4.9744	6.3545
2.9	120	17.1573	2262.950	5.1196	6.6532
3.1	120	15.4289	2199.39	5.2573	6.9420

Chapter 8

Conclusions and further work

The present work was designed to investigate thermal convection in a fluid saturated porous medium. Throughout the thesis we used the Darcy and Brinkman models to describe the flow in a porous material. The linear instability and nonlinear stability analyses were employed to determine the critical thresholds as well as examine the effects of the various physical parameters for the onset of thermal convection. The D^2 Chebyshev tau and the compound matrix techniques were implemented to solve the eigenvalue problems.

In Chapter 2 the Cattaneo-Christov law for the heat flux was proposed to study a model for thermal convection in a porous medium when the Guyer-Krumhansl equation was employed to describe the evolution of the heat flux. The energy balance equation and the Christov-Morro equation for the heat flux was derived. We found precise conditions for the Guyer-Krumhansl term, $\lambda < \frac{1}{\pi^2} \simeq 0.101321183$, in which the stationary convection will occur. The results of the linear instability theory showed that, for a chosen value of the inertia term A, the convection mechanism commences as oscillatory convection when the parameter P_2 is sufficiently large. As P_2 became smaller the convection mechanism switches to the stationary convection at transition value λ_c with narrower cells. These results indicate that the presence of Guyer-Krumhansl terms has a significant effect on the convection mechanism. Satisfactory numerical results were achieved by using D^2 Chebyshev tau method.

A similar model to that of Chapter 2 was investigated in Chapter 3 but here an alternative Cattaneo type theory for the heat flux was presented. The linear insta-

bility thresholds show that employing the Cattaneo-Fox law together with inclusion of the Guyer-Krumhansl terms for the heat flux lead to an a very interesting effect in the propagation heat mechanism. In particular, herein we showed that depending on the range of the Guyer-Krumhansl values λ, the instability convection can be stationary or oscillatory. It was found that the oscillatory convection depends strongly on the parameter P_2, Guyer-Krumhansl term λ, and inertia term A. As expected inclusion of the Guyer-Krumhansl term and once P_2 increase, the onset of convection is always by oscillatory. Also we note that the oscillatory wave numbers at the transition values λ_c are larger than that of stationary unless P_2 is large enough, and λ is likewise large. These results indicate the effect of the Guyer-Krumhansl term when the Cattaneo-Fox law for the heat flux is used.

In Chapter 4 the porous medium was assumed to have a large porosity and for this purpose we used Brinkman model to describe the flow in a porous medium. The employing of the Cattaneo-Christov theory effects on the thermal instability threshold was investigated. We have derived analytically the convection instability threshold for stationary and oscillatory convection in the case of free surfaces, while for the fixed surfaces the resulting eigenvalue problem was solved numerically by using the D^2 Chebyshev tau technique. It was showed that by introducing the Cattaneo-Christov theory in the institutive equation for heat flux which plays an important role in the thermal instability threshold. Through investigation we found that the stationary convection depends on λ only, whereas oscillatory convection depends on λ, A, and P_2. In general, the onset of convection is by stationary convection for small value of P_2. As P_2 increase the convection mechanism switches from the stationary convection to the oscillatory convection with narrower cells. The effects of increasing P_2 were seen to destabilize the system. This indicates that the thermal convection occurs more easily. Whilst increasing the value of λ as well as decreasing the value of A it was observed that the transition from the stationary mode to the oscillatory mode occurred sooner. It may be argued from the results that the critical Rayleigh numbers R_a and the critical wave numbers a_c are greater in the case of fixed-fixed boundaries than in the case of the free-free boundaries when all values of λ and A are considered. Also we observed that in the transition from

the stationary to the oscillatory convection in the case of fixed-fixed boundaries the value of P_2 is always smaller than in the free-free boundaries.

Chapter 5 presented the problem of a fluid saturated anisotropic porous Darcy medium. The analysis was restricted to the situation when the permeability varied in the vertical direction. It was found that the global nonlinear stability threshold was achieved. In sense that, the optimum results was obtained. The numerical solution was carried out via the D^2 Chebyshev tau method and the compound matrix method. It may be argued from the results that, in general, the effect of increasing the anisotropy parameter ξ, for a fixed value of q is to increase the critical Rayleigh number and the critical wave number. Thus, the anisotropic parameter was seen to have a profound impact on the stability regions.

Finally, in Chapters 6 and 7 we explained how the Taylor number due to the rotation effects the onset of thermal convection in an anisotropic Darcy porous medium. We allowed to the Vadasz number, V_a, to be infinite in Chapter 6. Our analysis showed that the effect of rotation is to enhance the stability of the system. Also, these results are reinforcing the fact that the linear instability analysis is accurately capturing the physics of the onset of convection. Inclusion of the inertia term was established in Chapter 7, the effect of inertia (Vadasz number) V_a, Taylor number $\tilde{T}^2$, and the anisotropy parameter ξ was investigated. Increasing the value of Taylor number leads to the onset of convection is by oscillatory convection for large value of the anisotropy parameter provided that $\tilde{T}^2 > (\Lambda^2 + V_a\beta)/\pi^2 (\Lambda - V_a)$, and $V_a < \Lambda$. As γ increases the convection mechanism switches from the oscillatory convection to the stationary convection (normally with narrower cells). These results indicate the effect of incorporating rotation in an anisotropic porous medium.

In future work we plan to investigate instability for the case of thermal convection in a rotating porous medium when the inertia coefficient is anisotropic. Straughan [123] has studied this effect in double diffusive convection but in the non-rotating case. He argues that there are several instances in real life where the inertia itself may be anisotropic.

Another class of the problem we plan to study is thermal convection under condition of local thermal non-equilibrium. This is when the solid skeleton of the

porous media and the saturating fluid have different temperatures. This topic has been creating much attention in the recent research literature, see e.g. Straughan [122], Celli et al. [18], Rees [89], Nield and Kuznetsov [81], Malashetty and Swamy [74], and Kuznetsov and Nield [62].

Bibliography

[1] S. Agarwal and B.S. Bhadauria. Natural convection in a nanofluid saturated rotating porous layer with thermal non-equilibrium model. *Transport in Porous Media*, 90:627–654, 2011.

[2] S.M. Alex and P.R. Patil. Thermal instability in an anisotropic rotating porous medium. *Heat Mass Transfer*, 36:159-163, 2000.

[3] A. Bagchi and F.A. Kulacki. Natural convection in fluid-superposed porous layers heated locally from below. *Int. J. Heat Mass Transfer*, 54:3672–3682, 2011.

[4] P. Bera and A. Khalili. Influence of Prandtl number on stability of mixed convective flow in a vertical channel filled with a porous medium. *Phys. Fluids*, 18:124103, 2006.

[5] P. Bera, J. Kumar, and A. Khalili. Hot springs mediate spatial exchange of heat and mass in the enclosed sediment domain: A stability perspective. *Advances in Water Resources*, 34:817–828, 2011.

[6] H.C. Brinkman. A calculation of viscous force exerted by a flowing fluid on a dense swarm of particles. *Appl. Sci. Res.*, 1:27–34, 1947.

[7] F. Capone, M. Gentile, and A.A. Hill. Anisotropy and symmetry in porous media convection. *Acta Mech.*, 208:205–214, 2009.

[8] F. Capone, M. Gentile, and A.A. Hill. Penetrative convection via internal heating in anisotropic porous media. *Mech. Research Communications*, 37:441–444, 2010.

[9] F. Capone, M. Gentile, and A.A. Hill. Penetrative convection in anisotropic porous media with variable permeability. *Acta Mech*, 216:49–58, 2011.

[10] F. Capone, M. Gentile, and A.A. Hill. Double-diffusive penetrative convection simulated via internal heating in an anisotropic porous layer with throughflow. *Int. J. Heat Mass Transfer*, 54:1622–1626, 2011.

[11] F. Capone, M. Gentile, and A.A. Hill. Convection Problems in Anisotropic Porous Media with Nonhomogeneous Porosity and Thermal Diffusivity. *Acta Appl Math.*, 122:85-9154, 2012.

[12] F. Capone and R. De Luca. Ultimately boundedness and stability of triply diffusive mixtures in rotating porous layers under the action of the Brinkman law. *Int J Non–Linear Mech.*, 47:799–805, 2012.

[13] F. Capone F and S. Rionero. Inertia effect on the onset of convection in rotating porous layers via the "auxilliary system method". *Int J Non–Linear Mech.*, 57:192–200, 2013.

[14] C. Carotenuto and M. Minale. Shear flow over a porous layer: velocity in the real proximity of the interface via rheological tests. *Physics of Fluids*, 23:063101, 2011.

[15] M. Carr and S. de Putter. Penetrative convection in a horizontally isotropic porous layer. *Continuum Mech. Thermodyn.*, 15:33-43, 2003.

[16] G. Castinel and M. Combarnous. Critere dápparition de la convection naturelle dans une couche poreuse anisotrope. *C. R. hebd. Seánc. Acad. Sci. Paris*, B287:701–704, 1974.

[17] C. Cattaneo. Sulla conduzione del calore. *Atti Sem. Mat. Fis. Univ. Modena*, 3:83–101, 1948.

[18] M. Celli, A. Barletta, and L. Storesletten. Local thermal non-equilibrium effects in the Darcy-Bénard instability of a porous layer heated from below by a uniform flux. *Int. J. Heat Mass Transfer*, 67:902-912, 2013.

[19] S. Chandrasekhar. Hydrodynamic and hydromagmetic stability. Oxford Univ. Press, 1961.

[20] X. Chen, S. Wang, J. Tao, and W. Tan. Stability analysis of thermosolutal convection in a horizontal porous layer using a thermal non-equilibrium model. *Int. J. Heat Fluid Flow*, 32:78–87, 2011.

[21] C.I. Christov. On frame indifferent formulation of the Maxwell-Cattaneo model of finite-speed heat conduction. *Mechanics Research Communications*, 36:481–486, 2009.

[22] C.I. Christov and P.M. Jordan. Heat conduction paradox involving second sound propagation in moving media. *Phys. Rev. Lett.*, 94:154301, 2005.

[23] M. Ciarletta and B. Straughan. Uniqueness and structural stability for the Cattaneo-Christov equations. *Mech. Res. Communications*, 37:445–447, 2010.

[24] M. Ciarletta, B. Straughan, and V. Tibullo. Christov-Morro theory for non-isothermal diffusion. *Nonlinear Analysis, Real World Applications*, 13:1224–1228, 2012.

[25] V.A. Cimmelli, A. Sellitto, and V.A. Triani. generalized Coleman-Noll procedure for the exploitation of the entropy principle. *Proc. Roy. Soc. London A*, 466:911-925, 2010.

[26] V.A. Cimmelli, D. Jou, and A. Sellitto. Propagation of temperature waves along core-shell nanowires. *J. Non-Equilibrium Thermodynamics*, 35:267–278, 2010.

[27] R. Courant and D. Hilbert. Methods of Mathematical Physics. Volume I. Interscience Publishers, New York, 1953.

[28] P.C. Dauby, M. Nélis, and G. Lebon. Generalized Fourier equations and thermoconvective instabilities. *Rev. Mex. Fis.*, 48:57–62, 2002.

[29] Y. Dhananjay, R. Bhargava, and G.S. Agrawal. Boundary and internal heat source effects on the onset of Darcye Brinkman convection in a porous layer saturated by nanofluid. *Int. J. Therm. Sci.*, 60:244–254, 2012.

[30] E. Diaz and L. Brevdo. Absolute/ convective instability dichotomy at the onset of convection in a porous layer with either horizontal or vertical solutal and inclined thermal gradients, and horizontal throughflow. *J. Fluid Mech.*, 681:567–596, 2011.

[31] J.J. Dongarra, B. Straughan, and D.W. Walker. Chebyshev tau-QZ algorithm methods for calculating spectra of hydrodynamic stability problems. *Appl. Numer. Math.*, 22:399–435, 1996.

[32] J.F. Epherre. Critere dápparition de la convection naturelle dans une couche poreuse anisotrope. *Rev. Geń. Thermique.*, 168:94S950, 1975.

[33] G. Evans. Practical Numerical Integration. Wiley, Chichester, 1993.

[34] N. Fox. Low temperature effects and generalized thermoelasticity. *J. Inst. Maths. Applics.*, 5:373–386, 1969.

[35] N. Falcón. Compact star cooling by means of heat waves. RevMexAA (Serie de Conferencias), 2001. See also, http://adsabs.harvard.edu/full/2001RMxAC..11..41F.

[36] P. Falsaperla, A. Giacobbe, and G. Mulone. Does Symmetry of the Operator of a Dynamical System Help Stability?. *Acta Appl. Math.*, 122:239-253, 2012.

[37] F. Franchi. Wave propagation in heat conducting dielectric solids with thermal relaxation and temperature dependent electric permittivity. *Riv. Mat. Univ. Parma*, 11:443–461, 1985.

[38] F. Franchi and B. Straughan. Thermal convection at low temperature. *J. Non– Equilib. Thermodyn.*, 19:368–374, 1994.

[39] S.N. Gaikwad and I. Begum. Onset of Double-Diffusive Reaction-Convection in an Anisotropic Rotating Porous Layer. *Transp. Porous Media*, 98:239-257, 2013.

[40] S. Govender. On the Effect of Anisotropy on the Stability of Convection in Rotating Porous Media. *Transp. Porous Media*, 64:413-422, 2006.

[41] S. Govender and P. Vadasz. The effect of mechanical and thermal anisotropy on the stability of gravity driven convection in rotating porous media in the presence of thermal non-equilibrium. *Transp. Porous Media*, 69:55-56, 2007.

[42] R. Guyer and J. Krumhansl. Dispersion relation for second sound in solids. *Phys. Review*, 133:1411–1417, 1964.

[43] R. Guyer and J. Krumhansl. Solution of the linearized Boltzmann phonon equation. *Phys. Review*, 148:766–778, 1966.

[44] R. Guyer and J. Krumhansl. Thermal conductivity, second sound, and phonon hydrodynamic phenomena in nonmetallic crystals. *Phys. Review*, 148:778–788, 1966.

[45] S.A.M. Haddad and B. Straughan. Porous convection and thermal oscillations. *Ricerche mat.*, 61:307–320, 2012.

[46] S.A.M. Haddad. Thermal Convection in a Cattaneo-Fox Porous Material with Guyer-Krumhansl Effects. *Transp. Porous Med.*, 100:363-375, 2013.

[47] S.A.M. Haddad. Thermal instability in Brinkman porous media with Cattaneo-Christov heat flux. *Int. J. Heat Mass Transfer*, 68:659-668, 2014.

[48] S.A.M. Haddad. Thermal convection in a Darcy porous medium with anisotropic spatially varying permeability. *Acta Applicandae Mathematicae*, doi:10.1007/s10440-014-9908-x.

[49] L. Herrera and N. Falcón. Heat waves and thermohaline instability in a fluid. *Physics Letters A*, 201:33–37, 1995.

[50] A.A. Hill and B. Straughan. Global stability for thermal convection in a fluid overlying a highly porous material. *Proc. R. Soc. A*, 465:207–217, 2009.

[51] A.A. Hill and M.S. Malashetty. An operative method to obtain sharp nonlinear stability for systems with spatially dependent coefficients. *Proc Roy Soc London A*, 468:323–336, 2012.

[52] A.A. Hill and M. Carr. The influence of a fluid-porous interface on solar pond stability. *Advances in Water Resources*, 52:1–6, 2013.

[53] A.A. Hill and M. Carr. Stabilising solar ponds by utilising porous materials. *Advances in Water Resources*, 60:1–6, 2013.

[54] D. Jou, V.A. Cimmelli, and A. Sellitto. Nonequilibrium temperatures and second-sound propagation along nanowires and thin layers. *Physics Letters A*, 373:4386–4392, 2009.

[55] D. Jou, A. Sellitto, and F.X. Alvarez. Heat waves and phononwall collisions in nanowires. *Proc. Roy. Soc. London A*, 467:2520-2533, 2011.

[56] P.N. Kaloni and A. Mahajan. Stability of magnetic fluid motions in a saturated porous medium. *ZAMP*, 62:529–538, 2011.

[57] J.P. Kelliher, R. Temam, and X. Wang. Boundary layer associated with the Darcy-Brinkman-Boussinesq model for convection in porous media. *Physica D*, 240:619–628, 2011.

[58] A. Kumar, P. Bera, and A. Khalili. Influence of inertia and drag terms on the stability of mixed convection in a vertical porous-medium channel. *Int. J. Heat Mass Transfer*, 53:23–24, 2010.

[59] A. Kumar, P. Bera, and J. Kumar. Non-Darcy mixed convection in a vertical pipe filled with porous medium. *Int. J. Thermal Sciences*, 50:725–735, 2011.

[60] A. Kumar and B.S. Bhadauria. Thermal instability in arotating anisotropic porous layer saturated by aviscoelastic fluid. *Int. J. Non–Linear Mech.*, 46:47-56, 2011.

[61] A.V. Kuznetsov and D.A. Nield. Thermal instability in a prous medium layer saturated by a nanofluid: Brinkman model. *Transp. Porous Media*, 81:409–422, 2010.

[62] A.V. Kuznetsov and D.A. Nield. The effect of Local Thermal Nonequilibrium on the onset of convection in a porous medium layer saturated by a Nanofluid:Brinkman model. *J. Porous Media*, 14:285–293, 2011.

[63] A.V. Kuznetsov and D.A. Nield. The onset of convection in a tridisperse porous medium. *Int. J. Heat Mass Transfer*, 54:3485–3493, 2011.

[64] O. Kvernvold and P.A. Tyvand. Non-linear thermal convecticm in anisotropic porous media. *J. Fluid Mech.*, 90:609–624, 1979.

[65] G. Lebon and A. Cloot. Bénard-Marangoni instabiity in a Maxwell-Cattaneo fluid. *Phys. Lett. A*, 105:361-364, 1984.

[66] G. Lebon and P.C. Dauby. Heat transport in dielectric crystals at low temperature: A variational formulation based on extended irreversible thermodynamics. *Phys. Review A*, 42:4710–4715, 1990.

[67] J. Lee, I.S. Shivakumara, and A.L. Mamatha. Effect of nonuniform temperature gradients on thermogravitational convection in a porous layer using a thermal nonequilibrium model. *J. Porous Media*, 14:659–669, 2011.

[68] S. Lombardo, G. Mulone, and M. Trovato. Nonlinear stability in reaction-diffusion systems via optimal Lyapunov functions. *J Math. Anal. Appl.*, 342:461–476, 2008.

[69] Lord Rayleigh. On convection currents in horizontal layer of fluid when the higher temperature is on the under side. *Philos. Mag. Ser.*, 32:529-546, 1916.

[70] M.S. Malashetty and M. Swamy. The effect of rotation on the onset of convection in a horizontal anisotropic porous layer. *Int. J. Thermal Sc.*, 46:1023–1032, 2007.

[71] M.S. Malashetty and M. Swamy. Combined effect of thermal modulation and rotation on the onset of stationary convection in a porous layer. *Transp. Porous Media*, 69:313-330, 2007.

[72] M.S. Malashetty and B.S. Biradar. The onset of double diffusive reaction-convection in an anisotropic porous layer. *Phys. Fluids*, 23:064102, 2011.

[73] M.S. Malashetty and B.S. Biradar. The onset of double diffusive convection in a binary Maxwell fluid saturated porous layer with cross-diffusion effects. *Phys. Fluids*, 23:063101, 2011.

[74] M.S. Malashetty and M. Swamy. Effect of rotation on the onset of thermal convection in a sparsely packed porous layer using a thermal non-equilibrium model. *Int. J. Heat Mass Transfer*, 53:3088-3101, 2010.

[75] M.S. Malashetty, I. Pop, and R. Heera. Linear and nonlinear double diffusive convection in a rotating sparsely packed porous layer using a thermal non-equilibrium model. *Continuum Mech. Thermodyn.*, 21:317–339, 2009.

[76] C.B. Moler and G.W. Stewart. An algorithm for generalized matrix eigenproblems. *SIAM J. Numer. Amal.*, 10:241–256, 1973.

[77] A. Morro. Evolution equations and thermodynamic restrictions for dissipative solids. *Math. Computer Modelling*, 52:1869–1876, 2010.

[78] A. Morro. Evolution equations for non-simple viscoelastic solids. *J. Elasticity*, 105:93–105, 2011.

[79] C.E. Nanjundappa, M. Ravisha, J. Lee, and I.S. Shivakumara. Penetrative ferroconvection in a porous layer. *Acta Mechanica*, 216:243–257, 2011.

[80] Nield, D.A., Barletta, A.: Extended Oberbeck–Boussinesq approximation study of convective instabilities in a porous layer with horizontal flow and bottom heating. Int. J. Heat Mass Transf 53, 577–585 (2010)

[81] D.A. Nield and A.V. Kuznetsov. The Effect of Local Thermal Nonequilibrium on the Onset of Convection in a Nanofluid. *J. Heat Transfer*, 132:052405, 2010.

[82] D.A. Nield and A.V. Kuznetsov. The effect of vertical throughflow on thermal instability in a porous medium layer saturated by a nanofluid. *Transp. Porous Media*, 87:765–775, 2011.

[83] D.A. Nield and A.V. Kuznetsov. The Onset of Convection in a Layer of a Porous Medium Saturated by a Nanofluid: Effects of Conductivity and Viscosity Variation and Cross-Diffusion. *Transp. Porous Media*, 92:837–846, 2012.

[84] D.A. Nield and A. Bejan. Convection in Porous Media. 4th edn., Springer, New York, 2013.

[85] N.C. Papanicolaou, C. Christov, and P.M. Jordan. The influence of thermal relaxation on the oscillatory properties of two-gradient convection in a vertical slot. *European J. Mech. B/Fluids*, 30:68–75, 2011.

[86] L.E. Payne, J.F. Rodrigues, and B. Straughan. Effect of anisotropic permeability on Darcýs law. *Math. Meth. Appl. Sci.*, 24:427–438, 2001.

[87] Puri, P. and P.M. Jordan. Wave structure in Stokes's second problem for a dipolar fluid with nonclassical heat conduction. *Acta Mech.*, 133:145-160, 1999.

[88] P. Puri and P.M. Jordan. Stokes's first problem for a dipolar fluid with nonclassical heat conduction. *J. Eng. Math.*, 36:219240, 1999.

[89] D.A.S. Rees. The Effect of Local Thermal Nonequilibrium on the Stability of Convection in a Vertical Porous Channel. *Transp. Porous Media*, 87:459–464, 2011.

[90] D.A.S. Rees. The onset of Darcy-Brinkman convection in a porous layer: an asymptotic analysis. *Int. J. Heat Mass Transfer*, 45:2213–2220, 2002.

[91] D.A.S. Rees and A. Postelnicu. The onset of convection in an inclined anisotropic porous layer. *Int. J. Heat Mass Transfer*, 44:4127-4138, 2001.

[92] S. Rionero. A new approach to nonlinear L^2-stability of double diffusive convection in porous media: necessary and sufficient conditions for global stability via a linearization principle. *J. Math. Anal. Appl.*, 333:1036–1057, 2007.

[93] S. Rionero. L^2-energy stability via new dependent variables for circumventing strongly nonlinear reaction terms. *Nonlinear Analysis, Theory Methods and Applications*, 70:2530–2541, 2009.

[94] S. Rionero. Long-time behaviour of multi-component fluid mixtures in porous media. *Int. J. Engng. Sci.*, 48:1519–1533, 2010.

[95] S. Rionero. Onset of convection in porous materials with vertically stratified porosity. *Acta Mechanica*, 222:261–272, 2011.

[96] S. Rionero. Absence of subcritical instabilities and global nonlinear stability for porous ternary diffusive-convective fluid mixtures. *Phys. Fluids*, 24:104101, 2012.

[97] S. Rionero. Global non-linear stability in double diffusive convection via hidden variables. *Int. J. Non–Linear Mechanics*, 47:61–66, 2012.

[98] S. Rionero. Triple diffusive convection in porous media. *Acta Mechanica*, 224:447–458, 2013.

[99] N. Rudraiah, B. Vecrappa, and S. Balachandra Rae. Effects of nonuniform thermal gradient and adiabatic boundaries on convection in porous media. *J. Heat Transfer*, 102:154–260, 1980.

[100] S. Saravanan and D. Brindha. Linear and non-linear stability limits for centrifugal convection in an anisotropic layer. *Int. J. Non-Linear Mech.*, 46:65–72, 2011.

[101] S. Saravanan and T. Sivakumar. Onset of thermovibrational filtration convection: departure from thermal equilibrium. *Phys. Rev. E*, 84:026307, 2011.

[102] A. Sellitto, F.X. Alvarez, and D. Jou. Phonon-wall interactions and frequency-dependent thermal conductivity in nanowires. *J. Appl. Phys.*, 109:064317, 2011.

[103] A. Sellitto, D. Jou, and J. Bafaluy. Non-local effects in radial heat transport in silicon thin layers and graphene sheets. *Proc. Roy. Soc. London A*, 468:1217-1229, 2012.

[104] I.S. Shivakumara, J. Lee, and K.B. Chavaraddi. Onset of surface tension driven convection in a fluid layer overlying a layer of an anisotropic porous medium. *Int. J. Heat Mass Transfer*, 54:994–1001, 2011.

[105] I.S. Shivakumara, J. Lee, M. Ravisha, and R.G. Raddy. Effects of MFD viscosity and LTNE on the onset of ferromagnetic convection in a porous medium. *Int. J. Heat Mass Transfer*, 54:2630–2641, 2011.

[106] I.S. Shivakumara, J. Lee, K. Vajravelu, and A.L. Mamatha. Effects of thermal nonequilibrium and non-uniform temperature gradients on the onset of convection in a heterogeneous porous medium. *Int. Communications Heat Mass Transfer*, 38:906–910, 2011.

[107] I.S. Shivakumara, Chiu-On Ng, and M.S. Nagashree. The onset of electrothermoconvection in a rotating Brinkman porous layer. *Int. J. Engng. Sci.*, 49:6464–663, 2011.

[108] R.D. Simitev. Double-diffusive convection in a rotating cylindrical annulus with conical caps.*Physics of the Earth and Planetary Interiors*, 186:183–190, 2011.

[109] L. Storesletten. Natural convection in a horizontal porous layer with anisotropic thermal diffusivity, *Transp. Porous Media*, 12:19–29, 1993.

[110] B. Straughan and F. Franchi. Bénard convection and the Cattaneo law of heat conduction. *Proc. Roy. Soc. Edinburgh A*, 96:175-178, 1984.

[111] B. Straughan and D.W. Walker. Anisotropic porous penetrative convection. *Proc. R. Soc. Lond. A*, 452:97-115, 1996.

[112] B. Straughan and D.W. Walker. Two very accurate and efficient methods for computing eigenvalues and eigenfunctions in porous convection problems. *J. Cornput. Phys.*, 127:128–141, 1996.

[113] B.Straughan. The Energy Method, Stability, and Nonlinear Convection. Springer-Verlag, New York, 1992.

[114] B. Straughan. A sharp nonlinear stability threshold in rotating porous convection. *Proc. R. Soc. London. A*, 457:8793, 2001.

[115] B. Straughan. The energy method, stability, and nonlinear convection, Ser. Appl. Math. Sci, second ed., vol. 91, Springer, New York, 2004.

[116] B. Straughan. Stability and wave motion in porous media. Appl. Math. Sci. Ser. Vol. 165, Springer, 2008.

[117] B. Straughan. Porous convection with Cattaneo heat flux. *Int. J. Heat Mass Transfer*, 53:2808–2812, 2010.

[118] B. Straughan. Thermal convection with the Cattaneo–Christov model.*Int. J. Heat Mass Transfer*, 53:95–98, 2010.

[119] B. Straughan. Acoustic waves in a Cattaneo–Christov gas. *Physics Letters A*, 374:2667–2669, 2010.

[120] B. Straughan. Tipping points in Cattaneo–Christov thermohaline convection. *Proc. Roy. Soc. London A*, 467:7–18, 2011.

[121] B.Straughan. Heat Waves. Appl. Math. Sci. Ser. Vol. 177, Springer, 2011.

[122] B. Straughan. Porous convection with local thermal non-equilibrium temperatures and with Cattaneo effects in the solid. *Proc. R. Soc. A*, 469:20130187, 2013.

[123] B. Straughan. Anisotropic inertia effect in microfluidic porous thermosolutal convection. *Microfluid Nanofluid*, 6:361-368, 2014.

[124] Sunil, P. Sharma, and A. Mahajan. Onset of Darcy-Brinkman ferroconvection in a rotating porous layer using a thermal non-equilibrium model: A nonlinear stability analysis. *Transp. Porous Media*, 88:421–439, 2011.

[125] V. Tibullo and V.A. Zampoli. uniqueness result for the Cattaneo–Christov heat conduction model applied to incompressible fluids. *Mechanics Research Communications*, 38:77–79, 2011.

[126] P.A. Tyvand. Thermohaline Instability in Anisotropic Porous Media. *Water Resour. Res.*, 16:325–330, 1980.

[127] R. Usha, S. Millet, H. BenHaddid, and F. Rousset. Shear thinning film on a porous substrate: stability analysis of a one-sided model. *Chem. Engng. Sci.*, 66:5614–5627, 2011.

[128] P. Vadasz. Stability of free convection in a narrow porous layer subject to rotation. *Int. Comm. Heat Mass Transfer*, 21:881–890, 1994.

[129] P. Vadasz. Stability of free convection in a rotating porous layer distant from the axis of rotation. *Transp. Porous Media*, 23:153–173, 1996.

[130] P. Vadasz. Convection and stability in a rotating porous layer with alternating direction of the centrifugal body forc. *Int. J. Heat Mass Transfer*, 39:1639–1647, 1996.

[131] P. Vadasz. Coriolis effect on gravity-driven convection in a rotating porous layer heated from below. *J. Fluid Mech.*, 376:351–375, 1998.

[132] P. Vadasz. Flow and thermal convection in rotating porous media. in: K. Vafai edn., Handbook of Porous Media, Marcel Dekker, New York, 395–440, 2000.

[133] P. Vadasz and S. Govender. Stability and stationary convection induced by gravity and centrifugal forces in a rotating porous layer distant from the axis of rotation. *Int. J. Eng. Sci.*, 39:715–732, 2001.

[134] J.J. Vadasz, S. Govender, and P. Vadasz. Heat transfer enhancement in nanofluids suspensions: possible mechanisms and explanations. *Int. J. Heat Mass Transfer*, 48:2673–2683, 2005.

[135] P. Vasseur, C.H. Wang, and S. Mihir. The Brinkman model for natural convection in a shallow porous cavity with uniform heat flux. *Numer. Heat Trnsfer*, 15:231–142, 1989.

[136] P. Vasseur and L. Robillard. The Brinkman model for natural convection in a porous layer: effects of nonuniform thermal gradient. *Int. J. Heat Mass Transfer*, 36:4199–4206, 1993.

[137] R.K. Vanishree and P.G. Siddheshwar. Effect of Rotation on Thermal Convection in an Anisotropic Porous Medium with Temperature-dependent Viscosity. *Transp. Porous Media*, 81:73-87, 2010.

[138] M. Wang, N. Yang, and Z.Y. Guo. Non-Fourier heat conductions in nanomaterials. *J. Appl. Phys.*, 110:064310, 2011.

[139] D. Yang, R. Zeng, and D. Zhang. Numerical simulation of convective stability of the short-term storage of CO_2 in saline aquifiers. *Int. J. Greenhouse Gas Control*, 5:986–994, 2011.

[140] S. Wang and W. Tan. The onset of Darcy-Brinkman thermosolutal convection in a horizontal porous media. *Phys. Lett. A*, 373:776–780, 2009.

Appendix A

Cattaneo theories

A.1   Cattaneo-Fox law and Cattaneo-Christov law

To clarify the Cattaneo-Fox law and the Cattaneo-Christov law we begin with the Maxwell-Cattaneo law of heat conduction [17],

$$\tau Q_{i,t} + Q_i = -\kappa T_{,i}. \tag{A.1.1}$$

When equation (A.1.1) is combined with the conservation of energy equation it leads to the hyperbolic telegraph equation for the temperature field. Thus the temperature can propagate as a damped travelling wave. However, equation (A.1.1) is insufficient to describe heat transfer in a moving fluid [28], or heat conduction in nanomaterials see, e.g., Wang et al. [138], and references therein. As a result, the equation governing the heat flux must involve an objective derivative.

Straughan and Franchi [110] proposed the following modification on the Maxwell-Cattaneo law (A.1.1)

$$\tau \left(\dot{Q}_i - \varepsilon_{ijk} w_j Q_k \right) = -Q_i - \kappa T_{,i}, \tag{A.1.2}$$

which has come to be known as the Cattaneo-Fox heat flux law. Here $\mathbf{w} = \mathrm{curl}\,\mathbf{v}/2$, a superposed dot denotes the material time derivative. The derivative $\tau \left(\dot{Q}_i - \varepsilon_{ijk} w_j Q_k \right)$ is an objective (Jaumann) time derivative of Fox [34] for the heat flux.

Christov [21] proposed an appropriate objective derivative for the heat flux when dealing with a Cattaneo type theory for a fluid. He suggests the following Lie

derivative which is a frame indifferent objective rate,

$$\tau \left(Q_{i,t} + v_j Q_{i,j} - Q_j v_{i,j} + v_{j,j} Q_i \right) = -Q_i - \kappa T_{,i}, \qquad \text{(A.1.3)}$$

which has come to be known as The Cattaneo-Christov law .

The Cattaneo-Christov theory has been placed on a sound thermodynamic basis by Morro [77]. Straughan [119] showed that the Cattaneo-Christov theory yields a well defined thermo-acoustic theory for wave propagation in a gas.

A.2 Guyer-Krumhansl model

The generalization of equation (A.1.1) which follows from the solution of the linearized Boltzmann equation is a well-known Guyer-Krumhansl equation for heat flux [42–44]. This equation has been analysed by Lebon and Dauby [66] by means of variational argument in the context of extended thermodynamics, which has form

$$\tau Q_{i,t} + Q_i = -\kappa T_{,i} + \hat{\tau} \Delta Q_i + 2\hat{\tau} Q_{k,ki}. \qquad \text{(A.2.4)}$$

Here $\hat{\tau} = \tau \tau_N c_s^2 / 5$ where τ_N is a relaxation time and c_s is the mean speed of phonons.

Franchi and Straughan [38] proposed modifying equation (A.1.2) by incorporating the Guyer-Krumhansl terms for heat flux. Then one would modify equation (A.1.2) to

$$\tau \left(\dot{Q}_i - \varepsilon_{ijk} w_j Q_k \right) = -Q_i - \kappa T_{,i} + \hat{\tau}(\Delta Q_i + 2Q_{k,ki}). \qquad \text{(A.2.5)}$$

Franchi and Straughan [38] employed equation (A.2.5) to study problem of thermal convection.

Appendix B

The D^2 Chebyshev tau method

In this Appendix, we describe how the Chebyshev polynomials are used in hydro-dynamic stability problems. For this purposes we introduce some recurrence rela-tionship between the functions and the Chebyshev polynomials. We then illustrate, by using the Bénard problem for the Brinkman model discussed in Chapter 1, the Chebyshev tau method employing a chebyshev representation of the second deriva-tive operator (D^2 Chebyshev tau method).

B.1 The Chebyshev polynomials

The Chebyshev polynomial of the first kind, denoted by $T_n(x)$, is polynomial of the nth degree defined by the relation

$$T_n(x) = \cos n\vartheta, \qquad \text{whene } x = \cos \vartheta, \qquad (B.1.1)$$

where $-1 \leq x \leq 1$ (the range of the corresponding variable $\vartheta \in [0, \pi]$), and $n = 0, 1, 2, \ldots$. The first two polynomials may be deduced from (B.1.1)

$$T_0(x) = 1,$$

$$T_1(x) = x.$$

From the trigonometric identities, we have

$$
\begin{aligned}
T_{n+1}(x) &= \cos(n+1)\vartheta \\
&= \cos n\vartheta \cos \vartheta - \sin n\vartheta \sin \vartheta, \qquad (B.1.2)
\end{aligned}
$$

and

$$
\begin{aligned}
T_{n-1}(x) &= \cos(n-1)\vartheta \\
&= \cos n\vartheta \cos\vartheta + \sin n\vartheta \sin\vartheta.
\end{aligned}
\tag{B.1.3}
$$

By combining (B.1.2) and (B.1.3) we find

$$
T_{n+1}(x) + T_{n-1}(x) = 2\cos n\vartheta \cos\vartheta,
$$

and so we have the fundamental recurrence relation

$$
T_{n+1}(x) = 2xT_n(x) - T_{n-1}(x), \qquad n = 1, 2, 3, \ldots.
\tag{B.1.4}
$$

Together with $T_0(x) = 1$, and $T_1(x) = x$ we can obtain the rest of the set of Chebyshev polynomials

$$
T_2(x) = 2x^2 - 1,
$$

$$
T_3(x) = 4x^3 - 3x,
$$

$$
T_4(x) = 8x^4 - 8x^2 + 1,
$$

$$
T_5(x) = 16x^5 - 20x^3 + 5x,
$$

$$
\text{etc.}
$$

The Chebyshev polynomials are orthogonal polynomials in the interval $(-1, 1)$ with respect to the weighting function $1/\sqrt{(1 - x^2)}$. In particular,

$$
\langle T_n, T_m \rangle = \int_{-1}^{1} \frac{T_n(x)T_m(x)}{\sqrt{1 - x^2}} dx = \begin{cases} \pi & \text{if } m = n = 0, \\ \dfrac{\pi}{2} & \text{if } m = n \neq 0, \\ 0 & \text{if } m \neq 0. \end{cases}
\tag{B.1.5}
$$

To proceed to (B.1.5) we consider the weighted inner product of $T_n(x)$ and $T_m(x)$ on the interval $-1 < x < 1$,

$$
\int_{-1}^{1} \frac{T_n(x)T_m(x)}{\sqrt{1 - x^2}} dx = \int_{0}^{\pi} \cos n\vartheta \cos m\vartheta d\vartheta.
\tag{B.1.6}
$$

In the case of $n = m = 0$, we have

$$
\begin{aligned}
\int_{0}^{\pi} \cos n\vartheta \cos m\vartheta d\vartheta &= \int_{0}^{\pi} d\vartheta \\
&= \pi,
\end{aligned}
$$

and when $n = m \neq 0$, then

$$
\begin{aligned}
\int_0^\pi \cos n\vartheta \cos m\vartheta d\vartheta &= \frac{1}{2} \int_0^\pi [\cos(n+m)\vartheta + \cos|n-m|\,\vartheta]\,d\vartheta \\
&= \frac{1}{2} \int_0^\pi [\cos(n+m)\vartheta + 1]d\vartheta \\
&= \left[\frac{\sin(n+m)\vartheta}{2(n+m)}\right]_0^\pi + \frac{\pi}{2} \\
&= \frac{\pi}{2}.
\end{aligned}
$$

Finally. in case of $n \neq m$, we have

$$
\begin{aligned}
\int_0^\pi \cos n\vartheta \cos m\vartheta d\vartheta &= \frac{1}{2} \int_0^\pi \cos(n+m)\vartheta + \cos|n-m|\,\vartheta d\vartheta \\
&= \left[\frac{\sin(n+m)\vartheta}{2(n+m)}\right]_0^\pi + \left[\frac{\sin|n-m|\,\vartheta}{2|n-m|}\right]_0^\pi \\
&= 0.
\end{aligned}
$$

Thus, we have proved that equation (B.1.5) is achieved.

B.2 The Chebyshev differentiation matrix D^2

In this section, before proceeding to derive the coefficients of the matrix D^2 we introduce the differentiating Chebyshev polynomials $T_n(x)$ with respect to x,

$$
\begin{aligned}
\frac{dT_n}{dx} &= \frac{dT_n}{d\vartheta} \cdot \frac{d\vartheta}{dx} \\
&= \frac{n\sin n\vartheta}{\sin \vartheta},
\end{aligned}
$$

and so

$$
T'_{n+1}(x) = \frac{(n+1)\sin(n+1)\vartheta}{\sin \vartheta}, \tag{B.2.7}
$$

$$
T'_{n-1}(x) = \frac{(n-1)\sin(n-1)\vartheta}{\sin \vartheta}. \tag{B.2.8}
$$

By adding (B.2.7)-(B.2.7), and then using trigonometric identities, we have

$$
\begin{aligned}
\frac{T'_{n+1}(x)}{n+1} - \frac{T'_{n-1}(x)}{n-1} &= \frac{1}{\sin \vartheta}[\sin(n+1)\vartheta - \sin(n-1)\vartheta] \\
&= 2\cos n\vartheta \\
&= 2T_n(x), \qquad \text{for } n \geq 2.
\end{aligned}
$$

In the case of $n = 0$, and $n = 1$, respectively, we find that $T_1'(x) = 1$ and $T_0'(x) = 0$. Therefore, the recurrence relation for $n \geq 0$ as follows

$$2T_n(x) = \frac{1}{n+1}T_{n+1}'(x) - \frac{1}{n-1}T_{|n-1|}'(x). \tag{B.2.9}$$

Now, let consider the Chebyshev expansion of a continuously differentiable function $f \in (-1, 1)$,

$$f(x) = \sum_{n=0}^{\infty} a_n T_n(x), \tag{B.2.10}$$

where a_n are the Chebyshev expansion coefficients. Similar expressions for $f'(x)$, $f''(x), \ldots$, are assumed so that

$$f^{(k)}(x) = \sum_{n=0}^{\infty} a_n^{(k)} T_n(x), \tag{B.2.11}$$

where $f^{(k)}$ is the kth derivative of f, and $a_n^{(k)}$ are the Chebyshev expansion coefficients of the kth derivative. Therefore, considering the first-order derivative, one finds

$$
\begin{aligned}
\frac{d}{dx}\sum_{n=0}^{\infty} a_n T_n(x) &= \sum_{n=0}^{\infty} a_n^{(1)} T_n(x) \\
&= \frac{1}{2}\sum_{n=0}^{\infty} a_n^{(1)}\left(\frac{1}{n+1}T_{n+1}'(x) - \frac{1}{n-1}T_{|n-1|}'(x)\right) \\
&= \frac{1}{2}\frac{d}{dx}\sum_{n=0}^{\infty} a_n^{(1)}\left(\frac{1}{n+1}T_{n+1}(x) - \frac{1}{n-1}T_{|n-1|}(x)\right) \\
&= \frac{1}{2}\frac{d}{dx}\left(\left(2a_0^{(1)} - a_2^{(1)}\right)T_1 + \frac{\left(a_1^{(1)} - a_3^{(1)}\right)}{2}T_2 + \frac{\left(a_2^{(1)} - a_4^{(1)}\right)}{3}T_3 + \cdots\right).
\end{aligned}
$$

Equating coefficients of $T_i(x)$, $i \geq 1$ gives the recurrence relation,

$$2pa_p = c_{p-1}a_{p-1}^{(1)} - a_{p+1}^{(1)}, \qquad \text{for } p \geq 1, \tag{B.2.12}$$

where $c_0 = 2$ and $c_p = 1$ for $p \geq 1$.

Proceeding by summing both sides of equation (B.2.12) over p with $p+n = $ odd, from $p = n+1$ to $p = \infty$, then

$$
\begin{aligned}
2\sum_{\substack{p=n+1 \\ p+n=\text{odd}}}^{\infty} pa_p &= \sum_{\substack{p=n+1 \\ p+n=\text{odd}}}^{\infty} c_{p-1}a_{p-1}^{(1)} - a_{p+1}^{(1)} \\
&= \left(c_n a_n^{(1)} - a_{n+2}^{(1)}\right) + \left(c_{n+2}a_{n+2}^{(1)} - a_{n+4}^{(1)}\right) + \left(c_{n+4}a_{n+4}^{(1)} - a_{n+6}^{(1)}\right) + \cdots,
\end{aligned}
$$

since $c_p = 1$ for $p \geq 1$. Simplifying the foregoing equation gives

$$a_n^{(1)} = \frac{2}{c_n} \sum_{\substack{p=n+1 \\ p+n=odd}}^{\infty} p a_p.$$

Thus, in general we obtain

$$a_n^{(k)} = \frac{2}{c_n} \sum_{\substack{p=n+1 \\ p+n=odd}}^{\infty} p a_p^{(k-1)}, \ n \geq 0, \tag{B.2.13}$$

Now, we replace $a_p^{(k-1)}$ by its expression in terms of the infinite series and so equation (B.2.13) may be written as

$$
\begin{aligned}
a_n^{(k)} &= \frac{2}{c_n} \sum_{\substack{p=n+1 \\ p+n=odd}}^{\infty} p \frac{2}{c_p} \sum_{\substack{m=p+1 \\ p+m=odd}}^{\infty} m a_m^{(k-2)}, \ c_p = 1 \ \text{for} p \geq 1 \\
&= \frac{4}{c_n} \sum_{\substack{p=n+1 \\ p+n=odd}}^{\infty} p \sum_{\substack{m=p+1 \\ p+m=odd}}^{\infty} m a_m^{(k-2)} \\
&= \frac{4}{c_n} (n+1) \left[(n+2) a_{n+2}^{(k-2)} + (n+4) a_{n+4}^{(k-2)} + (n+6) a_{n+6}^{(k-2)} + \cdots \right] \\
&\quad + \frac{4}{c_n} (n+3) \left[(n+4) a_{n+4}^{(k-2)} + (n+6) a_{n+6}^{(k-2)} + (n+8) a_{n+8}^{(k-2)} + \cdots \right] \\
&\quad + \frac{4}{c_n} (n+5) \left[(n+6) a_{n+6}^{(k-2)} + (n+8) a_{n+8}^{(k-2)} + (n+10) a_{n+10}^{(k-2)} + \cdots \right] \\
&= \frac{4}{c_n} (n+1)(n+2) a_{n+2}^{(k-2)} \\
&\quad + \frac{4}{c_n} [(n+1) + (n+3)] (n+4) a_{n+4}^{(k-2)} \\
&\quad + \frac{4}{c_n} [(n+1) + (n+3) + (n+5)] (n+6) a_{n+6}^{(k-2)} \\
&\quad + \frac{4}{c_n} [(n+1) + (n+3) + (n+5) + (n+7)] (n+8) a_{n+8}^{(k-2)} + \cdots \\
&= \frac{4}{c_n} \sum_{\substack{p=n+2 \\ p+n=even}}^{\infty} p a_p^{(k-2)} \sum_{\substack{m=n+1 \\ m+n=odd}}^{p-1} m. \tag{B.2.14}
\end{aligned}
$$

Next by expanding the inner summation, we obtain

$$
\begin{aligned}
\sum_{\substack{m=n+1 \\ m+n=odd}}^{p-1} m &= (n+1) + (n+3) + (n+5) + \cdots + (p-1) \\
&= \sum_{i=0}^{\frac{1}{2}(p-n)-1} (n+1+2i) \\
&= (n+1) \sum_{i=0}^{\frac{1}{2}(p-n)-1} 1 + 2 \sum_{i=1}^{\frac{1}{2}(p-n)-1} i \\
&= \frac{1}{2}(n+1)(p-n) + \frac{1}{2}\left(\frac{1}{2}(p-n) - 1\right)(p-n) \\
&= \frac{1}{4}\left(p^2 - n^2\right).
\end{aligned}
$$

Substituting back into equation (B.2.14), we have

$$
a_n^{(k)} = \frac{1}{c_n} \sum_{\substack{p=n+2 \\ p+n=even}}^{\infty} p\left(p^2 - n^2\right) a_p^{(k-2)} \tag{B.2.15}
$$

Further, we truncate the Chebyshev expansion of $a^k(x)$ at the $n = $ Nth term as follows

$$
a^{(k)}(x) = \sum_{n=0}^{N} a_n^{(k)} T_n(x) + e_{N+1}(x), \tag{B.2.16}
$$

where e_{N+1} is the error term. Suppose that e_{N+1} is small, we may therefore approximate $a^{(k)}(x)$ in term of finite series $\hat{a}^{(k)}(x) = \sum_{n=0}^{N} \hat{a}_n T_n$, where the coefficients $\hat{a}_n$ are evaluated by using the Clenshaw-Curtis quadrature formula, we refer the reader to the book by Evans [33].

Let now define a vector $\hat{\mathbf{a}}^{(k)} = \left(\hat{a}_0^{(k)}, \hat{a}_1^{(k)}, \hat{a}_2^{(k)}, \ldots, \hat{a}_N^{(k)}\right)^T$, then upon substituting into equation (B.2.15) we find,

$$
\hat{a}_n^{(k)} = \frac{1}{c_n} \sum_{\substack{p=n+2 \\ p+n=even}}^{\infty} p\left(p^2 - n^2\right) a_p^{(k-2)}. \tag{B.2.17}
$$

Thus, we may obtain an upper triangular matrix D^2 such that $\hat{\mathbf{a}}^{(k)} = D^2 \hat{\mathbf{a}}^{(k-2)}$,

where D^2 is given by

$$D^2 = \begin{pmatrix} 0 & 0 & 4 & 0 & 32 & 0 & 108 & \cdots \\ 0 & 0 & 0 & 24 & 0 & 120 & 0 & \cdots \\ 0 & 0 & 0 & 0 & 48 & 0 & 192 & \cdots \\ 0 & 0 & 0 & 0 & 0 & 80 & 0 & \cdots \\ \cdots & \cdots & \cdots & \cdots & \cdots & \cdots & \cdots & \cdots \end{pmatrix}.$$

In the next section, we discuss the application of the D^2 Chebyshev tau method.

B.3   Application of the D^2 Chebyshev tau method to the Bénard problem for the Brinkman model

The Bénard problem for the Brinkman model is studied in Chapter 1. For the present section the D^2 Chebyshev tau method will be used to solve the eigenvalue problem (1.3.7) in Section 1.3. This is rewritten for clarity

$$W'' - a^2 W = \lambda \left(W'''' - 2a^2 W'' + a^4 W \right) - a^2 R\Theta,$$
$$0 = RW + \Theta'' - a^2 \Theta. \tag{B.3.18}$$

The corresponding boundary conditions, when we consider fixed surfaces, are

$$W = W' = \Theta = 0, \quad \text{at } z = 0, 1. \tag{B.3.19}$$

The system (B.3.18) is an eigenvalue problem for R, given a and λ. The key idea is to write (B.3.18) as a system of second order equations. Therefore, we introduce variable $\chi = W'' - a^2 W$ and so we may rewrite the system (B.3.18) in the form

$$W'' - a^2 W - \chi = 0,$$
$$\lambda \chi'' - \lambda a^2 \chi - \chi = Ra^2 \Theta, \tag{B.3.20}$$
$$\Theta'' - a^2 \Theta = -RW.$$

Next, we recast equations (B.3.20) and the boundary conditions (B.3.19) in the interval $(-1, 1)$, and then we write W, Θ, and χ in the form of a series of Chebyshev polynomials. Truncating each sum, so that

$$\hat{W}(z) = \sum_{n=0}^{N} W_n T_n(z), \quad \hat{\chi}(z) = \sum_{n=0}^{N} \chi_n T_n(z), \quad \hat{\Theta}(z) = \sum_{n=0}^{N} \Theta_n T_n(z), \tag{B.3.21}$$

and

$$\hat{W}''(z) = \sum_{n=0}^{N} W_n^{(2)} T_n(z), \quad \hat{\chi}''(z) = \sum_{n=0}^{N} \chi_n^{(2)} T_n(z), \quad \hat{\Theta}(z) = \sum_{n=0}^{N} \Theta_n^{(2)} T_n(z).$$

(B.3.22)

Thus, from (B.3.20) we conclude

$$4\hat{W}^{(2)}(z) - a^2\hat{W}(z) - \hat{\chi}(z) = \tau_1 T_{N-1} + \tau_2 T_N,$$

$$4\lambda\hat{\chi}^{(2)}(z) - \lambda a^2\hat{\chi}(z) - \hat{\chi}(z) - Ra^2\hat{\Theta}(z) = \tau_3 T_{N-1} + \tau_4 T_N,$$

(B.3.23)

$$4\hat{\Theta}^{(2)}(z) - a^2\hat{\Theta}(z) + R\hat{W}(z) = \tau_5 T_{N-1} + \tau_6 T_N,$$

where τ_i are tau coefficients which may be used to measure the error associated with truncation in (B.3.21), and (B.3.22).

To remove τ_i's we take the weighted Chebyshev inner product of equation (B.3.23) with the polynomial T_i for $i = 0, 1, \ldots, N-2$, and then we let $\hat{W} = (W_0, W_1, \ldots, W_N)^T$, $\hat{\Theta} = (\Theta_0, \Theta_1, \ldots, \Theta_N)^T$, and $\hat{\chi} = (\chi_0, \chi_1, \ldots, \chi_N)^T$, with similar forms for $\hat{W}^{(2)}$, $\hat{\Theta}^{(2)}$ and $\hat{\chi}^{(2)}$ and make the substitutions $\hat{\mathbf{W}}^{(2)} = D^2\hat{\mathbf{W}}$, $\hat{\mathbf{\Theta}}^{(2)} = D^2\hat{\mathbf{\Theta}}$, and $\hat{\mathbf{\chi}}^{(2)} = D^2\hat{\mathbf{\chi}}$.

Next, we add two rows of zeros to the bottom of D^2 to make the matrix square, and these rows can be overwritten by the boundary conditions (B.3.19), where the relations $T_n(\pm 1) = (\pm 1)^n$, $T_n'(\pm 1) = (\pm 1)^{n-1} n^2$ are used, as follows

$$\sum_{n=0}^{N} W_n = 0, \quad \sum_{n=0}^{N} (-1)^n W_n = 0, \quad \sum_{n=0}^{N} \Theta_n = 0, \quad \sum_{n=0}^{N} (-1)^n \Theta_n = 0,$$

$$\sum_{n=0}^{N} n^2 W_n = 0, \quad \sum_{n=0}^{N} (-1)^{n-1} n^2 W_n = 0,$$

or upon simplification,

$$BC1: \ W_0 + W_2 + W_4 + \cdots + W_{N-1} = 0,$$

$$BC2: \ W_1 + W_3 + W_5 + \cdots + W_N = 0,$$

$$BC3: \ W_1 + 3^2 W_3 + 5^2 W_5 + \cdots + N^2 W_N = 0,$$

$$BC4: \ 4W_2 + 4^2 W_4 + \cdots + (N-1)^2 W_{N-1} = 0,$$

$$BC5: \ \Theta_0 + \Theta_2 + \Theta_4 + \cdots \Theta_{N-1} = 0,$$

$$BC6: \ \Theta_1 + \Theta_3 + \Theta_5 + \cdots \Theta_N = 0.$$

Thus, the system (B.3.23) may be arranged as

$$4D^2\hat{\mathbf{W}} - a^2\hat{\mathbf{W}} - \hat{\boldsymbol{\chi}} = 0,$$

$$\lambda 4D^2\hat{\boldsymbol{\chi}} - \lambda a^2\hat{\boldsymbol{\chi}} - \hat{\boldsymbol{\chi}} = Ra^2\hat{\boldsymbol{\Theta}},$$
(B.3.24)

$$4D^2\hat{\boldsymbol{\Theta}} - a^2\hat{\boldsymbol{\Theta}} = -R\hat{\mathbf{W}}.$$

The system (B.3.24) represent a matrix equation of the form

$$A\mathbf{x} = RB\mathbf{x},$$
(B.3.25)

where A and B are $(N+1) \times (N+1)$ matrix given by

$$A = \begin{pmatrix} 4D^2 - a^2I & -I & 0 \\ BC1 & 0\cdots0 & 0\cdots0 \\ BC2 & 0\cdots0 & 0\cdots0 \\ 0 & \lambda(4D^2 - a^2I) - I & 0 \\ BC3 & 0\cdots0 & 0\cdots0 \\ BC4 & 0\cdots0 & 0\cdots0 \\ 0 & 0 & 4D^2 - a^2I \\ 0\cdots0 & 0\cdots0 & BC5 \\ 0\cdots0 & 0\cdots0 & BC6 \end{pmatrix},$$

$$B = \begin{pmatrix} 0 & 0 & 0 \\ 0\cdots0 & 0\cdots0 & 0\cdots0 \\ 0\cdots0 & 0\cdots0 & 0\cdots0 \\ 0 & 0 & a^2I \\ 0\cdots0 & 0\cdots0 & 0\cdots0 \\ 0\cdots0 & 0\cdots0 & 0\cdots0 \\ -I & 0 & 0 \\ 0\cdots0 & 0\cdots0 & 0\cdots0 \\ 0\cdots0 & 0\cdots0 & 0\cdots0 \end{pmatrix}.$$

The matrix equation (B.3.25) is solved by employing the QZ algorithm of Moler and Stewart [76]. More details of employing the Chebyshev tau method may be found in Dongarra et al. [31].